UC Santa Barbara
UC Santa Barbara Electronic Theses and Dissertations

Title
Quantum Aspects of Spacetime Geometry

Permalink
https://escholarship.org/uc/item/0jk9n0m6

Author
Trevino, Gabriel

Publication Date
2021

Peer reviewed|Thesis/dissertation

eScholarship.org Powered by the California Digital Library
University of California

University of California
Santa Barbara

Quantum Aspects of Spacetime Geometry

A dissertation submitted in partial satisfaction
of the requirements for the degree

Doctor of Philosophy
in
Physics

by

Gabriel Treviño Verástegui

Committee in charge:

Professor Gary Horowitz, Chair
Professor Xi Dong
Professor David Stuart

September 2021

The Dissertation of Gabriel Treviño Verástegui is approved.

Professor Xi Dong

Professor David Stuart

Professor Gary Horowitz, Committee Chair

July 2021

Quantum Aspects of Spacetime Geometry

Copyright © 2021

by

Gabriel Treviño Verástegui

To my parents

Acknowledgements

First and foremost, I would like to thank my advisor, Gary Horowitz, for his continual support throughout my PhD. It has been a pleasure—and truly an inspiration—to work, do research, and learn physics with him. In particular, I want to thank him for encouraging me to explore many fascinating corners in gravitational physics—especially those that are not so well-appreciated by the community. I know that without him, I wouldn't have learned as much of what gravity has to offer as I did. I would also like to thank him for making me appreciate the value in having a clear and intuitive explanation for physics. I'm pleased to have had him not just as an advisor, but also as a teacher.

I want to thank the professors in the physics department that were part of my journey during these years. I thank Don Marolf for being a fantastic teacher and mentor. He always encouraged me to go ask him about anything—and whenever I did, he always had time for me. I'm pleased that I got to be part of his General Relativity course series, as well as three different special topics courses. It has been an invaluable experience to have had access to his insights in physics. I also want to thank Xi Dong for wonderful discussions, Steve Giddings for a very productive collaboration, and David Stuart for his useful guidance during graduate school.

My time in graduate school wouldn't have been the same without the valuable interactions I had with my friends and peers. I want to thank Seth Koren for a wonderful collaboration and for being someone I could always reach out for advice on physics, writing, and life. I also thank both Sergio Hernández-Cuenca and Diandian Wang for very insightful discussions and for teaching me so much during our group meetings. A special thank you goes to Alex Kinsella, Brianna Grado-White, Dillon Cisco, Eric Jones, Farzan Vafa, Neelay Fruitwala, and the rest of my classmates and friends who made of graduate school a wonderful adventure.

Next, I want to show gratitude to my family and friends back in Mexico for their constant support as I worked on my PhD far away from home. In particular, I thank my mother for always supporting and encouraging my curiosity for understanding the universe; and my father, who shared with me his dream of getting a PhD degree and inspired me to pursue my own.

I would also like to highlight the role that Daniel Sudarsky, Chryssomalis Chryssomalakos, Pablo Barberis, Elias Okon, and Miguel Alcubierre had on me as mentors in UNAM. They were central in preparing and motivating me to embark on my PhD. Finally, I want to express my appreciation for Stephen Hawking, who I was fortunate enough to thank in person, and whose books inspired me to get into physics in the first place.

This dissertation was supported by the UC MEXUS-CONACYT Doctoral Fellowship, and by two NSF grants: PHY-1504541 and PHY-1801805.

Curriculum Vitæ

Gabriel Treviño Verástegui

Education

2021	Ph.D. in Physics (Expected), University of California, Santa Barbara.
2018	M.A. in Physics, University of California, Santa Barbara.
2015	B.S. in Physics, Universidad Nacional Autónoma de México

Publications

"Boundary Causality Violating Metrics in Holography"
S. Hernández-Cuenca, G. T. Horowitz, G. Treviño, and D. Wang
[arXiv:2103.05014 [hep-th]]

"Exploring Strong-Field Deviations From General Relativity via Gravitational Waves"
S. Giddings, S. Koren, G. Treviño
Phys. Rev. D100 (2019) 044005, [arXiv:1904.04258 [gr-qc]]

"Reconstruction of an AdS Radiation/Boson Star Bulk Geometry Using Lightcone Cuts"
G. Treviño
JHEP **11**, 111 (2017) [arXiv:1708.03331 [hep-th]]

Abstract

Quantum Aspects of Spacetime Geometry

by

Gabriel Treviño Verástegui

In this dissertation, we investigate how some properties of quantum mechanics integrate in our description of the geometry of spacetime. This is done both at a theoretical and phenomenological level. In the first chapter, we give a brief introduction to the development of quantum mechanical ideas in our current understanding of spacetime and gravity. In particular, we motivate the necessity of a holographic description of gravity, as well as review some of the essential properties of the AdS/CFT correspondence.

In the second chapter, we use this holographic duality to ask how the geometry of a particular bulk system is encoded in a non-gravitational field theory. In particular, we review and use the light-cone cuts prescription, which has been proposed as a method to reconstruct the conformal metric of a holographic spacetime. With this framework, we explore how additional information about the bulk geometry gets encoded in the structure of these light-cone cuts. We pay special attention on how the hyperbolic angle related to a cusp in the light-cone cut encodes information about the matter content of the spacetime. We provide an explicit numerical example reconstructing the metric for a four-dimensional spacetime composed by the superposition of a boson star and a gas of radiation in AdS.

The full bulk path integral in a Lorentzian formulation of holography includes metrics that violate boundary causality. This leads to the following puzzle: The commutator of two field theory operators at spacelike-separated points on the boundary must vanish. However, if these points are causally related in a bulk metric, then the bulk calculation

of the commutator will be nonzero. It would appear that the integral over all metrics of this commutator must vanish exactly for holography to hold. This is puzzling since it must also be true if the commutator is multiplied by any other operator. Upon a careful treatment of boundary conditions in holography, in the third chapter of this thesis we show how the bulk path integral leads to a natural resolution of this puzzle.

In chapter four, we explore some phenomenological implications stemming from quantum modifications to a classical theory of gravity. Two new observational windows have been opened to strong gravitational physics: gravitational waves, and very long baseline interferometry. This suggests observational searches for new phenomena in this regime, and in particular for those necessary to make black hole evolution consistent with quantum mechanics. We describe possible features of "compact quantum objects" that replace classical black holes in a consistent quantum theory, and approaches to observational tests for these using gravitational waves. This is an example of a more general problem of finding consistent descriptions of deviations from general relativity, which can be tested via gravitational wave detection. Simple models for compact modifications to classical black holes are described via an effective stress tensor, possibly with an effective equation of state. A general discussion is given of possible observational signatures, and of their dependence on properties of the colliding objects. The possibility that departures from classical behavior are restricted to the near-horizon regime raises the question of whether these will be obscured in gravitational wave signals, due to their mutual interaction in a binary coalescence being deep in the mutual gravitational well. Numerical simulation with such simple models will be useful to clarify the sensitivity of gravitational wave observation to such highly compact departures from classical black holes.

Contents

Curriculum Vitae **vii**

Abstract **viii**

1 Introduction **1**
1.1 General Relativity 5
1.2 Entropy 10
1.2.1 Entanglement entropy in black holes 18
1.3 Holography 24
1.3.1 Gauge/gravity duality 26
1.3.2 AdS/CFT correspondence 28
1.3.3 Anti-de Sitter spacetime 31
1.4 Permissions and Attributions 35

2 Reconstruction of an AdS Radiation/Boson Star Bulk Geometry Using Light-cone Cuts **36**
2.1 Introduction 36
2.2 Light-cone Cuts 39
2.2.1 Review of the formalism 39
2.2.2 Cusp angle 41
2.3 AdS Radiation/Boson Star 42
2.3.1 Model 43
2.3.2 Geodesics 48
2.3.3 Recovering the metric 49
2.4 Discussion 53

3 Boundary Causality Violating Metrics in Holography **57**
3.1 Introduction 57
3.2 Specific examples 60
3.3 Operator dictionaries 63
3.4 Resolution 67

3.5 Discussion 73

4 Exploring strong-field deviations from general relativity via gravitational waves 76
4.1 Introduction 76
4.2 CQO models and observational challenges 81
4.3 Effective approach 85
4.4 Some simplified models for compact quantum objects 89
4.4.1 Generalities 89
4.4.2 Matched polytropes 96
4.5 Gravitational wave tests of compact quantum structure 100
4.5.1 Effective parameters 101
4.5.2 Love numbers 103
4.5.3 Evolution: effective models and expectations 106
Inspiral 106
Plunge and Merger 109
4.5.4 Quantum dynamics and expectations 110

A Uncertainty in k_2 calculations 113

Bibliography 115

Chapter 1

Introduction

> We live on an island surrounded by a sea of ignorance. As our island of knowledge grows, so does the shore of our ignorance.
>
> John Archibald Wheeler

Perhaps there is nothing in nature as fundamental and conspicuous as the four dimensions in which everything occurs: space and time. For Newton to build his Laws of Mechanics, it was important to have the notion of an absolute time that is in constant flow and exists independently of any observer. This universal time affected every observer at the same rate, and whenever two events were simultaneous for one observer, they were simultaneous for all observers. In concert, Newton introduced the notion of absolute space as the immutable stage on which all events of nature would take place. In this rigid space, motion was then the result of objects evolving their position according to the universal time.

This rigid and constant conception of space and time remained in the mainstream for more than 200 years until Albert Einstein came in 1905 and shook the universe with his ideas. Inspired by the robustly established equations of electrodynamics, he realized

that the rigidity of space and time as conceived by Newton was not compatible with the universality of Maxwell's equations for all inertial frames. In particular, the validity of these equations for all inertial observers implied the existence of a distinctive speed—the speed of light—whose value was constant independently of the frame in which it was measured. To preserve this property in electromagnetism, he argued, space and time needed to be observer-dependent and two sides of a unified entity: spacetime. Under this new theory, known as Special Relativity (SR), all clocks would no longer tick at the same rate; all rulers would no longer measure the same length; the notion of simultaneity would no longer be absolute. They all became observer-dependent. And similar to Newtonian mechanics, this is done without preferring any of the inertial observers over the other ones.

Einstein then took it one step further. He unified his ideas of relativistic spacetime with gravity. In this new theory, called General Relativity (GR), spacetime became malleable and dynamical. The gravitational force turned into the effect of the spacetime geometry on the motion of objects. As John A. Wheeler put it: "spacetime tells matter how to move; matter tells spacetime how to curve." GR then, under this paradigm shift, opened a new avenue for exploring the nature of spacetime. And even though the energy scales that put GR to its limits are not yet accessible in the experiments performed here on Earth, they are relevant for understanding the more profound aspects of the fabric of the universe.

The merging of space with time in SR, and then of spacetime with gravity in GR, follows from a principle of unification in physics. Indeed, every time two or more ideas previously thought to be incompatible with each other are united, progress is made in theoretical physics. This principle of unification has allowed for different theories to become compatible with each other, and by doing so, revealed new corners in the understanding of natural phenomena that were previously inaccessible by each independent

theory. Electricity and magnetism, for example, were unified in Maxwell's equations which then revealed that light was made of electromagnetic radiation. Classical field theories were then combined with SR and quantum mechanics (QM) to reveal the framework of quantum field theory (QFT). Once we arrived at QFT, we understood how particles are not point-like entities but rather excitations of the fundamental fields themselves, thus explaining how particles can come into existence or annihilate each other.

Even though GR puts forth a profound and elegant description of spacetime, it cannot be complete to the extent that it has left QM out of the equation. Undoubtedly, if we are to make progress toward a deeper formulation of spacetime, this will come from the exploration of the intersection of GR and QM, known as quantum gravity (QG). Given that GR is a classical field theory, one could ask: why not just quantize it like the other classical theories? The answer is that the standard perturbative quantization of GR gives a theory that is non-renormalizable [1, 2]. That is, after including all the appropriate counter-terms to make the perturbation series non-divergent, one is left with infinitely many parameters that need to be fixed by experiments to have any meaningful predictive power. Nonetheless, after long mathematical excursions, progress has started to take shape in the form of the holographic principle [3, 4]. This, in its most general form, states that a theory of QG has a dual description through a lower-dimensional quantum theory. The Anti-de Sitter/Conformal Field Theory (AdS/CFT) correspondence, discussed in this thesis, has proven to be the leading concrete realization of this principle [5]. Even though this duality is specific for geometries with a certain type of boundary condition, recent investigations (see, e.g., [6]) have argued that the insights learned from this framework can—and must—be exported into more general spacetimes. We thus take the attitude that by understanding this duality one can extract general results about how quantum phenomena are involved in the description of spacetime.

In this thesis, we explore some of the connections between quantum mechanics and

the emergence of spacetime and its geometry. First, we review the history of spacetime as it was first introduced by Einstein in his theory of GR. We then discuss the basics of this theory and the different tests and checks that the theory has passed throughout more than a century. In doing this, we also discuss some of the important limitations of the theory, as well as how they point us in the directions where new physics can be explored. Next, we review some of the ideas behind the entropy and thermodynamics of black holes. In this discussion, we make some important connections between classical information, causal horizons, and quantum entanglement. In particular, we will find an important connection between the entropy of an event horizon and the entanglement structure of a vacuum state. Then, this connection is used to motivate the introduction of the holographic principle. We next discuss this principle, first as a general property of QG, and then we will focus on the concrete framework of AdS/CFT.

In Chapter 2, we explicitly use an entry in the AdS/CFT holographic dictionary to recover the conformal metric of a bulk spacetime. We explain how the framework of light-cone cuts allows us to reconstruct the geometry inside of the bulk by using only boundary information. We also explore how some geometrical information—and the matter content from which it is determined—gets encoded in the structure of the light-cone cuts. Additionally, this method is illustrated in a concrete numerical example in which the geometry of a four-dimensional spacetime made from the superposition of a boson star and a gas of radiation in AdS is recovered. In Chapter 3, a causality puzzle in the holographic duality will lead us into thinking about how to properly include boundary causality violating metrics in a full gravitational path integral. After a careful analysis of this apparent contradiction, we provide a prescription for the bulk path integral in which this puzzle is resolved. We then explain how this resolution demands for the bulk dual of the boundary commutator to *not* be the limit of the naive bulk commutator. Finally, in Chapter 4 we explore how some of the quantum features of spacetime discussed in

this thesis require a modification of the predictions from classical GR in the strong regime. In particular, we argue for the necessity of new phenomena to make black hole evolution consistent with quantum mechanics. We also explain how these novel effects could in principle be observed in the gravitational waves signals that LIGO detects from the merger of black holes. We describe possible features of "compact quantum objects" that replace classical black holes in a consistent quantum theory, and approaches to observational tests for these. Simple models for compact modifications to classical black holes are described via an effective stress tensor, possibly with an effective equation of state. A general discussion is given of possible observational signatures, and of their dependence on properties of the colliding objects. Numerical simulation with such simple models will be useful to clarify the sensitivity of gravitational wave observation to such highly compact departures from classical black holes.

1.1 General Relativity

Similar to Newtonian physics—and based on our experience with nature—GR declares spacetime to be a continuum. Additionally, spacetime is required to look flat in the vicinity of any point. This condition is chosen to reflect Einstein's equivalence principle—namely, that local experiments in a freely falling laboratory are indistinguishable from those done in an inertial frame in flat space. The mathematical object that realizes these features is that of a manifold. The spacetime, represented by this manifold, is then allowed to warp in the presence of energy and stresses. The warped spacetime geometry is encoded by a metric field $g_{\mu\nu}$ that satisfies Einstein's field equations.

In this spacetime, the motion of particles is now universal. That is, massive objects in free-fall follow the same trajectory regardless of their mass. These trajectories are given by the geodesics of each particular geometry. Indeed, in the presence of different energy

sources, spacetime can take on a different geometry with a different geodesic structure. This proposal of a malleable spacetime was—albeit elegant—a radical departure from the known physics at the time. Therefore, for GR to become accepted by the physics community it needed to recreate known results as well as propose and confirm novel predictions.

The first success for the theory came in 1915 with Einstein's calculation of Mercury's orbit from which he found the correct answer for its perihelion precession. In this calculation, GR correctly added the 43"/century missing from the Newtonian prediction. This initial result used an approximation that was soon after corroborated with the appearance of the Schwarzschild metric. This spacetime provided an exact solution to Einstein's equations describing the geometry of a static and spherically symmetric source.

The next and perhaps more important check arrived four years later. Similar to how massive particles move according to the warped spacetime, massless particles also move along geodesics of the spacetime geometry. This implied that light rays traveling near a massive object (like our Sun) would get deflected by a specific angle computed by the theory. In May of 1919, Arthur Eddington and his collaborators took pictures of a particular group of stars before and during a solar eclipse. Their measurements accurately agreed with the GR prediction, thus providing at the time universal support for the new ideas introduced by Einstein regarding the nature of spacetime.

In the following years, additional tests were performed and one after the next one all corroborated the predictions made by GR. In 1959, Robert Pound and Glen Rebka Jr. measured the gravitational redshift of gamma rays emitted by a solid sample of iron-57 as they traveled 23 meters down from the top of a tower at Harvard University's Jefferson laboratory. More accurate tests of the same effect were observed in the spectral lines of the star Sirius B by the Hubble Space Telescope. Also, in 1966, the Shapiro time delay was observed by sending radar signals back and forth from Earth to Venus through the

gravitational well near the surface of the Sun. Today, these well-tested effects of GR are routinely used by the Global Positioning System (GPS) which employs a network of satellites in orbit to localize positions on the surface of planet Earth. Without taking into account the relativistic effects predicted by GR, the accuracy of GPS receivers would fail at a rate of about 10 km per day [7].

These effects—surprising as they are—do not push GR to its limits. To put some of the deepest ideas of GR to the test, one has to explore the strong field regime. Notably, many of these strong field effects have also been extremely well tested. In 1974, Russell Alan Hulse and Joseph Hooton Taylor Jr. started measuring the dynamics of a binary pulsar system composed of a pulsar and a neutron star [8]. These very compact objects orbit around their common center of mass, and by doing so, they lose energy through the radiation of gravitational waves. The existence of gravitational waves had been predicted by Einstein since 1916. Subsequent measurements of the orbital period for the pulsar showed that the system was losing energy at a rate predicted by GR. This observation hence provided the first indirect evidence for the existence of gravitational waves.

In 2016, a century after they were predicted, gravitational waves were finally detected directly by the Advanced Laser Interferometer Gravitational-Wave Observatory (aLIGO) [9]. This observatory uses Earth-based laser interferometry together with advanced noise reduction techniques to detect the fluctuations in space as a gravitational wave passes through its 4 km long arms. To successfully detect a gravitational wave, aLIGO needed to reach an accuracy of 10^{-19} meters, or roughly $1/10,000$th of the width of a proton. With its current specifications, aLIGO is designed to detect waves in the range from 10 Hz to 10kHz [10]. This range includes rotating neutron stars as well as the coalescence of compact binaries, and in particular of stellar black holes, i.e., those produced by the gravitational collapse of a star. Once a gravitational wave is detected—and after a very robust noise analysis—the signal is compared to different templates that have been

numerically simulated using solutions to Einstein's equations. The success that aLIGO has had matching their measurements with theoretical predictions of GR further supports the validity of the theory even in the strong field regime.

The current specifications of aLIGO, however, constrain the type of sources of gravitational waves that can detected. To expand this range, both the noise reduction and the arms length need to be improved. The Laser Interferometer Space Antenna (LISA) is a proposed gravitational wave detector that improves on these crucial points [11]. By orbiting in outer space, LISA will be able to have arms with a massive length of roughly 2.5 million km each, as well as eliminate noise from seismic sources. With a much longer wavelength, LISA will be able to access a lower frequency range which will make it ideal for the detection of gravitational waves from potential sources that include ultracompact binaries, supermassive black hole mergers, extreme mass-ratio inspirals, and possibly signals emitted in the early universe [12]. The last type is of particular interest because it could expand our understanding of how quantum fluctuations played a role in the moments after the Big Bang.

Most recently, the first direct observation of the region near a black hole horizon was obtained by the Event Horizon Telescope (EHT). This collaboration brings together an array of many radio telescopes located all around the globe. By combining the data from each telescope, this network effectively achieves a resolution sufficient to observe the region around a supermassive black hole at the scale of its event horizon. The two black holes that can be studied with the EHT are Sagittarius A*, located at the center of the Milky Way, and M87*, located at the center of the galaxy Messier 87. In the first image of M87*, published in 2019 [13], a dark shadow is shown at the center of a light ring. This qualitative image is predicted by GR. The shadow appears as a consequence of the black hole being illuminated from behind. On the other hand, the light ring could be composed of light emitted by matter that is orbiting near the horizon, or by light

coming from the photon ring due to the lensing effect of the black hole. Even though this first image might not have the resolution needed to clearly disambiguate the source of the observed light (cf. [14]), it certainly represents a step forward in the exploration of black hole physics. In March 2021, the EHT released a new image of M87*, this time in polarized light [15].

In all cases where it has been tested, spacetime behaves as instructed by GR: as a four-dimensional continuum that gets warped according to Einstein's equations. Indeed, more than one hundred years with many successful tests have strengthened GR as the leading theory for describing spacetime and gravity. Nonetheless, the theory is not flawless. For instance, even though the theory predicts the expansion of the universe, GR alone cannot explain what happened before or even in the very early moments after the Big Bang. During this hot and dense period of the universe, quantum mechanical effects were dominant. Therefore, to fully describe the physics of the Big Bang, a better understanding of how quantum effects interact with spacetime at extremely large energy scales is needed. All that GR has to offer in this limit is a mathematical singularity from which one cannot continue to evolve in order to learn about the state of the universe before the Big Bang.

Deep inside of black holes another problem is found. This is because at the center of each black hole one also finds a singularity, i.e., a region of spacetime with diverging curvature. Therefore, the evolution of any particle after it reaches the singularity inside of a black hole is impossible to predict using GR. One conceivable answer to this problem is that the continuous assumption for spacetime from GR is only a good approximation up to certain scales, but not all. It is possible that the continuum of spacetime is not elementary but rather an emergent property. The continuous property of water in fluid mechanics, for example, is emergent from the interaction of many individual molecules. While the collection of many water molecules behaves as a fluid, once we reach the

smallest of scales, it makes no sense to insist in describing the physics of the individual molecules using the laws of fluid mechanics. A different description is needed.

As we will see, the limitations of GR are not secluded to small scales. In fact, even at the scale of an event horizon (which for a supermassive black hole can be of order 10^9 km!) we will find issues as we try to reconcile the properties of GR with the tenets of QM [16]. The precise checks and tests that GR has passed throughout the time serve to reinforce the theory in those regimes where it makes accurate predictions; however, they also point at the shortfalls of the theory as important areas of research. Indeed, when a theory that agrees with many measurements fails to describe what happens in a particular configuration, that's a place where new physics is to be found!

1.2 Entropy

> Black hole thermodynamics is crazy, perhaps crazy enough to work.
>
> John Archibald Wheeler

The first indication that entropy was central for making progress in understanding the quantum nature of spacetime originated from the study of black holes. As originally conceived in statistical mechanics, entropy (S) is a measure that quantifies the uncertainty of a system. It counts the number of possible microscopic configurations of the system (known as microstates) that are compatible with the observable macroscopic properties such as temperature, volume, and pressure. The greater the entropy of a system, the more microstates it can in principle occupy. This, in turn, dilutes our detailed knowledge of the system. By having more available microstates that are macroscopically indistinguishable, we lose track of which particular microstate the system is occupying at any given time. We thus say that entropy quantifies our ignorance of the system.

Black holes in GR are fully described by very few parameters. The most general solution describing a stationary, rotating, and electrically charged black hole in four dimensions is characterized by its mass M, charge Q, and angular momentum J. This is known as the Kerr-Newman black hole [17, 18]. When the charge and angular momentum are zero, we recover the Schwarzschild black hole as a special case. That this is the most general solution for black holes in equilibrium was first suggested by John A. Wheeler [19]. He famously referred to this idea with the phrase "black holes have no hair" [20]. This conjecture was later supported by evidence from several uniqueness theorems [21, 22, 23]. Within GR, this result thus poses that it is impossible to distinguish between two black holes with the same parameters M, Q, and J, even if they were formed via two completely different collapse processes. Therefore, the number of classical configurations for a black hole that are compatible with its exterior observables is one. We say that our uncertainty about the internal details of the system is minimal and thus the entropy is zero. According to GR, black holes cannot have any non-zero entropy.

This, however, leads to an apparent problem regarding the thermodynamics of our universe. One could, for instance, consider the following thought experiment. Imagine taking a box that contains a certain amount of entropy and throwing it into the interior of a black hole. Since nothing can escape a black hole, the entropy of the box would then no longer be accessible to any outside observer. The thermal entropy of the universe outside the hole would decrease. At the same time, we know that the entropy of the hole cannot increase to account for this loss. Every detail of the infalling object is washed out into a final configuration that is uniquely determined by M, Q, and J. These simple parameters are not enough to account for the—in principle very complicated—information that was thrown inside. For an outside observer, entropy would have had decreased and the second law of thermodynamics would have been violated. This would not only create issues whenever boxes with entropy are thrown into black holes, but it would also render

the second law meaningless for outside observers in general.

Jacob Bekenstein, a Mexican-born physicist, worried about this disagreement with one of the tenets of thermodynamics: in a closed system, entropy must increase irreversibly. The solution, he argued, was to assign entropy to a different property of the black hole to compensate for the loss of entropy on the outside [24]. Bekenstein realized that when an object gets thrown into a black hole, while the mass of the object is lost inside, the area of the horizon increases irreversibly. Indeed, Stephen Hawking had proved that the surface area of a black hole cannot decrease in any kind of process within GR [25]. This is akin to the irreversible increase of entropy. Motivated by this connection, Bekenstein resolved that black holes should have entropy encoded by their horizon area. This entropy, he explained, was not meant to be a form of thermal entropy, but rather a measure of how much information is inaccessible from the outside. Namely, the kind of entropy used in statistical mechanics and information theory.

To get a quantity with units of entropy, the explicit formula included Boltzmann's constant k_B. Additionally, and to cancel the units of area, the horizon area was divided by Planck length squared ℓ_P^2. The inclusion of the latter was suggested to Bekenstein by Wheeler who insisted on the role that ℓ_P should play in an ultimate theory of quantum gravity [1]. Bekenstein thus arrived at the following equation [26]:

$$S_{BH} = \eta k_B \frac{A}{\ell_P^2} \tag{1.1}$$

where η represented a constant of proportionality still unknown to him. Through some thought experiments, however, he argued that η should be of order one. Therefore, since ℓ_P is very small, this formula assigns an enormous amount of entropy to a black hole,

[1] As Bekenstein said in his paper [26]: "...must have units of (length)$^{-2}$. But there is no constant with such units in classical general relativity. If in desperation we appeal to quantum physics we find only one truly universal constant with the correct units: h^{-1}, that is, the reciprocal of the Planck length squared"

which in turn reflects how irreversible the formation of a black hole is. In this form, this formula provided an enigmatic connection between gravity, thermodynamics, and the quantum.

Armed with this formula, Bekenstein turned to solve the original problem of entropy loss inside of black holes. He proposed a modification to the second law of thermodynamics. Rather than just the thermal entropy, he proposed that it is in fact the sum of the black hole entropy S_{BH} (given by its horizon area) and the regular thermal entropy outside the black hole S_{out} that together cannot decrease. With this new prescription, the entropy observed by an external observer would no longer decrease when the box with entropy gets thrown into a black hole. This is because even though the entropy of the outside seems to be going down, the sum of the black hole entropy and the exterior entropy both together go up. The area increases enough to compensate for the loss of entropy falling into the hole. This quantity is known as the generalized entropy:

$$S_{gen} = S_{BH} + S_{out}; \tag{1.2}$$

and the generalized second law then demands that under any process this entropy cannot decrease [26]:

$$dS_{gen} \geq 0. \tag{1.3}$$

The generalized entropy is thought-provoking because it combines two types of entropy that are—on a first look—different in nature. S_{BH} is geometric and measures information loss, while S_{out} deals with ordinary thermal matter and heat fluxes. Additionally, the area theorem was proved exactly using mathematical theorems, whereas the second law for thermal systems is meant to hold only to a very good approximation.

At the heart of (1.3) lies another puzzle. The increase in area of the black hole in GR

is determined by the energy of the object that falls to its interior. This energy is given by the mass of the object together with the velocity and the trajectory that the object is following. All of this data is independent of the type and amount of entropy encoded in the object. How then can the horizon area know how much entropy or information is stored in the object? And how does it always increase enough to compensate for the entropy that goes inside? To answer these questions, physicists needed to go beyond the classical theory; and by doing so, they were able to accelerate our understanding of how classical geometry is related to classical information and, eventually, to quantum information.

The connection between black holes and thermodynamics was made sharper with the introduction of the four laws of black hole mechanics [27]. In this paper, general formulas were derived for the physics of stationary axisymmetric black holes. The four laws of black hole mechanics are:

- **Zeroth Law**: The surface gravity κ of a stationary black hole is constant over the event horizon.
- **First Law**:
$$dM = \frac{\kappa}{8\pi G} dA + \Omega dJ + \Phi dQ. \tag{1.4}$$
- **Second Law**: The area A of the event horizon does not decrease with time.
- **Third Law**: It is impossible to reduce κ to zero by a finite sequence of operations.

These equations made explicit how the area of the horizon takes on the role of the entropy of the black hole. Similarly, in these equations κ behaves as the temperature of the hole. The event horizon of the black hole is said to be a Killing horizon if there exists a Killing field, χ^a, that is normal to the black hole horizon. This is always the case for

stationary black holes. The surface gravity κ is then defined as

$$\kappa^2 = -\frac{1}{2}(\nabla^a \chi^b)(\nabla_a \chi_b). \tag{1.5}$$

Physically, κ corresponds to the force per unit mass that an observer at infinity must apply in order to hold a particle at a fixed radius just outside the event horizon. Notice that by definition κ is an intensive quantity locally defined at the horizon. In a non-spherically symmetric horizon, e.g., in a rotating black hole, there is no a priori guarantee that κ will be constant everywhere on the horizon. Nonetheless, the Zeroth Law shows that κ takes on a constant value at the horizon of a stationary black hole (i.e., a black hole at equilibrium), thus making it a closer analog to the temperature of a thermal body at equilibrium.

The presence of κ in the First Law was obtained through mathematical manipulation of the equations describing the Kerr geometry. However, that κ belongs on the First Law can be argued physically as follows [28]. For a thermal system, an influx of heat dQ causes a change in entropy dS given by

$$dQ = TdS. \tag{1.6}$$

From an information theory perspective, the change in entropy measures a change in the amount of information contained inside the horizon. In particular, the simplest amount of information that could be added to the black hole would be a generic particle with 2 possible spin states. Since the number of black hole microstates is counted by e^{S_{BH}/k_B}, the minimum change of entropy after throwing in the particle is then $dS_{min} = k_B \ln 2$. Given the existence of this minimal change in entropy, there must be a corresponding minimal amount of heat $dQ_{min} = TdS_{min}$ that could be added to the black hole. One option

would be a particle with a tiny mass. However, the Compton wavelength for a particle with a small mass would eventually be larger than the black hole itself. Alternatively, one could slowly lower a particle very near the horizon so that its Killing energy is almost zero. The energy of the particle is given by the product of its mass m and the norm of the Killing vector at that location. At the horizon, the norm vanishes. Near the horizon, the norm is proportional to the surface gravity κ and grows linearly as the proper distance from the horizon to the center of mass of the object [29]. The minimal value for this distance is naturally characterized by the size ℓ of the object. The Killing energy of the particle is then proportional to the product $m\ell\kappa$. Since κ is determined by the black hole, one could imagine making this energy arbitrarily small by considering the limit $\ell \to 0$. However, taking into account QM, the product $m\ell$ is bounded from below by the uncertainty principle. The minimum amount of energy is then given by $dQ_{min} \sim \hbar\kappa$; and the corresponding temperature is given by

$$T = \frac{dQ_{min}}{dS_{min}} \sim \frac{\hbar\kappa}{k_B \ln 2}. \tag{1.7}$$

This indeed highlights the role of κ in the First Law as the temperature.

The similarities found between the four laws of black hole mechanics and the four laws of thermodynamics were remarkable. However, it was made clear at the time that these equations were supposed to be taken just as an analog rather than direct evidence claiming that black holes were thermal objects. If black holes had a real temperature they would have to radiate. This, in turn, would require particles to come out from inside the black hole, which is strictly forbidden by general relativity. Furthermore, taking (1.7) as a real temperature creates a thermodynamical issue. If a black hole is immersed in a thermal bath with lower temperature, the black hole will absorb more radiation and thus more entropy than it can compensate for by increasing its area. This would then violate

the generalized second law if the black hole couldn't radiate in thermal entropy. This was an early suggestion that quantum radiation at this temperature was needed in the black hole. Additionally, the inclusion of Planck's constant in both the formula for the entropy and the temperature suggested the possibility of some quantum process allowing for this radiation.

The breakthrough came two years later when Stephen Hawking published his seminal work on the black hole radiation. In [30], Hawking robustly showed how in the presence of quantum fields a black hole would necessarily radiate particles with a thermal temperature given by $T_{BH} = \hbar\kappa/2\pi k_B$. This turned out to be the precise temperature needed to preserve the generalized second law. At the same time, the formula for the black hole entropy was determined to be $S_{BH} = A/4\ell_P^2$. This radiation occurs because the vacuum state around the black hole is unstable to form fluctuations outside the horizon that are correlated with fluctuations on the inside. Physically, this is described as particle pair creation just outside the horizon with one partner with positive energy escaping to infinity and thus carrying energy away from the black hole, while the other partner with negative energy falls to the interior. As Hawking argued, this process will continue until the black hole evaporates after having radiated all of its mass.

This evaporation of black holes created a troubling puzzle. The process would seem to allow for information to be destroyed inside of black holes. This is because when an object—and all of the information that it carries—is thrown inside of a black hole, it can no longer escape outside the horizon. Meanwhile, the black hole radiates until it fully evaporates. The radiation, being thermal, doesn't bring out any information from the interior. The problem arises once the black hole is gone because at that time all of the information that was stored in its interior is effectively removed from the universe. This is troubling because conservation of information is a fundamental principle of physics as we know it. In particular, consistency with QM demands unitary evolution. Indeed, if

there exists a region in the universe where unitarity is being violated even a little bit, then the whole theory would be inconsistent and would have no predictive power [31]. This was referred to as the black hole information paradox. Upon its inception it was not obvious how this problem could be resolved. However, it quickly became clear that given its crucial location at the intersection of GR and QM, this was going to become a resourceful place where the connection between spacetime and quantum phenomena could be explored.

1.2.1 Entanglement entropy in black holes

Progress was first made by understanding the origin of the entropy S_{BH} assigned to black holes. Since the classical theory didn't offer enough degrees of freedom to account for this vast entropy, a quantum origin was expected. The problem was that the Hilbert space associated to a black hole was not yet known, and thus a direct count of microstates was unavailable. The key insight needed here is that the horizon of a black hole is not a special region of spacetime. It is, in fact, a smooth region with potentially small curvature depending on the size of the black hole. Furthermore, the equivalence principle demands that the experience of an infalling observer as they cross the horizon is locally indistinguishable from that of an inertial observer in flat space. One then could ask what the connection is between this seemingly ordinary region of spacetime and the entropy associated to the radiation of the black hole.

One year after Hawking radiation was introduced, William Unruh found a similar effect in flat space [32]. Unruh was interested in understanding how a particle detector would interact with the radiation outside of a black hole. Stationary detectors at a fixed radius outside the horizon in the Schwarzschild metric follow trajectories that are analogous to those of uniformly accelerated detectors in Minkowski space. In light of the

equivalence principle, one would then expect that the physics each one of these detectors experience is locally indistinguishable from one to the other. Indeed, Unruh found that accelerated particle detectors will detect particles in the vacuum even in flat spacetime. A detector that uniformly accelerates with proper acceleration a finds itself immerse in a thermal bath of temperature $T = \hbar a/2\pi k_B$. This is known as the Unruh effect[2] and is derived using properties of QFT on a fixed spacetime background [1]. The particle detector actually reacts to the field states that have positive frequency with respect to its own proper time and not to some universal time from which the vacuum state is defined. This might sound inconsistent with the perspective of an inertial Minkowski observer for which the state of the fields is the actual vacuum state. But in fact, when the accelerating detector gets excited by absorbing a field quanta, a generic Minkowski observer regards that process as the emission of a field quanta by the detector [32]. Furthermore, the energy needed for this emission, according to the inertial observer, is provided by the field that is accelerating the detector in the first place. In QFT, therefore, the notion of what a particle is depends on the state of motion of the observer. From this result, it seems as if this observer-dependence for the state of the fields would prevent from a unique definition of a ground state. However, in Minkowski spacetime it is possible to demand for the only physically reasonable detectors to be those following geodesics. By doing this, they can all agree to define the vacuum as the state of the fields for which none of them detect any particles.

To further see how the Unruh effect is related to the entropy of a black hole, it is instructive to analyze the entropy associated to an acceleration horizon. Consider the Minkowski spacetime written in hyperbolic coordinates (also known as Rindler coordi-

[2]This, incidentally, is a fitting name since Unruh means restless in German, and this radiation is observed by a restless detector.

nates):

$$ds^2 = -\xi^2 d\eta^2 + d\xi^2 + dy^2 + dz^2 \tag{1.8}$$

where the range $\eta \in (-\infty, +\infty)$ and $\xi \in (0, +\infty)$ covers only the right wedge $x > |t|$ of the full flat spacetime, known as the Rindler wedge (see Fig. 1.1). These coordinates make explicit the existence of the timelike Killing vector ∂_η. Under the symmetry generated by ∂_η, known as a Lorentzian boost, the right Rindler wedge gets map onto itself. This region corresponds to the only part of flat spacetime that is accessible to the Rindler observers, i.e., uniformly accelerated observers. And the boundary of this region is known as the acceleration horizon. Accelerated observers in these coordinates are described by $\xi = constant$, and their proper time is proportional to η. Thus, the ∂_η Killing vector provides a natural definition of positive and negative frequency modes for these accelerated observers. However, it is important to remark that this notion of positive and negative modes is not the same as the one associated to the usual t-translation symmetry in Minkowski time used to define the vacuum state for inertial observers (see Fig. 1.2).

To understand how this acceleration horizon creates a thermal radiation one needs to consider the vacuum state in Minkowski space. As mentioned before, this state is defined as the zero-energy eigenstate with respect to the Hamiltonian that generates t-translations in Minkowski coordinates. Rindler observers, however, only have access to the state restricted to the right Rindler wedge. The density matrix that describes the quantum state on the right wedge is then obtained by tracing out all the degrees of freedom from the left wedge, $\rho_R = Tr_L|0\rangle\langle 0|$. The result is a mixed density matrix that takes on the form of a thermal state in equilibrium with respect to the Hamiltonian that generates the boosts on the Rindler wedge, $\rho_R \propto \exp\left(-\frac{2\pi}{\hbar} H_\eta\right)$. Notice that this thermal state has an associated temperature given by $T = \hbar/2\pi$. The local temperature measured by one of the Rindler observers is found using the observer's internal clocks,

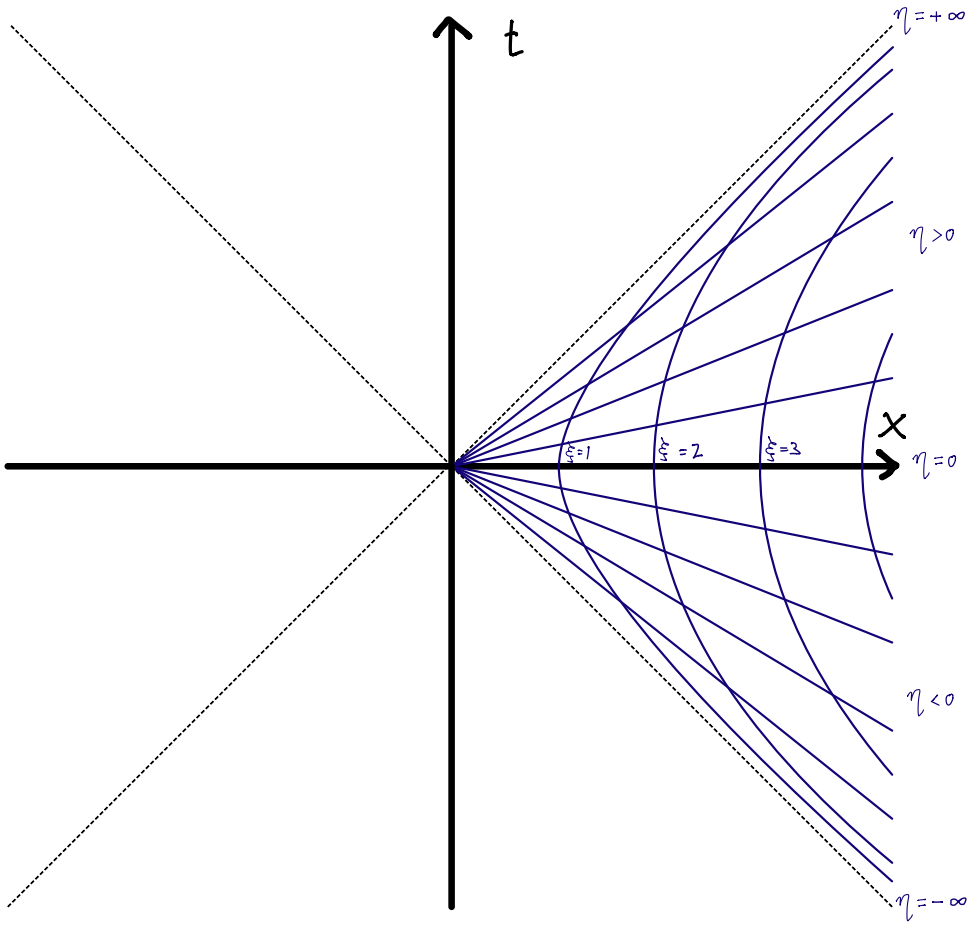


Figure 1.1: Minkowski space in Rindler coordinates η, ξ. Notice that the range $\eta \in (-\infty, +\infty)$ and $\xi \in (0, +\infty)$ covers only the right wedge $x > |t|$ of the space-time. This is known as the right Rindler wedge.

and is thus given by $T_{local} = a\hbar/2\pi = \hbar/2\pi l$, where a is the acceleration of the observer and l is the proper distance of the observer from the origin. For these Rindler observers, the acceleration horizon has a physical temperature that diverges as they get closer to it. If the origin of this temperature is approximated by a thermal gas, i.e., with an entropy density that scales as $s \sim T^3_{local}$, then an estimate of the entropy associated to the acceleration horizon is obtained as follows:

$$S \approx \int dV s = \int dA dl T^3_{local} \approx \frac{A}{\epsilon^2} \tag{1.9}$$

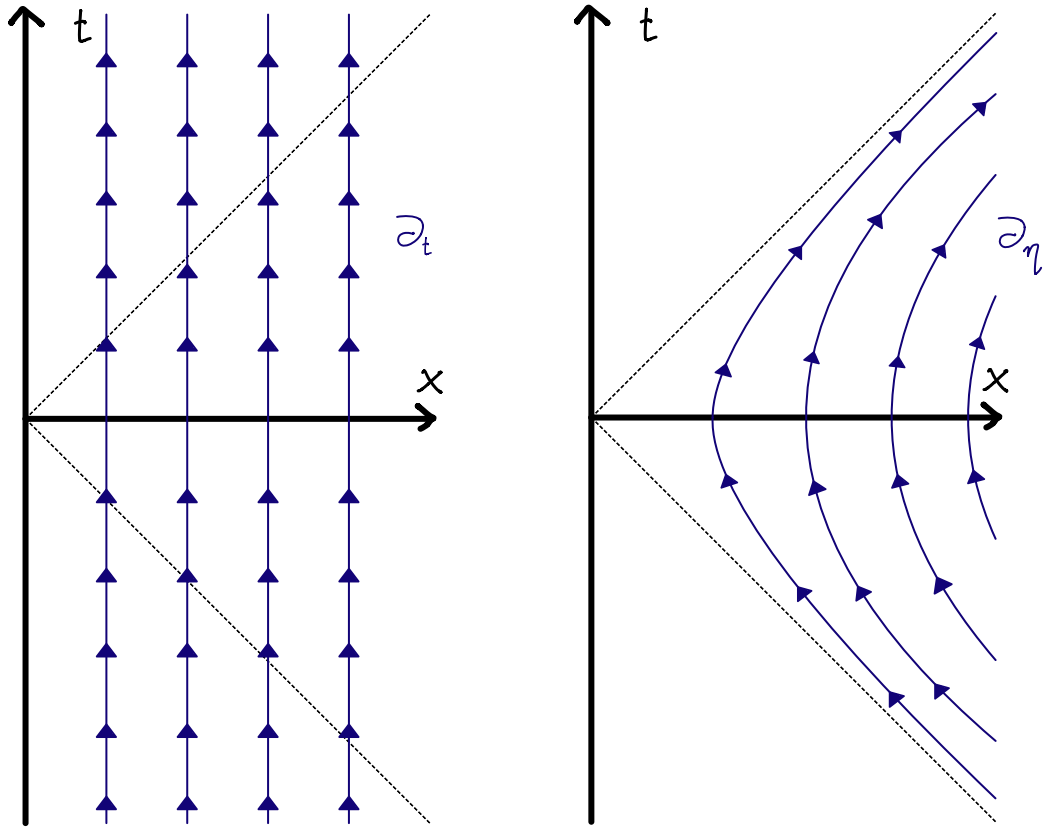


Figure 1.2: Left: symmetry generated by the usual t-translation in global Minkowski time. Right: symmetry generated by η-translations. Notice that under this "boost" transformation, the right Rindler wedge is mapped onto itself.

where ϵ is a short distance cutoff from the horizon. Notice that the entropy is proportional to the area of the horizon divided by the square of the natural cutoff of the system.

The result of (1.9) represents a coarse-grained type of entropy associated to the system, and as such, should be seen as an approximation to the real value. To obtained the more precise fine-grained entropy, i.e., a measurement that includes the detailed microscopic description of the system, we must look at the quantum entanglement structure of the vacuum state. In QFT, the entropy for the density matrix ρ_R is quantified by the

von Neumann entropy, a fine-grained entropy given by

$$S_{VN}(\rho_R) = -Tr(\rho_R \ln \rho_R). \tag{1.10}$$

This quantity measures the entanglement entropy between the degrees of freedom inside the right Rindler wedge and those outside. The fact that ρ_R is a mixed state reveals the presence of quantum correlations between the state of the fields inside and outside the Rindler wedge. Even though the Minkowski vacuum is a pure state, once the spacetime is partitioned by the acceleration horizon, the state of the fields for the Rindler observers will be incomplete, i.e., information will be missing from their perspective. Consequently, they assign a large entropy to their state and describe it as being thermal.

A similar result to (1.9) was found by Sorkin [33, 34], except that this time it was in terms of the von Neumann entropy. By using a 3-dimensional lattice of coupled harmonic oscillators as a toy model, Sorkin was able to show that the entanglement entropy for a mixed density matrix associated to a subregion of space is proportional to the area of the boundary of that region. Additionally, the entropy was found to be inversely proportional to the squared of the cutoff lattice length. Some years later, Ted Jacobson used this idea to argue that if one takes seriously the relation $S \sim A$, together with $dS = dQ/T$ where T is the Unruh temperature of vacuum, then one can show that the presence of entanglement entropy necessarily generates gravity [35]. He first argued that if a flux of energy flowing through an acceleration horizon changes its entropy, then it also must change its area. The acceleration horizon, however, is defined by the trajectory of null geodesics. Therefore, if the area of the horizon changes, this implies that there must be focusing of the null geodesics. This, in turn, reveals the existence of spacetime curvature. And this is precisely what GR taught us—in the presence of energy fluxes the geometry of spacetime changes. Indeed, by carefully using the equations for geodesic deviation,

Jacobson was able to derive Einstein's equations from this analysis. Additionally, he found that if $S = \alpha A$, then $G_N \sim 1/\alpha$. In other words, it is crucial for the entanglement entropy to be finite in order to have gravity. And conversely, as we discuss in the next section, the existence of gravity provides a cutoff for infinite entanglement entropy.

These results present entanglement entropy as one strong candidate for the entropy of the horizon of a black hole. Similar to the partition of Minkowski spacetime by the acceleration horizon, in the black hole spacetime the geometrical causal structure provides a natural partition of the degrees of freedom in the quantum state. The Unruh effect associated to this horizon is then the origin of Hawking radiation. The difference with the Minkowski case is that in a non-flat spacetime, like in the Schwarzschild geometry, it is possible to have two valid geodesic detectors such that for one the state of the fields looks like vacuum whereas for the other it looks as a many-particle state. Indeed, this feature of black holes will be part of the motivation in chapter 4. In particular, we will argue that modifications to our classical description of spacetime are needed even at large scales of order the horizon size. In the next section, we discuss how the lessons learned from the study of black hole entropy are important in developing the holographic principle—which itself is central to our current understanding of QG.

1.3 Holography

One of the most profound lessons that came from the study of black hole entropy is the holographic principle. In its most general form, it states that—in a theory that contains gravity—the description of a region of space and all the matter inside is fully encoded on its lower-dimensional boundary. This was first advanced by Gerard 't Hooft using general properties of black holes [3]. He started his argument by noticing that the maximum possible entropy that can be stored in a spherical region (with surface area A)

is given by the entropy of the black hole with that same size. Indeed, if it was possible to have more entropy without having a black hole, it would necessarily have to be in the form of some matter with lower energy than the mass of the black hole. One could then add into that region the remaining energy needed to create the black hole. Since the resulting black hole has less entropy by assumption, this process would violate the second law of thermodynamics. Therefore, this contradiction strongly suggests that the entropy of the region enclosed by the surface A is bounded from above by the entropy of the black hole given by:

$$S_{max} = \frac{A}{4\hbar G}. \tag{1.11}$$

This, in turn, provides an upper bound on the amount of information a region of space can store. 't Hooft used this idea to propose that microscopic black holes implement a physical cut-off at small scales.

For a typical non-gravitational quantum system, the maximum entropy for a region counts the number of degrees of freedom inside of it. In a system with n spins, for example, the dimension of the Hilbert space is given by $N = 2^n$. The maximum entropy for a state is then $S_{max} = \ln N \sim n$. On a spin-lattice, this entropy scales as the volume of a given region. Putting a tighter bound on the maximum entropy that scales not as the volume but as the area instead thus limits the number of physical degrees of freedom in that region.

Gravity is essential to provide this bound. Since the volume of a region typically scales faster than its surface area, one could try to violate this bound by extensibly increasing the volume of a region and the entropy contained in it. Alternatively, since higher entropy in a fixed volume requires access to higher energy states, one could fix the volume first and then increase the entropy by adding energy to the inside. In both cases, however, a black hole will form before the bound is surpassed. In other words, a

black hole is the object that has the largest number of states in a gravitational theory. In this way, gravity implements a natural cut-off for highly energetic states.

't Hooft took this as an indication for a fundamental property in a theory of QG: given any closed region, all internal degrees of freedom can be entirely represented on its surface. This is analogous to how a hologram encodes a 3D image in a 2D surface. He even argued that this property should be taken to the extreme in which the surface area is pushed all the way to infinity so that the enclosed region contains the whole universe. Under this holographic principle, the entirety of the degrees of freedom in the bulk are also encoded on its boundary. Leonard Susskind supported this argument soon after by providing a proposal on how this holographic principle could be realized in string theory [4].

1.3.1 Gauge/gravity duality

The most concrete realization of holography corresponds to the Gauge/Gravity duality. In its most general version, this duality states that a theory of QG can be found within every non-Abelian gauge theory [36]. In order to have gravitational interactions, we would need to find the graviton—a spin-two particle—hidden in the field theory. The most feasible possibility for this to happen would be to have the graviton as a composite state of two spin-one gauge bosons. However, such an option would seem to be explicitly forbidden by the Weinberg-Witten no-go theorem [37]. In fact, the loophole that is needed here is provided by the holographic principle: namely, that the gravitational theory we are looking for lives in a different, higher dimensional spacetime. Therefore, the graviton would not propagate in the same spacetime as the gauge bosons. Remarkably, this holographic insight turns out to be allowed.

For this duality to take form, we would need to find an extra dimension within the

degrees of freedom of the gauge theory. Many results from gauge theory suggest that the energy scale has the properties needed to act as the extra dimension r. In particular, it is known that the renormalization group for these theories is local with respect to the energy [36]. Indeed, following the heuristics from before we find that if the gauge theory is four-dimensional, then this energy scale r, together with the position x^μ of the center of mass for the composite state, give five coordinates for the location of the graviton. One could then think of this as the higher-dimensional spacetime on which the gravitational interactions take place. Furthermore, it is known that these dualities work best in scale invariant QFT, also known as conformal field theory (CFT). Then, this additional assumption allows us to find the geometry of this five-dimensional spacetime. This is because the metric of this spacetime needs to be invariant under uniform rescaling of $x^\mu \to \lambda x^\mu$. At the same time, the energy scale needs to transform as $r \to r/\lambda$. These symmetries must be present in a geometry that also preserves the usual Poincaré invariance on x^μ. The most general metric that satisfies these symmetries is

$$ds^2 = \frac{L^2}{r^2}dr^2 + \frac{r^2}{L^2}\eta_{\mu\nu}dx^\mu dx^\nu \tag{1.12}$$

which is called Anti-de Sitter space (or AdS) in Poincaré coordinates, where L is AdS radius.

We want a limit in which classical gravity is recovered. For this to happen, the characteristic length scale of the spacetime must be larger than the Planck length. Therefore, we require $L \gg \ell_P$. Then, the characteristic black hole in this spacetime will have size of order L. Its entropy, in turn, will be of order $S_{BH} \sim L^2/\ell_P^2$, and thus very large. To match this entropy in the field side, we then need many degrees of freedom available. Particularly, in gauge theories with a $SU(N)$ symmetry, this is possible by taking a large N limit. Indeed, 't Hooft showed us [38] that the sensible way of taking the $N \to \infty$

limit in these theories involves keeping $\lambda = g_{YM}^2 N$ fixed. Here, g_{YM} is the coupling constant and λ is the coupling strength of the gauge theory. Not only do we want λ to be fixed, but we also want it to be very large. Intuitively, this is because we need an effective strong-coupling in order for the composite state of two spin-one particles on the field theory to look like a single spin-two particle in the gravitational theory. The correct limit then is $N \to \infty$ together with $\lambda = \text{fixed} \gg 1$. Indeed, 't Hooft had already discovered that under these conditions a $1/N$ perturbation series of the gauge theory resembles a perturbative string expansion [38]. And in fact, in the examples where this duality is understood, the gauge theory is not dual to gravity alone, but instead to string theory—a theory of quantum gravity.

1.3.2 AdS/CFT correspondence

We now focus on the explicit construction of the AdS/CFT correspondence introduced by Juan Maldacena [5]. In this construction, a type-IIB string theory on $AdS_5 \times S^5$ (the bulk theory) is dual to a $\mathcal{N} = 4$ supersymmetric Yang-Mills (YM) theory with $SU(N)$ gauge group in four dimensions (the boundary theory). The $SU(N)$ YM theory is a simplified toy model that does not describe our universe. However, it shares many properties with quantum chromodynamics (which describes the strong force) and, therefore, some of these lessons can find real-world applications in the realm of condensed matter and nuclear physics. Importantly, this gauge theory on the boundary does not include gravity—that is, independently of this duality. The type-IIB string theory, on the other hand, represents a full theory of QG in the bulk. The "II" refers to the existence of two gravitinos. In contrast to type-IIA string theory, the two gravitinos in type-IIB have the same chirality and, as such, the theory is only defined on orientable spacetimes. The fields in this theory include a metric, a dilaton, a Neveu-Schwarz field (NS), and various

Ramond-Ramond gauge fields (RR). These RR and NS gauge fields should be thought of as higher-dimensional analogs of the gauge field in a Maxwell-Einstein theory. Even though the string theory lives in a ten-dimensional space, the gravitational theory is effectively five-dimensional with the other five compact dimensions represented by the S^5 frequently playing a secondary role in the duality.

The reason for using type-IIB supergravity (the low energy limit of type-IIB string theory) is that the theory admits D$p-$brane solutions of odd p [39]. In terms of the usual $p+1$ coordinates $x_\parallel$ parallel to the brane and the $9-p$ coordinates $x_\perp$ perpendicular to the brane, the string metric of these brane solutions is given by

$$ds^2_{string} = H_p^{-1/2} dx^2_\parallel + H_p^{1/2} dx^2_\perp \tag{1.13}$$

where H_p is only a function of $x_\perp$ and solves

$$\partial^2_\perp H_p = -(7-p)\Omega_{8-p} r_0^{7-p} \delta^{(9-p)}(x_\perp). \tag{1.14}$$

Here, r_0 has units of length and parameterizes the strength of the source. Ω_{8-p} is the volume of a unit $(8-p)-$sphere. As we mentioned, type-IIB supergravity has D1-, D3-, D5-, and D9-branes. The "D" is related to the fact that these branes serve as Dirichlet boundary conditions for strings in string perturbation theory. Of these, the D3-branes are of particular interest because they have a smooth horizon. For $p=3$, one finds $H_3 = 1 + r_0^4/r^4$. Additionally, near the horizon the geometry takes on the form of $AdS_5 \times S^5$ with radius L given as a function of the source in (1.14). This situation is analogous to the near-horizon limit of extremal Reissner-Nordstrom black holes in Maxwell-Einstein theory for which the geometry becomes $AdS_2 \times S^2$ [40].

The explicit AdS/CFT construction considers a stack of N coincident D3-branes.

Since these branes act as boundaries for string world-sheets, each additional brane adds a factor of the coupling g_s. Then, string perturbation theory on this system is good when $g_s N \ll 1$. In this weak-coupling regime, and after taking the low energy limit where the field theory on the brane decouples from the bulk, one is left with massless open strings attached to the branes. These are described by a $\mathcal{N} = 4$ $SU(N)$ four-dimensional gauge theory. The gauge coupling and the string coupling in this limit are related by $g_{YM}^2 = 4\pi g_s$. On the other hand, going to the strong-coupling regime $g_s N \gg 1$, one finds a low energy limit by approaching the near-horizon geometry of the branes. It is in this region that one discovers type-IIB string theory in $AdS_5 \times S^5$. The categorical statement of the AdS/CFT correspondence is that these two limits are dual to each other [5, 41]. In fact, even though it has not been proven conclusively, mounting evidence strongly suggests that this duality is true even at the non-perturbative level. This is the attitude that we take on this thesis.

These D3-branes, as three-dimensional objects immerse in ten dimensions, are surrounded by a five-sphere. Then, they carry a charge that sources a flux from F_5, a five-form field strength. This is similar to the two-form field strength $F_{\mu\nu}$ from electromagnetism. We say that these branes have both electric and magnetic fields. Following a similar argument to Dirac's quantization of magnetic monopoles, one can see that this flux from the D3-branes is quantized. Since each of the N branes contribute to this flux, the integral $\int_{S^5} F_5$ is proportional to N. Then, this connection between N and F_5, together with the equations of motion derived from the IIB supergravity action, can be used to express the radius L of the $AdS_5 \times S^5$ geometry found in the near-horizon limit as

$$\frac{L^4}{\ell_s^4} = 4\pi g_s N \tag{1.15}$$

where ℓ_s is the string length and is related to the Planck length by $\ell_P = g_s^{1/4} \ell_s$. This

relation allows us to see the complementary limits of this duality. Indeed, we have $L^4/\ell_s^4 = 4\pi g_s N = g_{YM}^2 N = \lambda$. Therefore, in the large N limit, and when $\lambda \gg 1$, the gauge theory is strongly coupled and gravity behaves classically. Alternatively, when $\lambda \ll 1$, the gauge theory is now weakly coupled and the gravitational theory is no longer classical.

1.3.3 Anti-de Sitter spacetime

Given its prominent role in the gauge/gravity duality, here we review some properties of empty Anti-de Sitter (AdS) spacetime. This geometry is a maximally symmetric Lorentzian manifold with constant negative scalar curvature. In $d+1$ dimensions, it is an exact solution of Einstein's equations in vacuum with a negative cosmological constant given by $\Lambda = -(d-1)d/(2L^2)$. As mentioned before, the length parameter L is known as the AdS radius. To visualize the $d+1$ AdS geometry, it is convenient to embed it in a higher-dimensional flat space. For this purpose, we use flat $\mathbb{M}^{2,d}$ which has two time coordinates T^1, T^2, and d space coordinates $X^1, \ldots, X^d$. In this ambient spacetime, consider the $d+1$-dimensional hyperboloid of radius L given by

$$(T^1)^2 + (T^2)^2 - \sum_{i=1}^{d} (X^i)^2 = L^2. \tag{1.16}$$

Notice that this hyperboloid is invariant under rotations in the T^1T^2 plane, as well as under two independent sets of isometries given by the $SO(d,1)$ Lorentz group—one for each set $\{T^1, X^i\}$ and $\{T^2, X^i\}$, respectively. Altogether, this hyperboloid enjoys a total of $(d+1)(d+2)/2$ symmetries given by the $SO(d,2)$ group. To find the AdS_{d+1} geometry, we need to first get the induced line element on this hyperboloid. For this, consider the parametrization given by $T^1 = \sqrt{L^2+r^2}\cos(\tau/L)$, $T^2 = \sqrt{L^2+r^2}\sin(\tau/L)$,

and $r^2 = \sum_i (X^i)^2$. Then, one finds that the induce metric on the hyperboloid is

$$ds^2_{AdS_{d+1}} = -(r^2/L^2 + 1)d\tau^2 + \frac{dr^2}{r^2/L^2 + 1} + r^2 d\Omega^2_{d-1} \tag{1.17}$$

where $d\Omega^2_{d-1}$ is the metric of the unit $(d-1)$-sphere. In this parametrization, however, the time coordinate τ is periodic with period 2π. This is an issue because it allows the existence of closed timelike curves. This can be solved by choosing to extend the range of τ so that it takes values on all of $\mathbb{R}$. This is known as the universal covering space of the hyperboloid (see Fig. 1.3). With this choice of coordinates, (1.17) is known as the $d+1$ AdS spacetime in global coordinates.

Notice that for large values of r we find that $g_{\tau\tau}$ increases. This is an indication that the gravitational potential for a massive particle grows as it moves away from $r = 0$. In fact, an explicit calculation of geodesics in this geometry shows that the motion of a massive particle that is put at rest at some large r will be oscillatory around the origin. This confining property of AdS makes of this geometry a toy model for gravity in a box. Massive particles with finite energy cannot reach infinite r. Additionally, massless particles can go to infinity and return to the origin in finite time.

To visualize the boundary structure of AdS, it is useful to introduce a new radial coordinate given by $R = \arctan(r/L)$. The range of this coordinate is from 0 to $\pi/2$, with $R = \pi/2$ representing the boundary at infinity. With this coordinate, the AdS metric becomes

$$ds^2_{AdS_{d+1}} = \frac{L^2}{\cos^2(R)} \left[-\frac{1}{L^2} d\tau^2 + dR^2 + \sin^2(R) d\Omega_{d-1} \right]. \tag{1.18}$$

Inside the bracket one finds the conformal metric for global AdS, which defines a smooth manifold with a timelike boundary. At $R = \pi/2$, the geometry for the conformal bound-

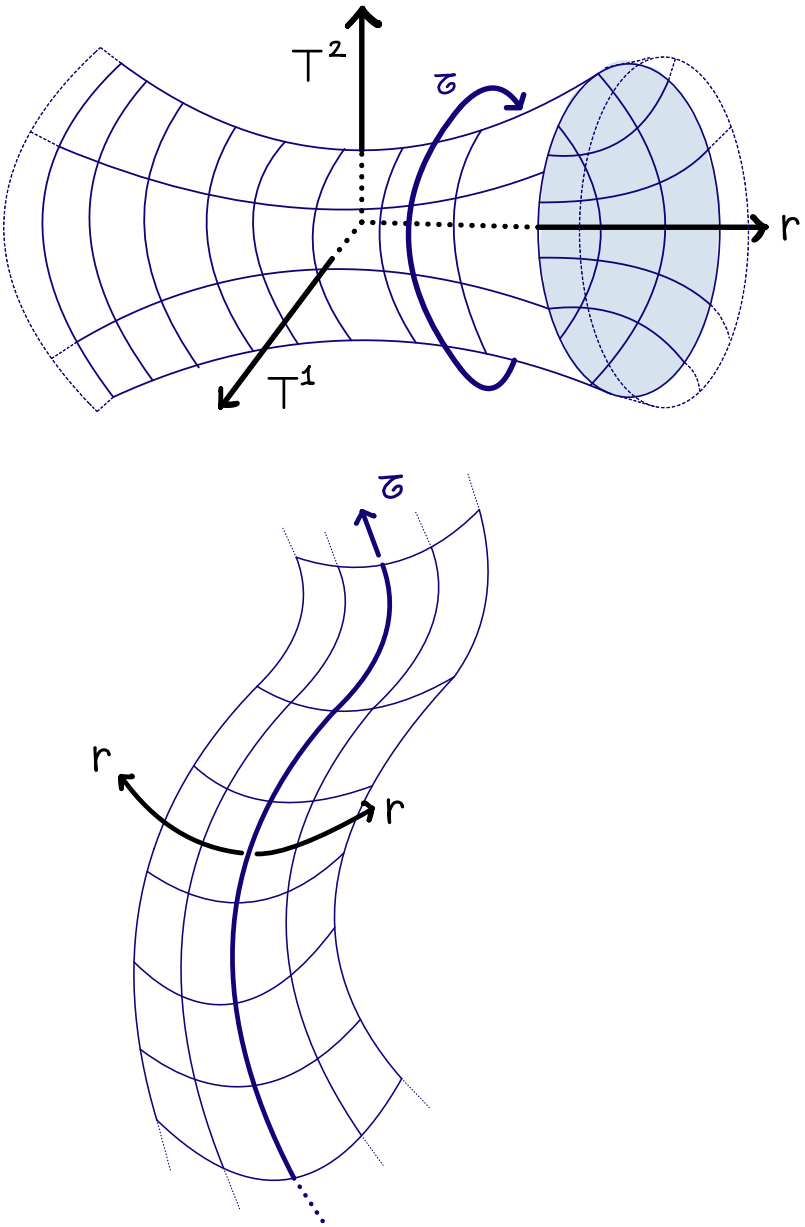


Figure 1.3: Top: $d+1$ hyperboloid embedded in flat $\mathbb{M}^{2,d}$ where $r^2 = \sum_i (X^i)^2$ represents the d spacial directions. The coordinate τ is periodic with period 2π which leads to the existence of closed timelike curves. Bottom: Universal covering space of the $d+1$ hyperboloid.

ary (as shown in Fig. 1.4) is just that of a flat cylinder $\mathbb{R} \times S^{d-1}$, known as the Einstein Static Universe (ESU).

Another useful set of coordinates to describe AdS is known as the Poincaré co-

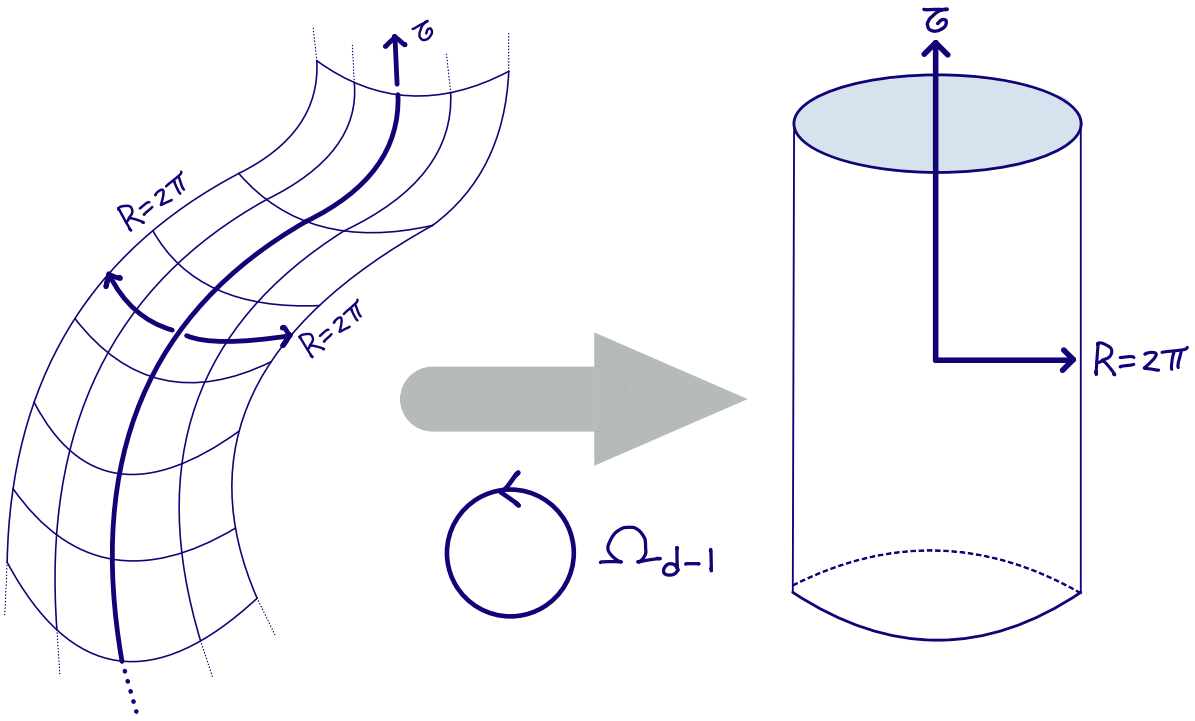


Figure 1.4: Anti-de Sitter spacetime and the ESU conformal boundary.

ordinates. We start with the hyperboloid in (1.16), and introduce coordinates $t = LT^2/(T^1 + X^d)$, $z = L^2/(T^1 + X^d)$, and $x^i = LX^i/(T^1 + X^d)$ for $i = i, \ldots, d-1$. In these coordinates, we find

$$ds^2_{AdS_{d+1}} = \frac{L^2}{z^2}\left[dz^2 - dt^2 + \sum_{i=1}^{d-1}(dx^i)^2\right]. \tag{1.19}$$

Notice that this is the same metric introduced in (1.12) with $z = L^2/r$. Unlike the global coordinates, these coordinates do not cover all of AdS. They cover a portion called the Poincaré patch. Once again, inside the bracket we find the conformal metric for AdS, this time in Poincaré coordinates. The boundary is now located at $z = 0$, and is given by the four-dimensional Minkowski spacetime (see Fig. 1.5). This, in turn, makes explicit the Poincaré symmetry associated to the coordinates t, x^i. Finally, since the Poincaré patch is contained in global AdS, we find that the ESU has a diamond patch that is

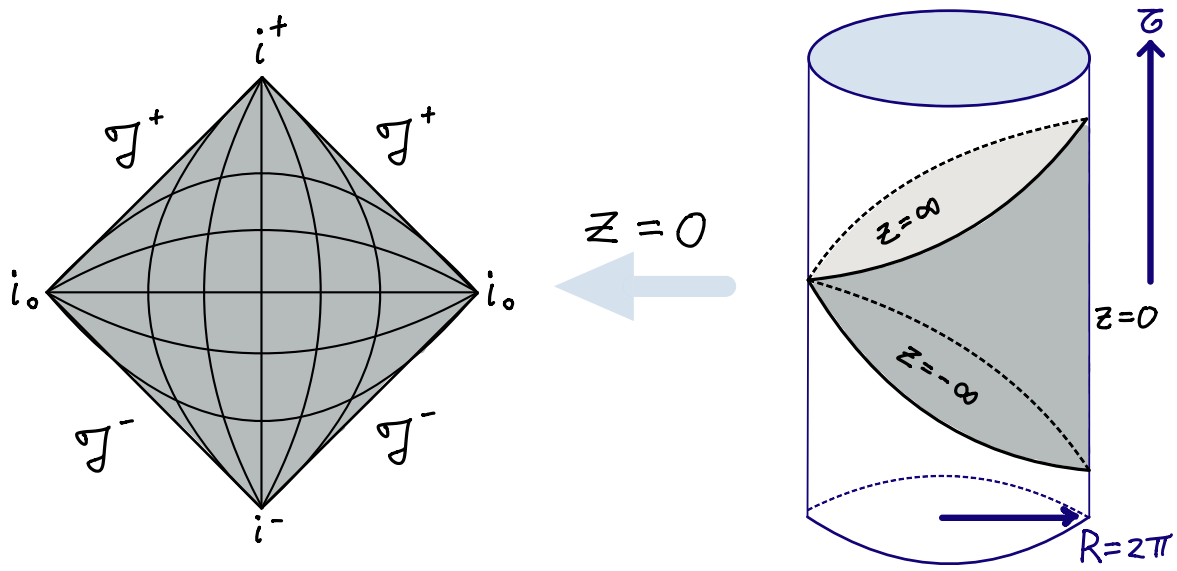


Figure 1.5: Right: Poincaré diamond patch in the ESU. Left: The $z = 0$ conformal boundary of the Poincaré patch is the Minkowski spacetime.

conformally equivalent to four-dimensional Minkowski spacetime.

1.4 Permissions and Attributions

1. The content of Chapter 2 has previously appeared in the Journal of High Energy Physics [42]. It is reproduced here with the permission of the International School of Advanced Studies (SISSA), Trieste, Italy. `https://jhep.sissa.it/jhep/help/JHEP/CR_OA.pdf`

2. The content of Chapter 3 is a result of a collaboration with Sergio Hernández-Cuenca, Gary Horowitz, and Diandian Wang [43].

3. The content of Chapter 4 is a result of a collaboration with Steve Giddings and Seth Koren, and has previously appeared in Physical Review D [16]. It is reproduced here with permission of the American Physical Society: `http://journals.aps.org/copyrightFAQ.html#thesis`.

Chapter 2

Reconstruction of an AdS Radiation/Boson Star Bulk Geometry Using Light-cone Cuts

> Remember to look up at the stars and not down at your feet. Try to make sense of what you see and wonder about what makes the universe exist. Be curious.
>
> Stephen Hawking

2.1 Introduction

The AdS/CFT correspondence [5, 41], first conjectured by Maldacena in 1997, provides a relation between gravitational theories with $(d+1)-$dimensional spacetimes that are asymptotically anti-de Sitter, and a $d-$dimensional non-gravitational gauge theory. This proposal has been one of the most important attempts to understand the inter-

play of quantum mechanics with gravity beyond the semi-classical approximation. One important program has been the development of the dictionary that describes how geometrical properties from the gravitational side get encoded in the information of the gauge theory. In principle, any physical quantity in the bulk theory should be obtainable from an observable in the boundary theory.

Perhaps the most remarkable element to consider is how the AdS/CFT correspondence changes our understanding of the nature of the metric. On the basis of this correspondence, many authors advocate for the emergence of the spacetime metric from fundamental quantum effects. For example, some approaches use the quantum entanglement in the dual field theory to recover information about the bulk metric [44, 45, 46, 47, 48, 49, 50, 51, 52, 53], where the entanglement entropy is the dual quantity to the area of extremal surfaces in the bulk. To reconstruct the metric, these techniques compare the entanglement entropy of neighboring regions in the boundary. On the other hand, some other attempts [54, 55] make use of the equations of motion in the bulk.

A new approach for reconstructing the bulk geometry from information in the boundary was recently introduced [56]. It was shown how the conformal metric of a holographic spacetime can be recovered from a set of distinguished spatial slices of the conformal boundary, known as "light-cone cuts." Using these light-cone cuts, the conformal metric is reconstructed point by point in the bulk. The prescription shows how the metric can be recovered purely from the location of the light-cone cuts in the boundary. These light-cone cuts can be obtained from the dual field theory by analyzing the divergent behavior of n-point functions in the boundary, following a prior work in [57, 58, 59]. Indeed, the n-point boundary correlation function has a divergence when all the points are null related to a single bulk vertex point, and energy-momentum at the vertex is conserved. This property can be used to determine the location of the vertex. This technique can

be applied to almost[1] any point inside the causal wedge of the conformal boundary.

It is of interest to inquire how the information gets encoded in the geometry of these slices in the boundary, apart from their location. Intuitively speaking, the light-cone cut of a bulk point p is given by the collection of points q in the boundary that are strictly null related to p, i.e., points q for which there exists a null curve connecting p to q but not a timelike curve. In general, matter in the spacetime creates a gravitational lensing effect on the null light rays. If two null geodesics intersect, they form a caustic in the bulk. A point q at the intersection of the boundary with any null geodesic that crosses a caustic inside the spacetime will fail to be strictly null related to p. The presence of these caustics creates a cusp in the light-cone cut at the boundary. This cusp is a distinguished conformal feature of the light-cone cut that encodes properties of the matter content of the bulk.

We want to understand in detail how the matter content is encoded in the cusp. The simplest case to provide an example for this method consists of a spherically symmetric and static spacetime. We consider the instructive case of a superposition of a radiation star and a boson star, in asymptotic AdS_4. For one radiation star, the geometry is parameterized by its central density ρ_c, which determines the total mass of the spacetime M_{Total}. This mass can be recovered from an integral at infinity, allowing for ρ_c to be recovered. To study a non-trivial example, we add a complex scalar field in the spacetime, creating a radiation/boson star in AdS. As shown in [60], boson stars in AdS are parameterized by the central value of the scalar field ϕ_c, which is also correlated to the total mass measured in the boundary. By considering the superposition of both of them, the total mass is now parameterized by ρ_c and ϕ_c. In this case, knowing the total mass from the boundary only provides a relation between both parameters; however, it does

[1]For static black holes, bulk vertices inside the photon sphere will in general fail to conserve energy-momentum from null related points at the boundary.

not allow one to completely identify the spacetime. We will use the angle of the cusp to find a second relation between the parameters, which allows the identification of the matter content of the spacetime.

The paper is organized as follows: in Section 2.2 we give a brief review of the light-cone cuts formalism, followed by the definition of a hyperbolic angle in the presence of a cusp on the light-cone cut. Next, Section 2.3 discusses the model for a 4-dimensional boson star in AdS superposed with a gas of radiation. We provide numerical results that show how this geometry can be reconstructed from information on the boundary. We conclude in Section 2.4.

2.2 Light-cone Cuts

2.2.1 Review of the formalism

This section provides a review of the pertinent properties of the light-cone cut formalism. We will follow the construction of [56].

The chronological future of a point p, $I^+(p)$, is defined as the collection of all points that are connected to p by a past-directed timelike curve. To include null curves, the causal future $J^+(p)$ of p is defined to be the set of all points connected to p through a past-directed timelike or null curve. Likewise, the chronological and causal past of a point p, $I^-(p)$ and $J^-(p)$ respectively, can be defined. We denote by M an asymptotically locally AdS spacetime[2] with conformal boundary ∂M. In this construction, the spacetime M is assumed to be C^2, connected, maximally extended, and AdS hyperbolic. In this work, we adopt the definition of AdS hyperbolic from [62]. This requirement corresponds to the absence of closed causal curves, together with the following condition: for any two

[2]We adopt the definition of asymptotically locally AdS spacetime from [61].

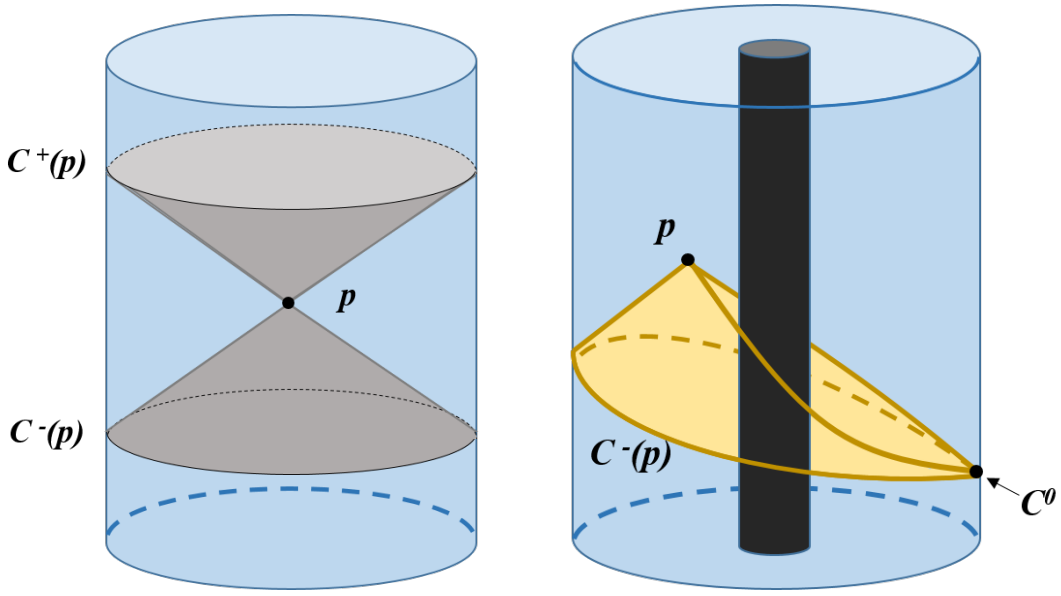


Figure 2.1: Left: Past and future light-cone cuts for a point p in pure anti-de Sitter geometry. Right: With matter content or a black hole in the bulk, the past light-cone cut $C^-(p)$ is continuous, but fails to be smooth in the cusp created by gravitational lensing.

points in the bulk $\{p, q\}$, if the AdS boundary has been conformally compactified, then the set $J^+(p) \cap J^-(q)$ is compact. The "future light-cone cut" of a point $p \in M$, denoted by $C^+(p)$, is defined as the intersection of the boundary of the causal future of p with ∂M: $C^+(p) \equiv \partial J^+(p) \cap \partial M$. The past light-cone cut of a point p, $C^-(p)$, can be obtained analogously. Figure 2.1 illustrates both the future and past light-cone cuts for a point inside pure AdS spacetime.

Some relevant properties of the light-cone cuts proved in [56] include:

- $C^\pm(p)$ is a complete spatial slice of ∂M.
- $C^\pm(p)$ is a continuous set.
- $C^\pm(p)$ is C^1 everywhere except on at most a measure zero set.
- $C^\pm(p)$ correspond to a unique bulk point: $C^\pm(p)$ and $C^\pm(q)$ agree on an open set if and only if $C^\pm(p) = C^\pm(q)$.

It is important to notice that, when gravitational lensing is present, the light-cone cut is not given by the intersection of the entire light-cone with the boundary. The future light-cone of a point p is defined as the set of all future-directed null geodesics fired from p. For a generic spacetime, null geodesics can focus and intersect, creating caustics. When a caustic is produced, the null geodesics leave the boundary of $J^+(p)$, and their intersection with ∂M do not belong to the future light-cone cut of the point p. This property of caustics in general geometries implies that the light-cone cuts are not necessarily smooth slices of ∂M. Moreover, even though the light-cone cuts are continuous, the presence of cusps in the cut will yield points where it fails to be C^1. See (b) in Figure 2.1 for an illustration.

2.2.2 Cusp angle

The presence of cusps in light-cone cuts is a feature of general spacetimes due to the effect of gravitational lensing on the light rays. The details of these cusps are determined by the distribution of matter in the bulk. Therefore, features of the matter content inside the spacetime are expected to be encoded in the structure of the cusp at the boundary. To parameterize the cut, we define a deficit angle for the cusp in the light-cone cut. This angle will represent a conformally invariant attribute of the light-cone cut that can be measured at the boundary.

In four dimensional geometries, the light-cone corresponds to a 3-dimensional Lorentzian hypersurface. For spherically symmetric spacetimes, using coordinates $\{t, r, \theta, \varphi\}$, we can further restrict the analysis to the equatorial plane $\theta = \pi/2$, reducing the light-cone to only two dimensions. We now introduce a new radial coordinate $\rho \equiv \arctan(r/L)$, where L is the AdS radius, locating the boundary at $\rho = \pi/2$. After a conformal rescaling, the metric in the boundary is chosen to be the Einstein Static Universe, that is, the static

cylinder $\mathbb{R} \times S^2$. Therefore, for $d = 4$, the conformal boundary metric restricted to the equatorial plane is given by

$$ds^2_{\partial M} = -dt^2 + d\varphi^2 \tag{2.1}$$

For this Lorentzian space, we can naturally define a hyperbolic angle. Let u and v be two spacelike vectors living in the boundary. We define the hyperbolic angle β between them by:

$$\cosh \beta = \frac{|u \cdot v|}{\sqrt{|u \cdot u||v \cdot v|}} \tag{2.2}$$

This angle corresponds to the absolute value of the boost parameter of the Lorentz transformation that relates both vectors, taking values in the interval $[0, \infty)$. The velocity of the associated boost is given by $v = \pm \tanh \beta$.

2.3 AdS Radiation/Boson Star

The set of light-cone cuts enable us to recover the conformal metric of the bulk spacetime. We now study how properties of this geometry get encoded in the structure of the light-cone cuts at the boundary, specifically in the hyperbolic angle of the cusp, and how to use that information to reconstruct the bulk metric.

According to the AdS/CFT dictionary, each bulk field has an associated dual operator in the boundary theory. Given a state in the CFT, for each non-vanishing one-point function of an operator in the boundary there exists a corresponding field in the bulk theory. In addition, when these one-point functions are static and spherically symmetric, their respective bulk fields will share these symmetries.

The simplest example of a static and spherically symmetric geometry that includes

matter is a perfect fluid with a radiation equation of state. This acts as an idealized model for a star in AdS. For these geometries, an examination of the non-vanishing correlation functions of the dual operators in the boundary will exhibit the presence of a massless field in the bulk. In our approximation, we will consider a state of radiation of that field, modeled by a perfect fluid. These solutions form a one-parameter family, characterized by their central density ρ_c. One characteristic of these solutions is that the total mass is a function of the central density, $M_{Total} = M_{Total}(\rho_c)$. The mass of the star can be computed as an integral at infinity, and thus the central density can be recovered from information on the conformal boundary. In order to provide a non-trivial example, where the cusp angle provides additional information, we will study the superposition of this radiation star with a boson star.

Boson stars with a negative cosmological constant have been studied for many years [63, 60]. In particular, the spherically symmetric solutions form a family parameterized by the central value of the scalar field ϕ_c. Similar to the case of a radiation star, the total mass of the geometry is a function of ϕ_c. By adding a complex scalar field to the spacetime, we introduce a degeneracy in solutions with the same total mass but different ρ_c and ϕ_c. Computing the mass at the boundary provides a relation between the 2 parameters. The cusp angle provides a second relation between these parameters, and thus the spacetime will be uniquely identified.

2.3.1 Model

The action of an AdS radiation/boson star in four dimensions is given by

$$S = \frac{1}{8\pi G_4}\int_{M_4} d^4x \left(\sqrt{-g}\frac{1}{2}(R - 2\Lambda) + \mathcal{L}_{boson} + \mathcal{L}_{rad}\right) \tag{2.3}$$

where the cosmological constant is given by $\Lambda = -3/L^2$, with L the AdS radius[3]. This action describes the evolution of a complex scalar field Φ minimally coupled to gravity, superposed with a gas of radiation. The Lagrangian density for a complex scalar field is defined by

$$\mathcal{L}_{boson} = \sqrt{-g}\left(g^{\mu\nu}\Phi^*_{,\mu}\Phi_{,\nu} + V(\Phi)\right) \tag{2.4}$$

where $V(\Phi)$ is the potential for the scalar field, and Φ^* denotes the complex conjugate of the field. We will restrict ourselves to a potential without any self-interaction terms. For our case $V(\Phi) = \mu^2\Phi^*\Phi$, where μ is the mass of the scalar field. The Lagrangian density (2.4) is invariant under the transformation of the scalar field by a global phase, $\Phi \to \Phi e^{-i\alpha}$; this symmetry gives rise to a conserved current

$$J^\mu = ig^{\mu\nu}\left(\Phi^*_{,\nu}\Phi - \Phi_{,\nu}\Phi^*\right) \tag{2.5}$$

The corresponding conserved charge can be identified as the number of scalar particles,

$$N = \int d^3x\sqrt{-g}J^t \tag{2.6}$$

Varying the action (2.3) with respect to the fields $g_{\mu\nu}$ and Φ yields the field equations

$$R_{\mu\nu} - \frac{1}{2}g_{\mu\nu}R - 3g_{\mu\nu} = 8\pi G_4\left[T^{rad}_{\mu\nu} + T^{boson}_{\mu\nu}\right], \tag{2.7}$$

$$\Box^2\Phi - \mu^2\Phi = 0, \tag{2.8}$$

[3]In this paper we use $c = L = 1$.

respectively. Here,

$$T^{rad}_{\mu\nu} = \rho(r)u_\mu u_\nu + p(r)\left(g_{\mu\nu} + u_\mu u_\nu\right) \tag{2.9}$$

is the stress-energy tensor for a perfect-fluid gas of radiation, where in four dimensions the pressure is related to the energy density by $p(r) = \rho(r)/3$; and

$$T^{boson}_{\mu\nu} = \partial_\mu\Phi^*\partial_\nu\Phi + \partial_\nu\Phi^*\partial_\mu\Phi - g_{\mu\nu}\left(\partial^\alpha\Phi^*\partial_\alpha\Phi + \mu^2|\Phi|^2\right) \tag{2.10}$$

is the stress-energy tensor for a boson star, where $\Phi = \phi_1 + i\phi_2$ is a complex scalar field assumed to be harmonic $\Phi = \phi(r)e^{-i\omega t}$. In these solutions, both stress-energy tensors are spherically symmetric and time independent. It is advantageous to use the metric in the form

$$ds^2 = -f(r)dt^2 + h(r)dr^2 + r^2d\Omega_2^2 \tag{2.11}$$

where $f(r)$ and $h(r)$ are functions of the radial coordinate r, and $d\Omega_2^2$ is the line element of a 2-sphere. From the tt component of equation (2.7), using the ansatz $\Phi = \phi(r)e^{-i\omega t}$, and setting $8\pi G_4 = 1$, we obtain

$$\frac{f(r)\left(h(r)\left[-1 + h(r) + 3r^2h(r)\right] + rh'(r)\right)}{r^2h^2(r)} = f(r)\rho(r) + 2\omega^2|\Phi|^2 + f(r)\left(-\frac{\omega^2}{f(r)}|\Phi|^2 + \frac{\left[\phi'(r)\right]^2}{h(r)} + \mu^2|\Phi|^2\right), \tag{2.12}$$

where the prime denotes derivative with respect to r. Similarly, from the rr component of equation (2.7), we obtain

$$-\left(3+\frac{1}{r^2}\right)h(r)+\frac{1+rf'(r)/f(r)}{r^2}= \frac{\rho(r)h(r)}{3}+2\left[\phi'(r)\right]^2-h(r)\left(-\frac{\omega^2}{f(r)}|\Phi|^2+\frac{\left[\phi'(r)\right]^2}{h(r)}+\mu^2|\Phi|^2\right), \quad (2.13)$$

Additionally, the scalar field equation of motion (2.8) yields

$$\frac{\omega^2}{f(r)}\phi(r)+\frac{1}{h(r)}\phi''(r)+\left[\frac{f'(r)}{2f(r)h(r)}-\frac{h'(r)}{2h^2(r)}+\frac{2}{rh(r)}\right]\phi'(r)-\mu^2\phi(r)=0 \quad (2.14)$$

One further condition can be obtained from conservation of the stress-energy tensor. Assuming that the scalar field satisfies its equation of motion, the bosonic stress-energy tensor from equation (2.10) is necessarily conserved. Consequently, by requiring that the divergence of the total stress-energy tensor vanishes, an expression for the conservation of the radiation stress-energy tensor is obtained,

$$\nabla_\mu T^{\mu\nu}_{rad}=\nabla_\mu\left[\rho(r)u^\mu u^\nu+p(r)\left(g^{\mu\nu}+u^\mu u^\nu\right)\right]=0 \quad (2.15)$$

A useful expression is given by the radial component $\nu = 1$:

$$2\frac{f'(r)}{f(r)}=-\frac{\rho'(r)}{\rho(r)} \quad (2.16)$$

From equations (2.12), (2.13), (2.14), and (2.15), one can solve for the coefficients of the metric, $f(r)$ and $h(r)$, the radiation density $\rho(r)$, and the radial component of the scalar field $\phi(r)$. To solve these equations we need to impose appropriate boundary conditions. By requiring a regular, non-singular spacetime at the origin, the components of the metric must satisfy $f(0) = 1$, and $h(0) = 1$. Additionally, we demand the solution

to be asymptotically AdS_4, giving the following boundary conditions at infinity:

$$f(\infty) \rightarrow \left[1 + r^2 + \mathcal{O}(\frac{1}{r})\right], \tag{2.17}$$

$$h(\infty) \rightarrow \left[1 + r^2 + \mathcal{O}(\frac{1}{r})\right]^{-1}, \tag{2.18}$$

The boundary conditions for the scalar field are $\phi(0) = \phi_c$, and $\phi'(0) = 0$, where ϕ_c is the central value of the scalar field. For the radiation energy density we have $\rho(0) = \rho_c$, with ρ_c the value at the origin. For each value of the scalar field mass μ, this family of solutions is described by two parameters: ϕ_c and ρ_c. Henceforth, we will set $\mu = 1$.

Given a family of solutions, it is important to identify the configurations that yield a stable solution. Figure 2.2 shows the total mass M_{Total} of the star as a function of ϕ_c, for different values of ρ_c. In the pure boson star case $\rho_c = 0$, the total mass is not a monotonic function of ϕ_c. This suggests the onset of a dynamical instability. Studies have been done discussing the stability of boson stars in 4 dimensions with $\Lambda = 0$, [64, 65, 66]. The transition between stability and instability of these solutions is located at the critical points in a plot of the mass as a function of the central value of the scalar field ϕ_c. For boson stars in AdS, the stability of solutions was studied in [60], with similar results: the maximum mass M_{max} represents the boundary between the regions of stability and instability. In essence, the transition from stable to unstable occurs when the solution admits a static perturbation (vanishing frequency $\omega = 0$) that doesn't change the mass of the solution. Likewise, as noted in [67], the self-gravitating gas of radiation has a similar behavior: for large central densities ρ_c, the mass becomes a non-monotonic function of ρ_c, suggesting the onset of a radial instability located at the maximum of the mass function. Following these results, in order to stay in a regime of stable configurations, only stars with $\rho_c \lesssim 0.6$ and $\phi_c \lesssim 0.6$ will be considered.

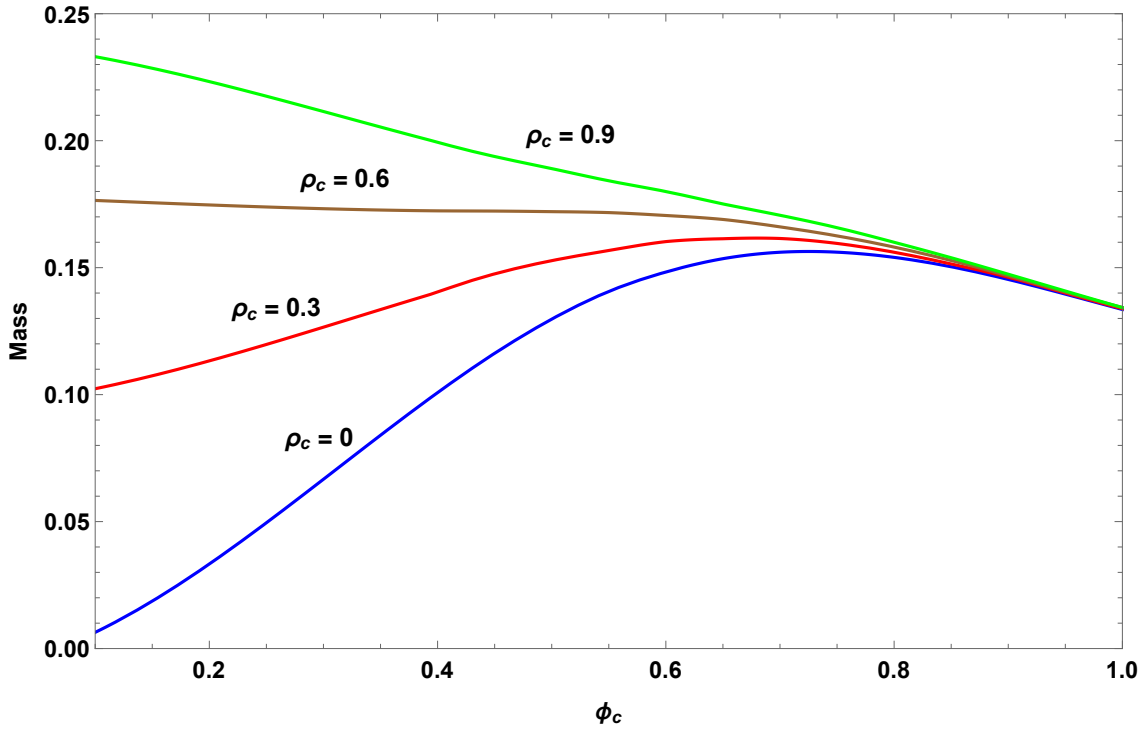


Figure 2.2: Mass of the spacetime as a function of ϕ_c and ρ_c.

2.3.2 Geodesics

The metric given by equation (2.11) has Killing fields associated to the time-translation symmetry and the azimuthal-rotation symmetry. In spherical coordinates (t, r, θ, φ), these correspond to $\xi = (1, 0, 0, 0)$ and $\eta = (0, 0, 0, 1)$, respectively. These Killing fields give rise to the energy (e) and angular momentum (l) as conserved quantities along any geodesic.

Let $u^\mu = (\dot{t}, \dot{r}, \dot{\theta}, \dot{\varphi})$ be the four velocity of a given geodesic. Then, the normalization condition corresponds to $g_{\mu\nu}u^\mu u^\nu = \kappa$, with $\kappa = -1$ for timelike geodesics, $\kappa = +1$ for spacelike geodesics, and $\kappa = 0$ for null geodesics. In our case, as we are interested in null geodesics that reach out to infinity, the normalization condition in terms of the energy

and angular momentum reads

$$f(r)h(r)\dot{r}^2 = e^2 - f(r)r^2\dot{\theta}^2 - f(r)\frac{1}{r^2\sin^2\theta}l^2 \tag{2.19}$$

Taking advantage of the spherical symmetry, it is convenient to restrict ourselves to the equatorial plane $\theta = \pi/2$. In general, the geodesics will be parameterized by both e and l. For null geodesics, it is possible to express these equations in terms of one parameter, which is $\alpha \equiv e/l$. By applying the chain rule, the geodesic equations can be written as functions of the radial coordinate:

$$\frac{d\varphi}{dr} = \pm\frac{1}{r^2}\sqrt{\frac{f(r)h(r)}{\alpha^2 - V(r)}}, \qquad \frac{dt}{dr} = \pm\frac{\alpha}{f(r)}\sqrt{\frac{f(r)h(r)}{\alpha^2 - V(r)}}. \tag{2.20}$$

with $V(r) \equiv f(r)/r^2$. Then, in order to find the intersection of the light-cone with the boundary, it suffices to integrate these expressions out to infinity. In these equations, the sign depends on the radial component of the tangent vector at the initial point. For an ingoing radial component, we must use the negative sign; conversely, for an outgoing radial component, the positive sign is chosen.

2.3.3 Recovering the metric

Now we can analyze the process of recovering the geometry of our model of a radiation/boson star in AdS. First, the total mass M_{Total} of the spacetime can be obtained through a boundary integral. Similar to the flat case, the asymptotic bulk metric can be expressed as $ds^2 = ds_0^2 + h_{\mu\nu}dx^\mu dx^\nu$, where ds_0^2 describes the asymptotic AdS metric, and $h_{\mu\nu}$ represent the deviations from it. The mass and other conserved quantities are expected to be obtained from information encoded in $h_{\mu\nu}$. One approach for locally asymptotically AdS_4 geometries has been proposed in [68]. The mass and the angular

momentum can be obtained as Noether charges for the asymptotic Killing fields, $\partial/\partial t$ and $\partial/\partial\varphi$. Many authors have discussed different methods, including a Hamiltonian formalism, to compute the mass in asymptotically AdS spacetimes; for a further discussion, see [60, 69, 70, 71, 72, 68, 73, 74]. These different methods give equivalent results. By calculating the total mass of the spacetime $M_{Total} = M_{Total}(\rho_c, \phi_c)$, we obtain a relation between ρ_c and ϕ_c.

The next step is to use β from equation (2.2), the angle of the cusp in the light-cone cuts, to get a second relation and disambiguate for the exact value of both parameters. In this analysis, we use the cusp in the future light-cone cut $C^+(p)$. For fixed ρ_c and ϕ_c, the angle of the cusp can only depend on the initial position of the point p, given by the radial coordinate r_0. This quantity relies upon the choice of a coordinate system for the bulk. We can find a more invariant description of the point using the time coordinate on the boundary by considering the difference $\Delta t = t_{max} - t_{min}$, where t_{min} and t_{max} are the time coordinates of the first and last point to reach the boundary in the light-cone cut, respectively. For a point p located in the middle of the spacetime, spherical symmetry guarantees a spherically symmetric light-cone cut. In this case, the time coordinate in the boundary is the same for every point in the light-cone cut; hence $\Delta t = 0$. As the point p moves towards the boundary, the difference Δt increases, and in the limit $r_0 \to \infty$ we recover the result associated to the light-cone cut being traced by a null geodesic traveling in the boundary, namely $\Delta t = \pi$. For the AdS radiation/boson star, the time difference is a monotonic function of the initial position r_0. Therefore, the position of the point p, and its respective light-cone cut, can be parameterized by Δt.

Using the static time coordinate in the bulk t_{bulk}, there is a preferred rest frame in the dual theory for which the bulk Killing vector $\partial/\partial t_{bulk}$ has unit norm when it gets extended to the boundary. This provides a natural choice of time coordinate t in the boundary theory.

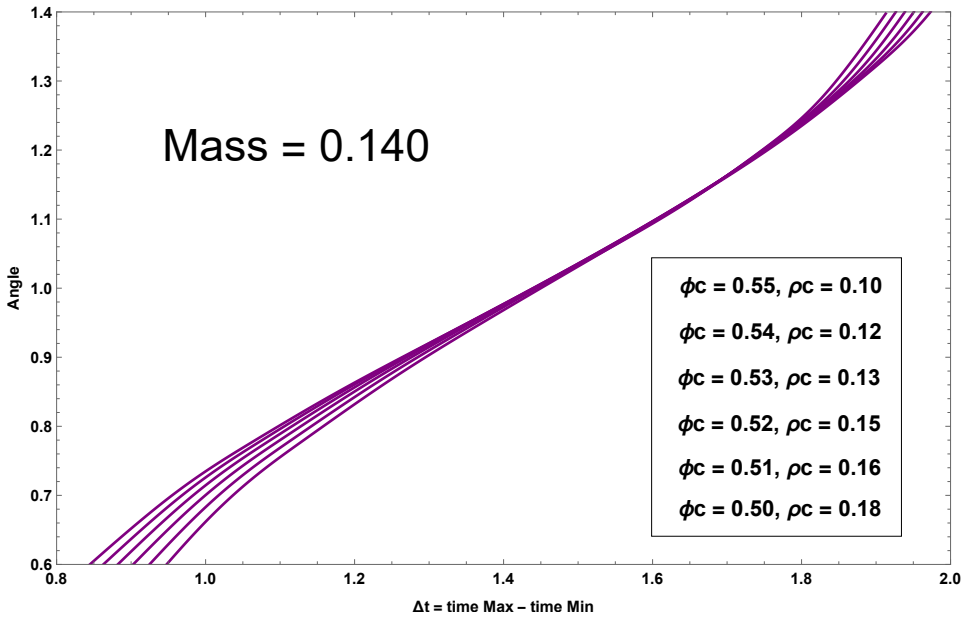


Figure 2.3: Plot of the angle β vs Δt for solutions with different values of ρ_c and ϕ_c, and total mass $M_{Total} = 0.140$.

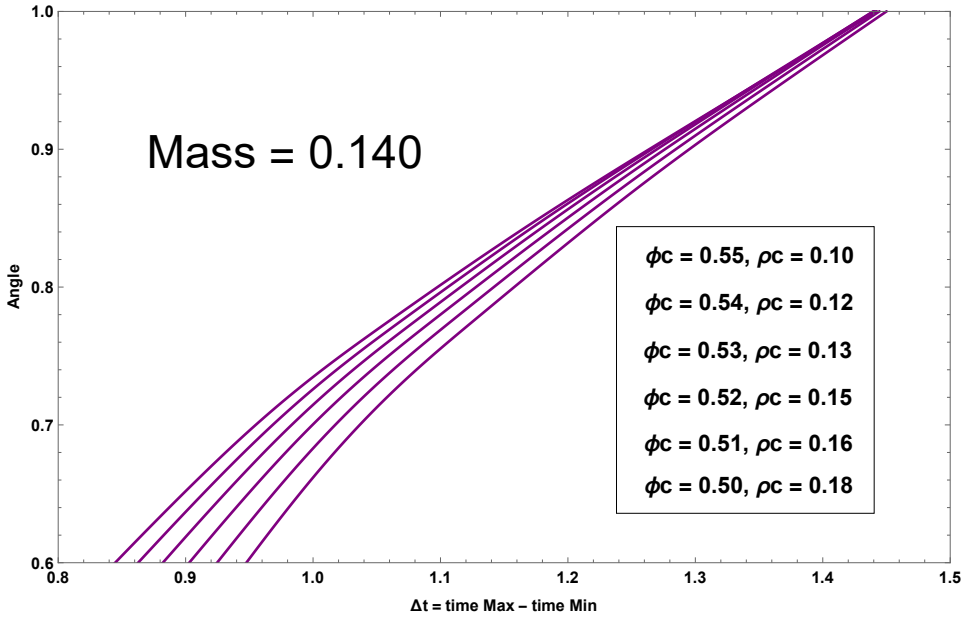


Figure 2.4: Close-up to the plot of the angle β vs Δt for solutions with different values of ρ_c and ϕ_c, and total mass $M_{Total} = 0.140$.

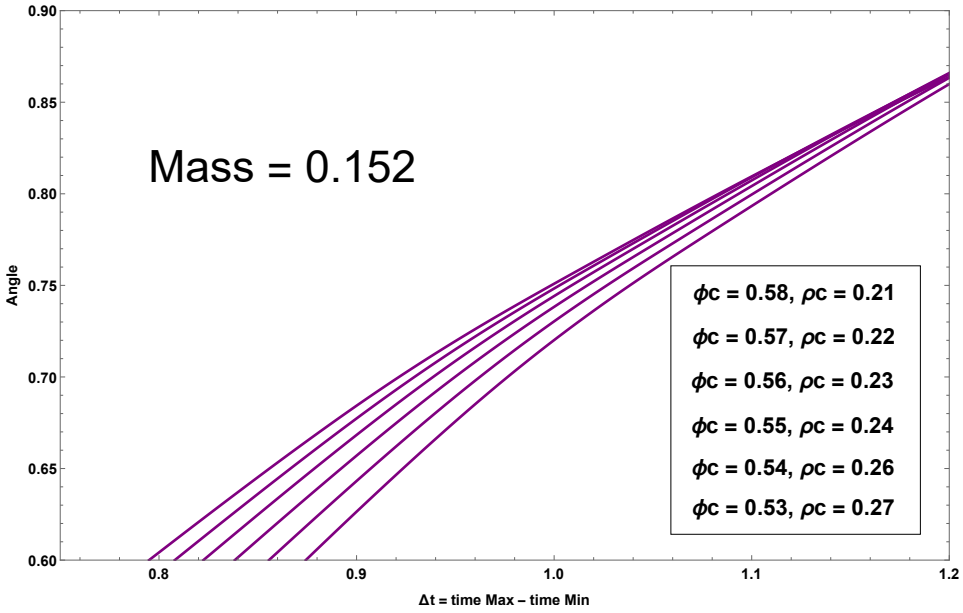


Figure 2.5: Close-up to the plot of the angle β vs Δt for solutions with different values of ρ_c and ϕ_c, and total mass $M_{Total} = 0.152$.

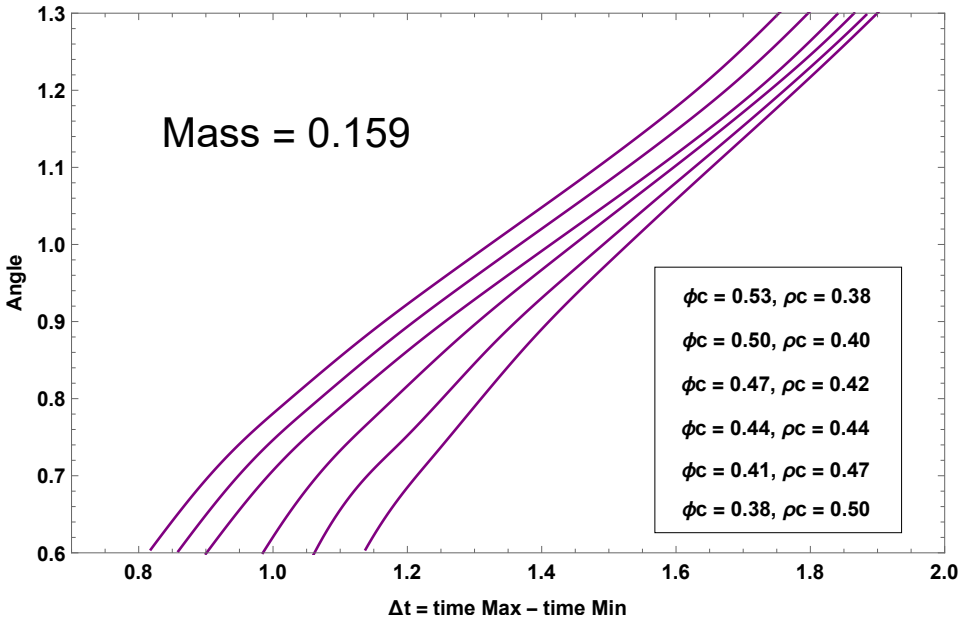


Figure 2.6: Close-up to the plot of the angle β vs Δt for solutions with different values of ρ_c and ϕ_c, and total mass $M_{Total} = 0.159$.

For a fixed $M_{Total} = M_0$, different parameters ρ_c and ϕ_c yield a different plot β vs Δt. These plots for geometries with M_0 can be compared: if none of the plots coincide with each other, identifying the particular plot gives the specific values of the parameters. Figure 2.3 shows the plot of the cusp angle as a function of Δt, for different values of ρ_c and ϕ_c, all for the same total mass $M_{Total} = 0.140$. As the radial coordinate of the bulk point approaches the origin, Δt goes to zero, the cusp becomes flat, and the angle β approaches zero. Conversely, as the radial coordinate of the bulk point approaches the boundary, Δt reaches the maximum value of π and the cusp angle becomes infinite. The latter case corresponds to the light-cone cut being created by light rays traveling in the boundary. The numerical results show that for the same mass, different values of ρ_c and ϕ_c yield distinct curves. Figure 2.4 shows a close-up view of Figure 2.3, in which different geometries with the same mass $M_{Total} = 0.140$ are compared. As we can see in Figure 2.4, there exists a region in the plots where each solution can be clearly identified: for a fixed value of Δt in this region, each solution has a different angle β. Figure 2.5 and 2.6 show the same pattern for solutions with total mass of $M_{Total} = 0.152$ and $M_{Total} = 0.159$, respectively. As discussed at the end of section 2.3.1, all the solutions considered in these figures have parameters ϕ_c and ρ_c within the region of stability. These numerical results exhibit how the cusp angle can be used to recover a second relation between the two parameters. Thus, the matter content and the geometry of this non-trivial bulk spacetime can be reconstructed purely from boundary information.

2.4 Discussion

We have presented a non-trivial example in which the geometry of the bulk can be reconstructed entirely from information in the boundary. We have used the light-cone cut construction of [56] and explored more features of the light-cone cuts. In the presence

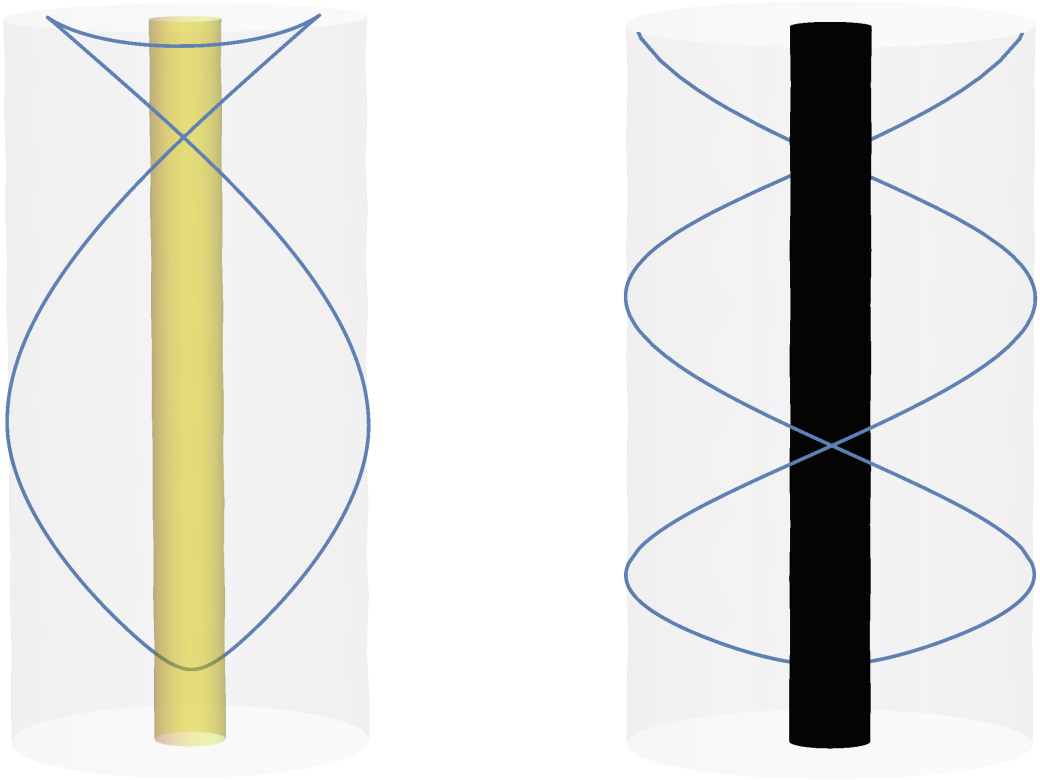


Figure 2.7: Intersection of the light-cone and ∂M for: Left: Self-gravitating radiation gas in AdS; Right: AdS Eternal Black Hole.

of matter, gravitational lensing will create caustics in the spacetime, generating cusps in the light-cone cuts. In this paper, we have explored and taken advantage of these cusps. By using the deficit angle of these cusps, we have included additional information from the boundary that allowed us to reconstruct the geometry of a superposition between a radiation and a boson star.

The light-cone cuts of the AdS radiation/boson star have the structure of the image (a) in Figure 2.7. In this figure we plot the intersection of the complete light-cone with the boundary of the spacetime; we will refer to this subset of the boundary as the "extended light-cone cut". This image shows the existence of three angles: one in the cusp of the light-cone cut, and two more angles on the top of the extended light-cone cut, one on each side. In the latter case, one can use equations (2.20) to find the value of the coordinates

t and φ of the null geodesic at the boundary. The locus of points $(t_{Bndy}, \varphi_{Bndy})$ describes a curve in the boundary as a function of α. As mentioned in [67], the slope of this curve is given by $(dt/d\varphi)_{Bndy} = 1/\alpha$. Indeed, in the case of an AdS radiation/boson star, we have obtained numerically this same result. This shows that the derivative of the curve on each side of the meeting point of the top angles arrives with the same value, giving a cusp with zero angle. Therefore, these additional angles don't contribute any additional information about the matter content of the spacetime.

Another feature of the bulk that can be identified from the light-rays structure is the existence of ultracompact objects. An ultracompact object is defined as one with a radius smaller than 3/2 its Schwarzschild radius, and so it exhibits a photon sphere. Defined this way, black holes are ultracompact objects, but there are also other non-black holes objects that admit a photon sphere [75]. The presence of a photon sphere leaves a characteristic imprint in the extended light-cone cut. The intersection of the boundary ∂M and the light-cone of a point p located outside the photon sphere radius $R = 3R_{Schw}/2$ is generated by all the null geodesics that remain outside of the photon sphere. The geodesics that pass close to this sphere will travel around the object several times before coming out to infinity. Given that they can travel arbitrarily close to this orbit, these geodesics experience a considerable time dilation, and so the time that it takes for one of these geodesics to come back out to infinity can be arbitrarily large. This effect leaves a signal in the form of an ongoing, extended light-cone cut, which intersects itself an infinite number of times. On the other hand, for non-ultracompact objects, the intersection of the light-cone with the boundary of the spacetime will be finite. Figure 2.7 shows the extended light-cone cuts for two different asymptotically AdS geometries: (a) a self-gravitating radiation star, and (b) an eternal black hole. In the first case, the extended light-cone cut is finite; in the second case, this extended cut intersects itself an infinitely number of times, and it is unbounded in the time direction. Using this

feature, and having access to the extended light-cone cut, one can identify ultracompact objects in the bulk from information in the dual theory at the boundary. A different approach to probe ultracompact objects in the bulk was studied in [67]. In this previous work, the authors discussed the relation between singularities of two-point functions and several causal properties of the bulk spacetime. In particular, they considered points in the boundary that are connected causally by a bulk null geodesic. With these "bulk-cone singularities", they argued how to use them to probe the bulk geometry in the context of different asymptotically AdS spacetimes, including ultracompact objects. For a recent discussion on how to extend the light-cone cuts framework to reconstruct the metric of the additional compact dimensions in any asymptotically locally $AdS_n \times S^k$ spacetime, see [76].

An avenue of interest for future work would be to consider how the light-cone cuts could be used to identify black holes from other ultracompact objects.

Chapter 3

Boundary Causality Violating Metrics in Holography

> Time, space, and causality are only metaphors of knowledge, with which we explain things to ourselves.
>
> Friedrich Nietzsche

3.1 Introduction

A bulk description of nonperturbative quantum gravity is not yet available. A popular approach is to consider a path integral over all bulk metrics. We will investigate some aspects of this approach. It is possible that the metric will turn out to be only a low-energy approximation of some other fundamental degrees of freedom. Our results will plausibly apply in that case also, since the issues we address can all be described by metrics with curvature well below the Planck (and string) scale.

We thus begin with a Lorentzian formulation of holography, in which one integrates

over all asymptotically anti-de Sitter (AdS) spacetimes and matter fields (with certain boundary conditions) to compute correlation functions in a dual quantum field theory. One often works in a large N or semiclassical limit in which one only includes classical supergravity solutions and small perturbations of them. Classically, spacetimes satisfy the null energy condition so the Gao-Wald theorem [77] ensures that the bulk preserves boundary causality. In other words, the fastest way to send a signal between two observers on the boundary is via a path that stays on the boundary. No trajectory that enters the bulk can arrive sooner. Semiclassically, the achronal averaged null energy condition ensures boundary causality [78].[1]

However, in full quantum gravity (finite N), the bulk path integral will include metrics that violate boundary causality. That is, two boundary points that are spacelike-separated with respect to the boundary metric can nevertheless be timelike-separated with respect to the bulk metric. These boundary causality violating metrics are not "rare". If a point p is timelike-related to another point q in one bulk metric, it remains timelike-related in any nearby metric. So these metrics include open sets in the space of all metrics. Given this, one might worry that they would contribute to a causality violating process in the dual field theory. Any small nonzero contribution would clearly be a problem. We stress that these bulk metrics are causally well-behaved as bulk geometries. There are no closed timelike curves or any other causal pathology, and (as already mentioned) the curvature is everywhere small compared to the Planck or string scale. So there is no reason to exclude them from the bulk path integral.

Consider, for example, the commutator of a dual field theory operator $\mathcal{O}$ at two spacelike-separated points on the boundary: $[\mathcal{O}(x), \mathcal{O}(y)]$. This must clearly vanish identically, but holography says that it should be given by a bulk path integral over metrics and a matter field ϕ dual to $\mathcal{O}$. If one computes the commutator $[\phi(p), \phi(q)]$ in

[1] A necessary and sufficient geometric condition for boundary causality is given in [79].

each metric g, and then follows the standard limiting procedure of taking $p \to x$ and $q \to y$, one expects a nonzero answer whenever x and y are causally related with respect to g.[2] This is not yet a contradiction, since we must still integrate this answer over metrics g weighted by $e^{\mathrm{im}S_g}$, and it could be that this vanishes exactly.

However, it is not just one quantity that must integrate to zero exactly. In principle, $\mathcal{O}$ can be any operator in the dual field theory, and one can multiply the commutator by any other operator. The corresponding bulk expressions would all be nonzero for some boundary causality violating bulk metrics g, but their integrals over metrics must still vanish identically. Since the gravitational weighting $e^{\mathrm{im}S_g}$ and measure are independent of the operator being considered, it is difficult to see how this is possible.

By studying the boundary conditions for the bulk path integral computation of commutators, we identify an ambiguity whenever the boundary theory is causal and unitary. We show that there is a way to fix this ambiguity so that boundary causality is manifestly preserved.

We begin by giving some examples of boundary causality violating metrics and showing that they can easily have the same action as pure AdS. This suggests that they are not immediately suppressed by oscillations of $e^{\mathrm{im}S_g}$. We then briefly review two operator dictionaries in holography, namely the "differentiate dictionary" and the "extrapolate dictionary". After these preliminaries we explain our resolution of this causality puzzle.

[2]While there are special cases where the commutator vanishes for timelike-separated points (such as free massless fields in even-dimensional Minkowski spacetime), this is generically not the case.

3.2 Specific examples

Consider the following family of static, spherically symmetric, four-dimensional metrics parameterized by $b \in \mathbb{R}$,

$$g_{(b)} = -f_b(r)\,\mathrm{d}t^2 + f_b(r)^{-1}\,\mathrm{d}r^2 + r^2\,\mathrm{d}\Omega_2^2. \tag{3.1}$$

The associated spacetime $\mathcal{M}$ is guaranteed to be asymptotically AdS with radius of curvature ℓ by demanding that $f_b(r) \approx r^2/\ell^2$ to leading order at large r, with the conformal boundary $\partial\mathcal{M}$ corresponding to $r \to \infty$. To avoid conical singularities, differentiability at $r = 0$ requires $f_b(0) = 1$ and $f_b'(0) = 0$. We connect this family at $b = 0$ to global AdS_4 by setting $f_0(r) = 1 + r^2/\ell^2$. In pure AdS, any two boundary points are null-separated on the boundary if and only if they are null-separated in the bulk. To see what properties the function f_b must have for the metrics in (3.1) to violate boundary causality, we now look at how the light cone in the bulk "opens up" or "closes" with respect to the light cone in pure AdS. Taking advantage of the spherical symmetry, it is convenient to restrict the analysis to radial null geodesics. Any such curve obeys $\mathrm{d}t = \pm f_b(r)^{-1}\mathrm{d}r$ and thus its crossing time from boundary to boundary is

$$t_\infty = 2\int_0^\infty \frac{\mathrm{d}r}{f_b(r)}. \tag{3.2}$$

Violating boundary causality then corresponds to opening up the light cones so that $t_\infty < t_\infty^{\mathrm{AdS}} = \pi$. Clearly, one sufficient condition is for $f_b(r)$ to be greater than the pure AdS value $f_0(r)$ everywhere.[3]

In Einstein gravity, the full gravitational bulk action for these geometries contains an

[3]It was noted in [80] that metrics of the form (3.1) have $R_{ab}k^ak^b = 0$, for all radial null geodesics with tangent k^a. This is in fact not sufficient to apply the Gao-Wald time delay theorem [77].

Einstein-Hilbert term, a Gibbons-Hawking boundary term, and the appropriate counter-terms. In four-dimensions, and with a negative cosmological constant $\Lambda = -3/\ell^2$, the bulk action is given by [81, 82]

$$S = \frac{1}{16\pi G}\int_{\mathcal{M}}\sqrt{-g}\left(R+\frac{6}{\ell^2}\right)+\frac{1}{8\pi G}\int_{\partial\mathcal{M}}\sqrt{\gamma}K-\frac{1}{8\pi G}\int_{\partial\mathcal{M}}\sqrt{\gamma}\left(\frac{2}{\ell}+\frac{\ell}{2}\mathcal{R}\right), \quad (3.3)$$

where γ is the induced metric on $\partial\mathcal{M}$, regulated to a hypersurface of constant $r = \ell/\epsilon$. Additionally, K is the trace of the extrinsic curvature of this hypersurface, and $\mathcal{R}$ is the Ricci scalar of γ. For the metrics in (3.1), the action (3.3) integrates exactly to a boundary term evaluated at the cutoff surface. By enforcing AdS asymptotics to leading order, we can in general write $f_b(\ell/\epsilon) = \epsilon^{-2}(1+\tilde{f}_b(\epsilon))$ with $\tilde{f}_b$ some function only required to satisfy $\lim_{\epsilon\to 0}\tilde{f}_b(\epsilon) = 0$. The action then reduces to

$$S = -\frac{\ell T}{4G}\lim_{\epsilon\to 0}\frac{\tilde{f}_b(\epsilon)}{\epsilon}, \quad (3.4)$$

where T is a time interval between two fixed-t hypersurfaces. This shows that any correction $\tilde{f}_b$ to pure AdS with $|\tilde{f}_b(\epsilon)|$ decaying to zero faster than linear in ϵ can be chosen to violate boundary causality (by making (3.2) integrate to $t_\infty < \pi$) while keeping the same action as AdS. In the remainder of this section we explore some explicit examples.

For convenience, set $\ell = 1$. A simple example which satisfies our boundary conditions and violates boundary causality is given by (3.1) with

$$f_b(r) = r^2 + 1 + b\frac{r^2}{1+r^4}. \quad (3.5)$$

As discussed above, these metrics violate boundary causality as long as $b > 0$ so that $f_b(r) \geq f_0(r)$ everywhere. Another example that shows explicitly how the light cone

opens up in the bulk is given by (3.1) with

$$f_b(r) = (r^2+1)\left[1 - \frac{b}{b - \left(\frac{1+(1+b^2)^2 r^2}{4r}\right)^2}\right], \tag{3.6}$$

again with $b = 0$ corresponding to pure AdS. For these metrics, the integral (3.2) can be computed exactly to obtain

$$t_\infty = \pi - \frac{8\pi b}{(1+b^2)\,(2+b^2)^2}, \tag{3.7}$$

so boundary causality is clearly violated for $b > 0$.

These static configurations only contribute to a path integral where the initial and final surfaces have induced metric $\mathrm{d}r^2/f_b(r) + r^2\mathrm{d}\Omega_2^2$. So one might ask if there are examples which violate boundary causality and have a simple classical solution interpolating between these initial and final surfaces. The answer is yes. The metric induced on a spacelike surface $t = b\,h(r)$ in global AdS has the desired form with $f_b(r) \geq f_0(r)$. To satisfy our asymptotic boundary condition, h must fall off like $1/r^2$ or faster. As a concrete example, one can take $h(r) = (r^2+1)^{-1}$ which leads to

$$f_b(r) = \frac{(r^2+1)^3}{(r^2+1)^2 - 4b^2r^2}, \tag{3.8}$$

defined for $b^2 < 1$. Global AdS clearly interpolates between two such surfaces.

Alternatively, to match a standard static surface in AdS, one can simply make the parameter b in our earlier examples time-dependent near the initial and final surfaces and set it to zero on them. More generally, one can match any given initial and final metric by making $g_{(b)}$ time-dependent near those boundaries without affecting the causality violating region in the middle. Furthermore, since the action is a global property of

the spacetime, we can modify the metric away from the causality violating region while making the action take any value we want, e.g., the same as pure AdS.

The set of metrics with the same action as AdS is a codimension-one surface in the space of metrics. So the metrics can vary in many ways without changing S_g. Furthermore, if boundary causality is violated in one metric g, it is violated in an open neighborhood of g. This is because if x is timelike-related to y in one metric, it remains timelike-related in all nearby metrics. So there are many causality violating metrics that are not suppressed by $e^{\mathrm{im}S_g}$ in the path integral.

Although we have focused on four-dimensional examples, it is clear that similar examples exist in all dimensions greater than two.

3.3 Operator dictionaries

Perhaps the most general and explicit statement of a holographic duality which makes sense irrespective of energy scale is as an equivalence between partition functions.[4] We thus take the proposal of [86, 41] as a well-established starting point, and postulate equivalent bulk and boundary partition functions,

$$\mathcal{Z}_{\mathrm{bulk}}[\phi_0] = \mathcal{Z}_{\mathrm{bdy}}[\phi_0], \tag{3.9}$$

as a general statement of holographic duality. Here, $\mathcal{Z}_{\mathrm{bdy}}$ is defined on some fixed Lorentzian manifold $(\mathcal{B}, \gamma)$, whereas the bulk theory has $\mathcal{Z}_{\mathrm{bulk}}$ path-integrated over space-

[4]Recent discussions have cast doubt even on this basic original postulate – see e.g. [83, 84, 85] for more details on the gravity/ensemble interpretation of the AdS/CFT correspondence. Concrete examples of these subtleties have mostly arisen within two-dimensional models of gravity, where there is not a sharp and general sense in which the bulk can violate boundary causality. Nonetheless, were these to extend to higher-dimensions, we would still expect our arguments to apply: The vanishing of commutators at spacelike separation will be preserved under ensemble averages over reasonable theories, and our analysis of the bulk side would be unchanged.

times $(\mathcal{M}, g)$ having $(\mathcal{B}, \gamma)$ as their conformal boundary. The notation ϕ_0 should be understood as a placeholder for all boundary conditions for dynamical fields on the bulk side, and as sources of operator deformations of the action on the boundary side. To make progress beyond the formal statement of (3.9), most work in the literature restricts to a saddle point approximation or perturbative corrections to it in a large N expansion. Here we test one aspect of (3.9) as a statement of holography in full quantum gravity, i.e., nonperturbatively in G.

In order to study real-time correlation functions, it is assumed that (3.9) applies in Lorentzian signature. From the standpoint of the boundary theory, clearly $\mathcal{Z}_{\rm bdy}[\phi_0]$ is just a standard field-theoretic generating functional. Explicitly [41],

$$\mathcal{Z}_{\rm bdy}[\phi_0] = \left\langle \exp\left\{ \mathrm{i}m \int_{\mathcal{B}} \sum_{\alpha} \phi_0^{\alpha}\, \mathcal{O}_{\alpha} \right\} \right\rangle_{\rm bdy} , \tag{3.10}$$

where $\langle\,\cdot\,\rangle_{\rm bdy}$ denotes the boundary path integral over quantum fields, and each $\mathcal{O}_{\alpha}$ is a gauge-invariant operator sourced by ϕ_0^{α}. In light of (3.9), the bulk object $\mathcal{Z}_{\rm bulk}[\phi_0]$ may be regarded as a generating functional of boundary correlation functions as well. As such, a general time-ordered n-point correlation function may be computed via

$$\langle \mathcal{T}\mathcal{O}_n(x_n)\cdots\mathcal{O}_1(x_1)\rangle_{\rm bdy} = \frac{1}{\mathrm{i}m^n} \frac{\delta}{\delta\phi_0^n(x_n)} \cdots \frac{\delta}{\delta\phi_0^1(x_1)} \left. \frac{\mathcal{Z}_{\rm bulk}[\phi_0]}{\mathcal{Z}_{\rm bulk}[0]} \right|_{\phi_0=0} , \tag{3.11}$$

where $\mathcal{T}$ denotes the time-ordering operator with respect to boundary time. The rationale so far is the one first proposed by [86, 41] and later coined the "differentiate dictionary" in [87]. Observe that, as presented here, this differentiate dictionary is an immediate implication of the basic postulate (3.9).

In practice though, one usually takes a leap and follows the logic of [88] (and implicitly [89]) to argue that a boundary correlator should be nothing but an appropriate limit of

bulk ones. More specifically, if ϕ is the bulk field dual to $\mathcal{O}$ and the latter has conformal dimension Δ, then one may propose[5]

$$\langle \mathcal{O}_n(x_n) \cdots \mathcal{O}_1(x_1) \rangle_{\text{bdy}} \overset{?}{\propto} \int \mathcal{D}g \, e^{\text{i}mS_g} \lim_{z \to 0} z^{\sum_\alpha \Delta_\alpha} \langle \phi_n(x_n, z) \cdots \phi_1(x_1, z) \rangle_g \,, \tag{3.12a}$$

where $\langle \cdot \rangle_g$ stands for the bulk path integral over quantum fields in a fixed metric g, and (x, z) are Fefferman-Graham coordinates [90] as canonically defined near the conformal boundary of any asymptotically locally AdS spacetime. (These provide a diffeomorphism invariant location for the bulk operators.) Alternatively, one could have chosen to switch the metric integration and the $z \to 0$ limit and write

$$\langle \mathcal{O}_n(x_n) \cdots \mathcal{O}_1(x_1) \rangle_{\text{bdy}} \overset{?}{\propto} \lim_{z \to 0} z^{\sum_\alpha \Delta_\alpha} \int \mathcal{D}g \, e^{\text{i}mS_g} \, \langle \phi_n(x_n, z) \cdots \phi_1(x_1, z) \rangle_g \,. \tag{3.12b}$$

We will consider both of these options below. While physically both (3.12a) and (3.12b) seem like reasonable proxies for boundary correlators, it is not obvious that they are equal, or whether they are mathematically consistent with (3.11).

The prescriptions in (3.12) are equivalent when gravity is treated semiclassically, and in this case were referred to as the "extrapolate dictionary" in [87], where their consistency with the differentiate one was carefully studied. Their findings established a nontrivial perturbative equivalence between these two dictionaries for self-interacting scalar fields in a fixed background with Euclidean AdS asymptotics.[6] Our main deviation from [87] is to study Lorentzian physics and at a nonperturbative level.

Let x and y be two boundary points at spacelike separation with respect to the

[5]Time-ordering operators are intentionally dropped from this expression. Whereas on the boundary the time order is solely dictated by the insertion points, in the bulk it subtly depends on the integrated-over metric in the gravitational path integral. This will be addressed in Section 3.4.

[6]They argued for their equivalence also with perturbative gravity in the bulk turned on, though some caveats arise in this case. Either way, as they carefully acknowledge, their considerations are intrinsically perturbative in nature.

boundary metric. In this case, the commutator of local operators inserted at these points clearly vanishes from the standpoint of the CFT. In the bulk, unless otherwise stated, it will in general be assumed that the theory has a perfectly well-defined and physical semiclassical limit whose on-shell metrics obey boundary causality. Despite this, there appears to be a problem with the extrapolate dictionary stemming from the presence of off-shell contributions to the gravitational path integral that do violate boundary causality.

Since both alternatives in (3.12) appear to have similar problems, we consider (3.12a) for definiteness here. For a commutator of an operator $\mathcal{O}$ at two points x and y which are spacelike-separated with respect to the boundary metric, (3.12a) becomes

$$0 = \langle [\mathcal{O}(x), \mathcal{O}(y)] \rangle_{\text{bdy}} \overset{?}{\propto} \int \mathcal{D}g \, e^{\text{i}mS_g} \lim_{z \to 0} z^{2\Delta} \langle [\phi(x,z), \phi(y,z)] \rangle_g \,. \tag{3.13}$$

Since the commutator on the right vanishes in all metrics that respect boundary causality, the integral over g can only receive contributions from bulk metrics for which x and y are causally related. As we have seen, these contain open sets of metrics and will generically yield nonzero commutators. However, if the extrapolate dictionary was valid, the integral on the right would have to vanish. Furthermore, any operator-valued function of the commutator that vanishes on the boundary when the commutator does should also vanish in the bulk. In other words, there are infinitely many integrals like (3.13) which the extrapolate dictionary says should give zero. Since the weighting $e^{\text{i}mS_g}$ and measure are the same while the integrands change, we do not expect all such path integrals to be identically zero. It thus appears that the extrapolate dictionary is not consistent with boundary causality.

3.4 Resolution

In the previous section, we have discussed the two holographic dictionaries and illustrated how the application of the extrapolate dictionary appears to lead to a causal issue. In this section, we will explain a subtlety that was omitted from the above discussion. With a proper interpretation of this subtlety, both dictionaries are consistent with boundary causality.

The easiest way to understand the commutator uses path integrals, i.e.,

$$\langle [\phi(p), \phi(q)] \rangle_g \equiv \langle \phi(p)\phi(q) \rangle_g - \langle \phi(q)\phi(p) \rangle_g \,, \tag{3.14}$$

each term computed via a path integral over field space. Here we have used the notation for a bulk computation on a fixed metric g, but our discussion here is general: Replacing $(\mathcal{M}, g)$ with $(\mathcal{B}, \gamma)$ does the job for the boundary field theory. Now, the path integral on the original manifold always computes a time-ordered correlator. To compute an out-of-time-order correlator, one needs to manufacture from the original manifold a *timefold*. It can be done as follows. Consider the n-point function for a field ϕ,

$$\langle \phi_+ | \phi(p_n) \cdots \phi(p_2)\phi(p_1) | \phi_- \rangle_g \,, \tag{3.15}$$

where $\phi_\pm$ are the initial and final states on Cauchy surfaces $\Sigma_\pm$.[7] Starting at Σ_-, one should use the forward evolution operator $\mathcal{U}$ up to a Cauchy surface containing p_1, at which point $\phi(p_1)$ can be inserted. To continue while preserving the ordering, one should then evolve to p_2 before inserting the second operator $\phi(p_2)$. If p_2 is to the future of

[7]Standard procedures exist for defining the initial and final states in the bulk given the initial and final states on the boundary. For instance, if the boundary initial state is vacuum, we can pre-pare the corresponding bulk initial state using a Euclidean path integral with no operator insertion (and "post-pare" the final state similarly). More generally, the boundary contour contains both Euclidean and Lorentzian sections, and it serves as boundary conditions for the bulk path integral [91, 92].

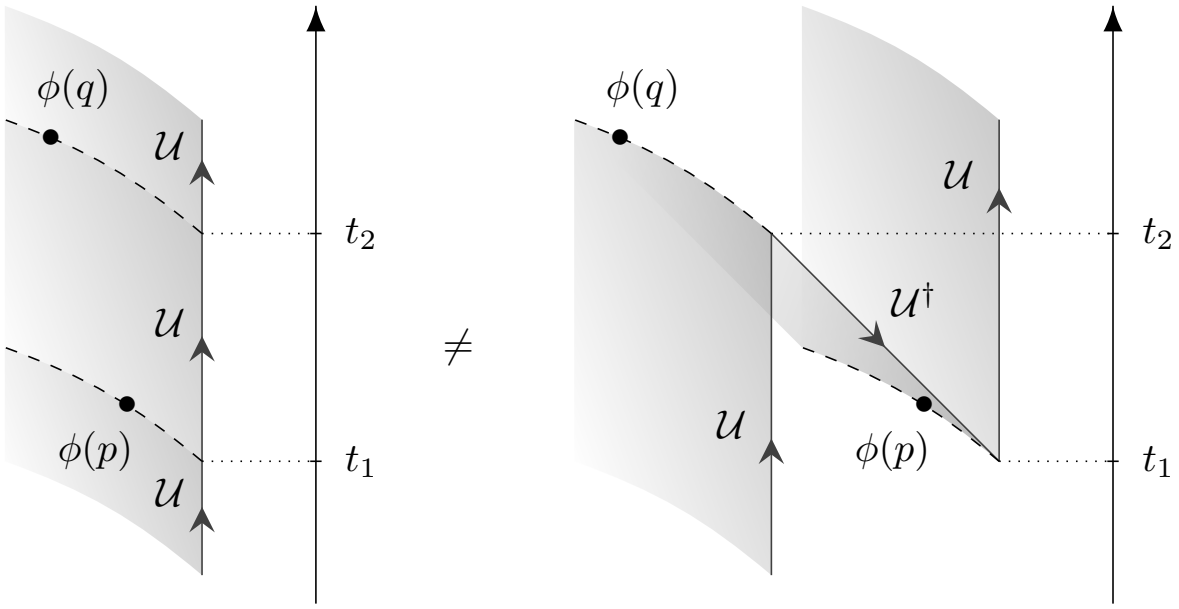


Figure 3.1: Inequivalent timefolds for the computation of two-point correlation functions involving a field operator ϕ inserted with different time orderings. It is assumed that point q is to the future of p, where p and q respectively lie at times t_1 and t_2, with $t_2 > t_1$. The left figure illustrates the computation of a standard time-ordered correlator $\langle\phi(q)\phi(p)\rangle$, where time-folding is trivial and time-evolution is simply implemented by $\mathcal{U}$ everywhere. In contrast, the right figure shows the nontrivial timefold required for the computation of the out-of-time-order correlator $\langle\phi(p)\phi(q)\rangle$, where backwards time-evolution via $\mathcal{U}^\dagger$ is needed between insertions. Generically, these give different results and thus one expects $\langle[\phi(p), \phi(q)]\rangle \neq 0$.

p_1, one could just use $\mathcal{U}$ again, but if p_2 is to the past of p_1, one should evolve back with the backwards evolution operator $\mathcal{U}^\dagger$ to where p_2 is for the insertion of $\phi(p_2)$. Then this procedure should be repeated until all n insertions are carried out properly before finally evolving to Σ_+. The whole process then creates what is called a timefold, a new zigzagged spacetime that ensures the correct ordering of operators. On each backward component, the path integral has a weighting $e^{-\mathrm{im}S_g}$, in contrast to the usual weighting $e^{\mathrm{im}S_g}$ on the forward components. Fig. 3.1 gives an example of this. Then, if the two points are timelike-related, the commutator, being a difference between two correlators computed on distinct timefolds, will be generically nonzero. In the case of spacelike-separated points, however, the two points can be inserted on the same Cauchy surface.

This means that the same timefold qualifies for computation of either ordering, yielding a vanishing commutator. We emphasize again that the discussion here applies to both boundary commutators $\langle[\mathcal{O}(x),\mathcal{O}(y)]\rangle_{\rm bdy}$ and bulk commutators $\langle[\phi(x,z),\phi(y,z)]\rangle_g$ on a specific metric, and therefore one has both boundary timefolds and bulk timefolds.

In general, the field theory $\mathcal{Z}_{\rm bdy}$ is naturally defined on some manifold $\mathcal{B}$, and $\mathcal{Z}_{\rm bdy}[\mathcal{B},\phi_0]$ is the generating functional of time-ordered correlation functions on $\mathcal{B}$. To compute an out-of-time-order correlator, one needs to extend $\mathcal{Z}_{\rm bdy}$ to an appropriate timefold spacetime $\mathcal{F}$ constructed out of $\mathcal{B}$ as described above. Then $\mathcal{Z}_{\rm bdy}[\mathcal{F},\phi_0]$ would allow one to compute the desired correlator. The statement of holography at the level of partition functions must account for this. Hence one has to more explicitly rewrite (3.9) as

$$\mathcal{Z}_{\rm bulk}[\mathcal{F},\phi_0]=\mathcal{Z}_{\rm bdy}[\mathcal{F},\phi_0], \tag{3.16}$$

where now $\mathcal{Z}_{\rm bulk}[\mathcal{F},\phi_0]$ path-integrates over all metrics with the timefold $\mathcal{F}$ as conformal boundary, and boundary conditions ϕ_0 appropriately distributed on $\mathcal{F}$.

For a causal and unitary boundary theory, if x and y are spacelike-separated, $\langle\mathcal{O}(y)\mathcal{O}(x)\rangle$ can be computed on either a trivial timefold (i.e. the original spacetime with no foldings), or a nontrivial timefold with $\mathcal{O}(x)$ on the first sheet[8] and $\mathcal{O}(y)$ on the second sheet (or vice versa) with the same result. This is just the statement that evolution forward and back – without operator insertions – is the identity. It is not obvious that the corresponding bulk partition functions will agree since we do not know (independent of holography) that the gravitational path integral describes unitary evolution. This leads to a potential ambiguity in the definition of $\mathcal{Z}_{\rm bulk}$. Since we are trying to understand how a basic property of the boundary theory follows from the bulk path integral, we have to resolve this ambiguity. If the boundary theory is causal and unitary, we adopt a *minimal timefold* approach,

[8]We will call the regions of spacetime separated by the creases the "sheets" of the timefold.

in which a fold is introduced only when needed to represent operators at causally-related points where the later operator appears first in the correlator. When folding minimally, backward evolution just needs to sweep causal diamonds between insertions at non-time-ordered points (including small neighborhoods for spacelike creases). Minimal timefolds are introduced to disambiguate inequivalent computations which should nonetheless give equivalent results—if the boundary theory is acausal or non-unitary, however, results will generically disagree and the minimal-timefold prescription does not apply.

We now show that with the minimal timefold, both the differentiate and extrapolate dictionaries predict no violation of boundary causality. Consider first the differentiate dictionary. Equation (3.11) tells us how the time-ordered correlators on the boundary are computed from the bulk, but we have so far not included out-of-time-order correlators in this equality. Extending the dictionary to general n-point functions, one has

$$\langle \mathcal{O}_n(x_n) \cdots \mathcal{O}_1(x_1) \rangle_{\text{bdy}} = \frac{1}{\text{im}^n} \frac{\delta}{\delta \phi_0^n(x_n)} \cdots \frac{\delta}{\delta \phi_0^1(x_1)} \left. \frac{\mathcal{Z}_{\text{bulk}}[\mathcal{F}, \phi_0]}{\mathcal{Z}_{\text{bulk}}[\mathcal{F}, 0]} \right|_{\phi_0 = 0}, \tag{3.17}$$

where $\mathcal{F}$ is a minimal *boundary* timefold constructed so as to order the operator insertions as given (cf. (3.11) when the left-hand side is time-ordered so $\mathcal{F}$ is just the trivial timefold $\mathcal{B}$). If x and y are two spacelike-separated points on the boundary, the minimal timefold for a two-point correlator is trivial, i.e., it is just the original spacetime. Since this is true regardless of the order of the operators, the only difference between the two terms in the commutator is the order in which one takes the derivatives with respect to ϕ_0. Since these derivatives commute, the commutator obviously vanishes. Note that this is completely independent of whether x and y are causally related with respect to some bulk metrics. All we use is that the integral over all metrics and matter fields is some function of the boundary conditions ϕ_0 on a trivial timefold. If x and y are causally related on the boundary, the situation is different. In that case, the two terms in the commutator

require different minimal timefolds: a trivial one $\mathcal{F}$ for the time-ordered correlator, and a nontrivial one $\mathcal{F}'$, for the out-of-time-order correlator. In the latter case, the source for the earlier operator is moved to the second sheet, so the commutator can be nonzero.

We now turn to the extrapolate dictionary (3.12). Consider first (3.12a). For a bulk metric relating x and y causally, one would expect $\langle\phi(x,z)\phi(y,z)\rangle_g \neq \langle\phi(y,z)\phi(x,z)\rangle_g$, as a result of being computed on different bulk timefolds. This nonzero commutator on g is the origin of the casuality puzzle. However, there is a subtlety: The boundary condition on g must be the same as for the differentiate dictionary. Namely, one must have a trivial boundary timefold when x and y are spacelike-related on the boundary. If one computes the commutator by a path integral over fields on the bulk metric g, the causality puzzle is resolved as follows. Recall that a field path integral on a trivial timefold always gives the time-ordered correlator. So when the two operators are in the asymptotic region, inside the bulk path integral each of the two terms in the commutator (3.14) should come with a time-ordering with respect to g, $\langle\mathcal{T}\phi(x,z)\phi(y,z)\rangle_g = \langle\mathcal{T}\phi(y,z)\phi(x,z)\rangle_g$, yielding a vanishing commutator. Indeed, if the two points are timelike-related in the bulk, in the limit $z \to 0$ a non-time-ordered correlator would require a bulk metric with a nontrivial timefold asymptotically, violating our boundary condition. In this case, the naive bulk commutator $\langle[\phi(x,z),\phi(y,z)]\rangle_g$ plays no role in computing the CFT commutator $\langle[\mathcal{O}(x),\mathcal{O}(y)]\rangle_{\text{bdy}}$.

Even with no timefold on the boundary, the bulk path integral includes timefolds that become trivial asymptotically.[9] Intuitively, the amount of time that one evolves backward goes to zero as $z \to 0$. This has no effect on the differentiate dictionary, since the differential operators only act on the boundary conditions. However, for the extrapolate dictionary, it introduces an ambiguity in the location of the bulk operators

[9]This is closely related to the fact that the bulk path integral should impose gravitational constraints which necessitates integration over both positive and negative lapse [93]. We thank Don Marolf for discussion about this point.

ϕ. If there are different sheets of the bulk timefold, then one has to specify which sheet the operator is on, in addition to giving its location on the sheet. If we use (3.12a) one expects this ambiguity to have no effect since we take the limit $z \to 0$ for each metric where the timefold becomes trivial.

In contrast, if we use (3.12b) there is a potential problem. For any nonzero z, there are bulk metrics where for timelike-separated points (x, z) and (y, z) there is a timefold that is trivial asymptotically, but both the time-ordered and out-of-time-order correlators can be obtained by placing the operators on different sheets.[10] In other words, the bulk contains a timefold that allows a nonzero commutator, but in the region outside the location of the operators, the timefold decays and completely disappears at the boundary. Under these conditions, it would appear that the integrand of (3.12b) can be nonzero, and one again is left with the puzzle of why the integral over metrics vanishes exactly.

However this conclusion follows only if we allow the bulk operators to move from one sheet of a timefold to another depending on the order of operators in a correlator. Since the choice of sheet is not fixed by the boundary correlator that we are trying to reproduce, one can adopt the rule that one fixes the ambiguity in the extrapolate dictionary by picking one sheet of a timefold for each operator independent of the location of the operator in the correlator. With this understanding, the integrand in (3.12b) remains zero for each g, consistent with boundary causality.

Finally, we extend the example of time-ordering the bulk path integrand when the two points are spacelike-separated on the boundary to general n-point functions and to allow for timefolds in the bulk interior. The two versions of the extrapolate dictionary

[10] We are using the fact that since the bulk timefolds do not have to be minimal, a nonzero commutator can be obtained from a single timefold, by moving the earlier operator from one sheet to another. For example, on the right-hand side of Fig. 3.1, one can compute the commutator by moving $\phi(p)$ to the first sheet.

then read

$$\langle \mathcal{O}_n(x_n)\cdots\mathcal{O}_1(x_1)\rangle_{\text{bdy}} \propto \int \mathcal{D}g\, e^{\text{im}S_g} \lim_{z\to 0} z^{\sum_\alpha \Delta_\alpha} \langle \mathcal{P}\phi_n(x_n,z)\cdots\phi_1(x_1,z)\rangle_g\,, \tag{3.18a}$$

$$\langle \mathcal{O}_n(x_n)\cdots\mathcal{O}_1(x_1)\rangle_{\text{bdy}} \propto \lim_{z\to 0} z^{\sum_\alpha \Delta_\alpha} \int \mathcal{D}g\, e^{\text{im}S_g} \langle \mathcal{P}\phi_n(x_n,z)\cdots\phi_1(x_1,z)\rangle_g\,, \tag{3.18b}$$

where g is restricted to metrics that asymptote to the minimal boundary timefold required to order the field theory correlator correctly (just as for the differentiate dictionary in (3.17)) and $\mathcal{P}$ is the ordering operator enforced by the field path integral on g, which reduces to the time-ordering operator $\mathcal{T}$ when g is a trivial timefold (cf. the order followed by the arrows in Fig. 3.1).

3.5 Discussion

In this paper, we have explained how the bulk theory manages to respect causality of a unitary boundary theory despite the bulk path integral involving boundary causality violating metrics. To do so, we formulated the bulk computation of correlators using minimal timefolds, where it becomes manifest that boundary microcausality prevails, i.e., local operators still commute at spacelike separation. With non-minimal timefolds we would still expect microcausality to hold so long as the boundary theory is causal and unitary. This way, however, one would have to rely on unexpected cancellations in the integral over metrics—in this sense, minimal timefolds are nothing but a simpler representation of the problem (cf. charge conservation via symmetry arguments vs checking all orders in perturbation theory).

Our results apply to both the differentiate dictionary as given in (3.17) and the

extrapolate dictionary in the form (3.12a). It also applies to the latter if one integrates first, with a suitable rule for how to place operators on bulk timefolds that are trivial at the boundary. The basic reason for this is that a nonzero commutator for two asymptotic bulk operators requires a bulk timefold that is nontrivial at infinity, but the minimal timefold for two spacelike-separated points on the boundary is trivial. So the bulk dual of the commutator of two field theory operators at spacelike-separated points vanishes.

The bulk dual of the commutator of two stress energy tensors on the boundary does not require any bulk matter fields. Nevertheless our argument using the differentiate dictionary still applies. Since the boundary metric is the source for the stress tensor, one should compute the path integral over bulk geometries with a general boundary metric. One then functionally varies the boundary metric at the location of the stress tensors. If the stress tensors are spacelike-related, there is no timefold on the boundary and hence the commutator vanishes. (There is an issue with even defining the extrapolate dictionary nonperturbatively in this case arising from the apparent need to split the degrees of freedom in the metric into background and fluctuations.) Our argument also applies to fermionic operators which anticommute at spacelike separations. For the differentiate dictionary, the difference in sign arises since the sources for these operators are also fermionic and hence their variations anticommute.

Although there is no problem with commutators at spacelike-separated points, boundary causality violating metrics do contribute to general field theory correlators. It would be interesting to understand what, if any, are the implications of this quantum gravity effect. We do not believe there are examples of holography in which a bulk classical solution violates boundary causality, but if there are, the boundary theory would have to be acausal or non-unitary. In this case, computations are timefold-dependent and our resolution does not apply.

Our discussion in this paper has been motivated by the microcausality property of the

boundary field theory, which requires local operators to commute at spacelike separation. However, there are other properties the field theory is expected to have, and they in general impose further constraints on the bulk state classically and semiclassically. For example, the invariance of von Neumann entropy under unitary transformations requires the causal wedge be contained within the entanglement wedge [62, 94]. (This is a stronger requirement as it implies the boundary causality condition [78].) As another example, a stricter causality requirement states that, for two bulk points causally connected in the bulk, boundary regions encoding each of the two points cannot be totally spacelike [95]. (This extends our discussion of the commutator between local operators to operators with support in a subregion.) Just like what we have been discussing, perturbatively it is expected that bulk states in physical theories will satisfy these conditions, but in a nonperturbative quantum gravitational path integral there will be configurations violating them. An interesting future direction would be to understand how the bulk path integral preserves these properties.

Chapter 4

Exploring strong-field deviations from general relativity via gravitational waves

> The years of anxious searching in the dark, with their intense longing, their alternations of confidence and exhaustion, and final emergence into light—only those who have experienced it can understand that.
>
> Albert Einstein

4.1 Introduction

With a steadily increasing number of gravitational wave observations from coalescing binaries[96], and with imminent new data from very long baseline interferometric (VLBI) observations of apparent black holes[97], we have entered a new era of observationally

testing strong-field gravity. As it endures increasingly precise tests in this strong field realm, general relativity (GR) so far appears to be holding firm.

Modifications to the classical behavior of black holes are of course possible, and many models with such modified behavior have been considered, with various motivations. But there is one very compelling reason to believe that a classical description of black holes *must* ultimately be modified: such a description appears inconsistent with quantum mechanics, which is thought to govern all physical phenomena. At first it was believed that this might only be important very near the center of a black hole, or in the late stages of black hole evaporation, and would be irrelevant outside the horizon of large black holes. However, deeper examination of the requirement of consistency of black hole evolution with quantum mechanics has led to a widespread view[98, 99, 100, 101, 102, 103, 104] that there need to be important corrections to classical black hole behavior *at horizon scales*. This is due to the requirement that for ultimate unitarity of black hole evolution, information needs to transfer out of a black hole while it is still of macroscopic size, in direct contradiction with a description based on classical geometry, together with small perturbations due to local quantum fields.

This raises a key question: can the modifications to classical behavior necessary for quantum consistency have observable effects?[1] Of course, often when physics has opened new observational regimes, new phenomena have been found, so it is important to model and investigate possible new phenomena in the strong gravity regime, independent of this question. But, quantum consistency serves as a particularly important motivator to focus on the specific class of effects that can restore consistency between the existence of black hole-like objects and quantum mechanics.

This leads to a particular focus on the near-horizon region, $r \sim 2M$ for a black hole

[1]For some earlier discussion of this question, see [105, 106, 107]. For other discussion of tests for deviations from GR for black holes, see *e.g.* [108, 109, 110, 111].

without spin. The origin of the unitarity problem (in some views, really a crisis) is in the physics of Hawking radiation, which can be thought of as originating near[2] $r \sim 3M$. Quantum consistency strongly motivates the possibility of new quantum effects in this region, or closer to the horizon[103].

A variety of scenarios have been considered for near-horizon modifications necessary for quantum consistency. The resulting objects, whose description is supposed to be consistent with quantum mechanics, have varying degree of departure from the classical black hole (CBH) description, depending on the scenario. In order not to prejudice a particular scenario at the outset, but given their quantum origin, we will refer to these objects generically as *compact quantum objects* (CQOs).[3]

A central question then becomes what non-CBH properties CQOs have, and how these might be detected. While VLBI is expected to provide an important window,[4] this paper will focus on gravitational waves. In order to predict the gravitational wave signature of coalescence resulting from a particular scenario or model, one needs to describe the full nonlinear evolution of the binary, analogous to the nonlinear evolution of GR. This *problem of nonlinear evolution* is a first challenge. This is particularly true given that while existing models for CQOs exhibit some of the behavior important for quantum consistency, they are not yet derived from a more complete underlying theory of quantum gravity. This is an example of a more general problem in observationally testing GR – the lack of good foils or alternatives to GR for describing nonlinear evolution of alternatives to CBHs, in the strong-gravity regime.

A second challenge for tests of highly compact objects is what we call the *problem*

[2]For recent discussion, see [112].

[3]A related terminology is exotic compact object (ECO). A CQO is intended to be something more specific than an ECO, since CQOs are presumed to owe their existence to the quantum dynamics necessary to make quantum evolution consistent for CBH-like objects – and quantum mechanics is certainly not exotic.

[4]Some discussion of this appears in [105, 113, 107].

of gravitational obscuration. Suppose we consider the collision of two objects that differ from CBHs only in a region close to the horizon. We might in general expect there to be little deviation from GR in the gravitational wave signal until the discrepant regions meet. However, this happens when the two objects are deep inside a gravitational well and we might expect that if the objects coalesce to form an object with horizon-like behavior, most of the discrepant signal is also absorbed into this final object and is not observed at infinity[106]. This potentially considerably lowers observational sensitivity.

Of course, it may be that there are signatures of CQO properties from inspiral, and CQO behavior may also affect observations by changing absorption and reflection probabilities for gravitational waves, but these may be more subtle effects.

Note that this discussion contrasts with another proposal for modifications to the CBH signal, that of gravitational echoes[114, 115, 116]. The key difference arises from the fact that the echo story assumes that the two objects coalesce to immediately form an object that does not have horizon-like behavior, *e.g.* by having or rapidly developing a "hard" barrier, from which the echoes reflect. This represents a more extreme departure from CBH behavior than appears to be required for quantum consistency. We instead focus on the possibility that the effects needed for a reconciliation with quantum mechanics involve less drastic departure from CBH behavior.

A goal of this paper is to begin work to investigate these related problems, in some simple models for departure from CBH behavior. In fact, a first model for a departure from a CBH merger is a merger of neutron stars, whose gravitational signatures exhibit important features.[5] Of course neutron stars cannot have the masses seen in many recent detections, so more general models are needed. But this suggests one general approach to investigating departures from CBHs that have consistent nonlinear evolution, namely to parametrize them in terms of an effective stress tensor, and in even simpler models, in

[5]See, *e.g.*, [117].

terms of an effective equation of state (EOS). Such models, if they produce objects with relevant masses, begin to provide simple foils for coalescence of CBHs.

After further discussion of motivation and CQO scenarios in the next section, section III will describe such an effective approach and its use to formulate simple models to test aspects of possible modifications to CBH behavior, such as with CQOs. Section IV will investigate spherically-symmetric solutions for such models, and in particular those with an EOS that permits them to be highly compact, in line with preceding comments. Section V will discuss parameters and features of such solutions, and their possible connection to observable deviations in gravitational wave signatures. While the models we study are limited in their ability to capture possible CQO properties, they should allow initial investigation of some of the basic questions regarding gravitational wave sensitivity to very compact departures from CBHs.

In particular, one ultimate goal is to understand how sensitive gravitational wave observations can be to highly compact deviations from CBHs, given the obscuration question. The models we describe provide a way to set up the problem, but probably the best way to test the role of obscuration – and other aspects of sensitivity to highly-compact deviations – is through numerical evolution of the kinds of solutions that we provide. This is an important step for future work.

In short, now that strong gravitational physics is an observational subject, it is important to try to parameterize possible deviations from the predictions of GR, and to test them against observation. This paper will begin to investigate some models for certain kinds of deviation from classical black hole behavior, in an effective approach.

4.2 CQO models and observational challenges

Gravitational dynamics has been quantitatively well tested primarily in weak-field regimes, perturbatively close to flat space (for a recent review, see [118]). This leaves as an important question the possibility of deviations from GR in strong-field regimes. GR is a mathematically beautiful and compelling framework, and it is commonly believed that it will be significantly modified only in strong *curvature* regimes. However, there are forceful arguments for some modification of the combined frameworks of GR and local quantum field theory (LQFT) in situations where classical GR predicts a black hole horizon would form. The vicinity of such horizons can also be thought of as strong-field regions; although for big black holes they are not expected to have high curvatures, the metric near a black hole horizon corresponds to a large perturbation of an ambient Minkowski space in which the black hole resides.

A primary motivation to expect such modification is the combination of facts: 1) black hole-like objects appear to exist and 2) attempts to describe black holes as objects in a quantum Universe, based on a combination of LQFT and GR, appear to produce a contradiction with basic principles of quantum mechanics. After much exploration of this "information paradox" or "unitarity crisis," many who have thought deeply about this puzzle have concluded that modifications to GR+LQFT are required, not just at very short distances, but, in the context of black holes, at scales given by the horizon size, which can be arbitrarily large for big black holes. This appears to be the most conservative approach to reconciling the existence of compact objects that have basic features of classical black holes with quantum mechanics.

A number of proposals have been considered for modifications to the GR+LQFT description at a scale given by the radius R of a classical black hole (BH) horizon, or at even larger scales, while respecting quantum principles. These can be divided into some

broad scenarios for CQOs:

1. *Massive remnants.* A very general scenario was proposed in [98]: at some stage in its evolution, a BH transitions to a new kind of star-like "massive remnant," truncating the Schwarzschild spacetime outside the would-be horizon, analogous to, *e.g.*, a neutron star.[6] In such a scenario the new physics outside the horizon is assumed to be characterized by some short (microscopic) distance scales, and thus be "hard;" one measure of this is typical momentum transfer to infalling matter.[7] A number of more specific variants of this basic hard picture have been proposed. These include gravastars[119], fuzzballs[101], firewalls[103], and Planck stars[120]. These may differ in their evolution subsequent to the transition.

2. *Soft gravitational atmospheres.* Another possibility is a "softer" departure from CBHs, in a near-horizon "atmosphere" region, which is similar to the near-horizon region of a CBH and in particular permits infalling observers to pass without undue violence[102, 121, 122, 123, 124]. The characteristic softness scale should be determined by a distance scale that at the least grows with black hole radius. The deviations present in the atmosphere are constrained by the fact that interactions with them must suffice to transfer information from the BH state to the environment of the BH, so that evolution is unitary. If these interactions are assumed to couple universally to all fields, two variants have been described. One is "strong" [123], with an effective description of the atmosphere in terms of $\mathcal{O}(1)$ but soft state-dependent metric fluctuations. A more minimal scenario is the "weak" scenario of [124], in which very small state dependent metric fluctuations are found to be sufficient to transfer information.

[6] A variant proposal is that such a massive remnant forms before a BH can form.

[7] Either the gravitational field may be characterized by hard scales, or other fields or structure may be characterized by such hard scales.

3. *Long distance modification of locality.* A third possibility is modification to the locality structure of LQFT on scales $\gg R$. A standard example of this is the ER=EPR proposal[125, 104], where mere entanglement of remote degrees of freedom is interpreted as corresponding to formation of a connection between them via a spacetime bridge.

In each of these scenarios for CQO behavior, a very interesting and important question is whether the required new effects could have any observational implications. This question becomes even more compelling with growing prospects for testing strong field gravity, both through gravitational wave observation with LIGO/VIRGO, and in the future with LISA, and with VLBI, specifically with EHT.

These two observational approaches have key differences. VLBI effectively provides an electromagnetic picture of the geometry, resulting from passage of light from, *e.g.* accreting matter, through the region near the (would-be) horizon. Thus, all that is required of a scenario is a prediction of how light propagates or interacts with the CQO replacement of a CBH. For example, in the "soft, strong" proposal of [123], one can perform ray-tracing through the perturbed geometry to determine possible modifications of images that could be visible to EHT[113]. Similar predictions of electromagnetic images are in principle possible from any other sufficiently explicit scenario.

As noted, tests of scenarios via gravitational waves (GWs) face the problem of nonlinear evolution; they require dynamics as opposed to simply providing "snapshots" of the configuration. Specifically, the prediction of the GW signal requires prediction of the full nonlinear evolution of the CQOs, analogous to the nonlinear evolution of GR. Although one or more of the broad scenarios outlined above may produce a logically-viable description of the quantum behavior, none of them is yet advanced enough to be based on an understanding of underlying gravitational dynamics that is sufficiently developed

to make predictions about the nonlinear evolution of CQO replacements for CBHs.

The second problem described above, obscuration, is also a potentially important challenge to using GWs as probes of novel structure that could modify a CBH. Specifically, suppose a CBH is replaced by a CQO departing from CBH behavior out to a radius[8] $R_a = R + \Delta R_a$. When two such objects collide after the end of inspiral, one naïvely expects significant modification to the GW signature from the regime where the modified structures come close to touching[106]. But, if $\Delta R_a \lesssim R$, this occurs when the CQOs are deep within their mutual gravitational well, suggesting that a significant part of the signal modification may be absorbed in the final object, if it indeed has basic features of a CBH. This seems particularly clear if $\Delta R_a \ll R$. Indeed, there are arguments that much of the final GW signal from coalescence of BHs is generated in the vicinity of the light ring of the final BH[114] (though for some counterpoints, see [126]). So, an important question is to what extent GW observations can be sensitive to possible near-horizon quantum structure.

Given the growing and anticipated amount of GW data and the lack of predictions of nonlinear evolution for complete quantum scenarios, one reasonable approach is to begin by exploring the questions of sensitivity of observations to new structure and obscuration in simple models for modification of CBH behavior. Specifically, if a CBH is replaced by a CQO with different properties, how much effect can this have on the GW signal – how sensitive are GW observations to *any* modification of structure in the near-horizon region? Since answering this question requires nonlinear evolution of the CQOs, one simple way to begin to explore this question is to assume that whatever the full description is of their configuration, it can be approximately described as possessing an effective four-dimensional metric $g_{\mu\nu}$, and that departures from the vacuum Einstein equations can

[8]For spherically symmetric objects, this can be precisely defined in terms of the standard Schwarzschild coordinate r, using the match to the Schwarzschild solution at $r > R_a$.

be consistently and approximately summarized by an effective stress tensor source, $T_{\mu\nu}$, in these equations.[9] If this stress tensor satisfies certain consistency conditions, such as conservation, this provides a model for how to incorporate modifications to CBH behavior with consistent nonlinear evolution.

Various specific models for departure from BH predictions for GW signatures have also been considered, including boson and fermion stars (see *e.g.* [127, 128, 129]) and Proca stars[130]. However, the resulting solutions have characteristic sizes determined by mass parameters of the underlying theory, so do not provide models for quantum behavior of BHs of arbitrary size, and also do not typically achieve the highest range of compactness. For this reason, we explore other forms of the stress tensor.

4.3 Effective approach

The complete quantum description of CQOs replacing BHs is so far unknown, and may at the fundamental level involve different quantum variables than a four-dimensional metric. However, in order to test sensitivity to departures from classical GR, we will assume the existence of a quantum variable $g_{\mu\nu}$ that plays the role of an effective four-dimensional metric, such that $\langle g_{\mu\nu}(x)\rangle$ is well behaved (non-planckian) in a typical state. This may or may not be true in various scenarios – for example in the cases of fuzzballs or firewalls, if a consistent fundamental description even exists for either of these proposals in situations corresponding to large, non-extremal BHs. In either a general such massive remnant scenario, or in that of a soft gravitational atmosphere, there may also be other quantum degrees of freedom that are excited in the vicinity of the would-be horizon. We will model the effect of these, and of possible corrections to classical Einsteinian

[9] In a full quantum theory, these are significant assumptions.

evolution, using an effective stress tensor,

$$\langle G_{\mu\nu}[g]\rangle = 8\pi G\langle T_{\mu\nu}\rangle \ . \tag{4.1}$$

If the underlying fundamental theory *were* a field theory, this would arise from an action

$$S = \int d^4x\sqrt{-g}\left(\frac{R}{16\pi G} + \mathcal{L}\right) \tag{4.2}$$

where $\mathcal{L}$ is a lagrangian summarizing other degrees of freedom as well as, for example, higher-curvature terms. The effective stress tensor is then

$$T_{\mu\nu} = -\frac{2}{\sqrt{-g}}\frac{\delta}{\delta g^{\mu\nu}}\int d^4x\sqrt{-g}\mathcal{L} \ . \tag{4.3}$$

While the origin of the quantum evolution law in a more fundamental description of quantum gravity may not be from such an action, *e.g.* in the case of a soft gravitational atmosphere, working with an effective stress tensor gives an approach to test sensitivity to some types of near-horizon deviations from CBH behavior. Such an effective stress tensor must obey certain consistency conditions; one is conservation,

$$\langle \nabla^\mu T_{\mu\nu}\rangle = 0 \ . \tag{4.4}$$

We ultimately wish to study coalescence of two CQOs in such a model, governed by the evolution law (4.1). We begin by considering the description of the individual objects. In the spherically-symmetric static case, with zero angular momentum, the stress tensor in spherical coordinates $x^\mu = (t, r, \theta, \phi)$ must take the form

$$\langle T^\mu_\nu\rangle = \mathrm{diag}[\rho(r), p_r(r), p_\theta(r), p_\theta(r)] \ . \tag{4.5}$$

The underlying quantum dynamics then determine ρ, p_r, p_θ, subject to conservation (4.4), as well as other consistency conditions. To proceed further, we need more information about relations between these variables, and the metric.

If the properties of the CQO can be described in this fashion, at least approximately, the relations between ρ, p_r, p_θ, and $g_{\mu\nu}$ would depend on the currently unknown full quantum dynamics. A goal of this paper is to begin to investigate sensitivity to such dynamics, replacing CBH behavior in the near-horizon region. Since a primary question is how much of the signal from colliding compact objects is absorbed into the final BH, we can start to explore this sensitivity by considering simplified models for CQOs. One highly simplified but pragmatic approach is to assume that the quantum stress tensor is well-approximated by (4.5), and moreover behaves like an isotropic ideal fluid with an equation of state,

$$p_r = p_\theta = p(\rho) \ . \tag{4.6}$$

In this case, one additional plausible consistency condition is that the speed of sound not exceed the speed of light, requiring

$$p'(\rho) \leq 1 \ . \tag{4.7}$$

For consistency with quantum mechanics, CBHs of arbitrary size must ultimately be replaced by CQOs. As noted above, this is not true for various specific microscopic models for $\mathcal{L}$, such as boson stars (see [131], and references therein), which have maximum masses that depend on the mass of the boson that is coupled to GR to find non-trivial solutions. A way to ensure the existence of solutions at arbitrary mass is if the effective dynamics has a scaling symmetry.

The basic scaling transformation replaces the metric configuration $g_{\mu\nu}(x)$ with a new

configuration,

$$g_{\mu\nu}(x) \to \tilde{g}_{\mu\nu}(x) = g_{\mu\nu}(\lambda x) \ . \tag{4.8}$$

This leaves the Minkowski metric invariant, but rescales perturbations of it:

$$ds^2 = [\eta_{\mu\nu} + h_{\mu\nu}(x)]dx^\mu dx^\nu \to d\tilde{s}^2 = [\eta_{\mu\nu} + h_{\mu\nu}(\lambda x)]dx^\mu dx^\nu \ . \tag{4.9}$$

For example, this transformation maps the Schwarzschild solution with mass M to a solution with mass M/λ. A change of integration variables shows that

$$S[\tilde{g}] = \int d^4x\sqrt{-\tilde{g}}\tilde{R} = \frac{1}{\lambda^2}\int d^4x\sqrt{-g}R = \frac{1}{\lambda^2}S[g] \ , \tag{4.10}$$

but of course the vacuum equations are invariant:

$$\tilde{G}_{\mu\nu}(x) = \lambda^2 G_{\mu\nu|_{\lambda x}} = 0 \ . \tag{4.11}$$

With a source, the equations will be scale invariant if the scaling transformation also acts as

$$T_{\mu\nu} \to \tilde{T}_{\mu\nu}(x) = \lambda^2 T_{\mu\nu}(\lambda x) \ . \tag{4.12}$$

For example, the stress tensor of a massless scalar,

$$T_{\mu\nu} = \partial_\mu\phi\partial_\nu\phi - \frac{1}{2}g_{\mu\nu}(\partial\phi)^2 \tag{4.13}$$

satisfies this condition, but it is violated if there is a scalar mass present.

For the stress tensor (4.5), there will be static solutions of all scales if given a solution $\rho(x), p_r(x), p_\theta(x)$, there is a solution $\lambda^2\rho(\lambda x), \lambda^2 p_r(\lambda x), \lambda^2 p_\theta(\lambda x)$. This is clearly violated by a given fixed equation of state, (4.6). Thus, to have solutions of all scales, one

must consider a *family* of equations of state; this is more plausible if $\langle T_{\mu\nu} \rangle$ summarizes some general properties of CQOs, as opposed to being determined directly by a specific microphysical $\mathcal{L}$. We return to this point later.

4.4 Some simplified models for compact quantum objects

New effects associated to a CQO replacement of a classical BH are plausibly only significant in the strong gravity region, near the would-be horizon of the classical BH. As was noted above, this raises the question of gravitational obscuration of any modification to the classical GR signal resulting from the collision of two such objects. In order to explore this question, we first explore possible compact solutions, in the effective approach outlined above.

4.4.1 Generalities

The general static, spherically-symmetric metric can be written

$$ds^2 = -e^{2\mu(r)}dt^2 + e^{2\lambda(r)}dr^2 + r^2(d\theta^2 + \sin^2\theta d\phi^2) \ ; \tag{4.14}$$

we assume this form for the effective metric $\langle g_{\mu\nu} \rangle$. One commonly introduces an effective mass $m(r)$ by

$$e^{-2\lambda(r)} = 1 - \frac{2m(r)}{r} \ . \tag{4.15}$$

With the stress tensor (4.5), Einstein's equations (4.1) take the form (see, *e.g.*, [132])

$$m' = 4\pi r^2 \rho \tag{4.16}$$

$$\mu' = \frac{1}{r}\left(4\pi r^2 p_r + \frac{m}{r}\right) e^{2\lambda} \tag{4.17}$$

$$\mu'' + (\mu' - \lambda')\left(\mu' + \frac{1}{r}\right) = 8\pi p_\theta e^{2\lambda} \ , \tag{4.18}$$

where we use units with $G = 1$ and prime denotes the r derivative. The Tolman-Oppenheimer-Volkov (TOV) equation generalizes to

$$p_r' = -\mu'(p_r + \rho) - \frac{2}{r}(p_r - p_\theta) = -\frac{1}{r}(p_r + \rho)\left(4\pi r^2 p_r + \frac{m}{r}\right) e^{2\lambda} - \frac{2}{r}(p_r - p_\theta) \ . \tag{4.19}$$

If a solution of these equations has vanishing $\langle T^\mu_\nu \rangle$ outside a radius R_a, and has total mass M, we can define the compactness of the solution to be $C = M/R_a$. Our focus is on sensitivity to merger of highly-compact solutions. While it is possible to find more compact anisotropic solutions[132, 133] (see also [134, 135] for recent discussions), we defer exploring these to future work and instead focus on the simpler isotropic case, $p_r = p_\theta = p$. In that case, the preceding equations can be shown to imply that, for positive p and ρ, the compactness is limited by the Buchdahl bound[136],

$$C < 4/9 \ . \tag{4.20}$$

However, the Buchdahl bound is not achievable using a physical equation of state (EOS). Specifically, the stiffest EOS satisfying the constraint (4.7) on the speed of sound is

$$p = \begin{cases} \rho - \rho_0, & \text{if } \rho > \rho_0 \\ 0, & \text{if } \rho < \rho_0 \ , \end{cases} \tag{4.21}$$

where ρ_0 is an EOS parameter. It has been shown[137] that this EOS yields the isotropic solutions with the highest compactness[138] satisfying the causality condition(4.7).[10] The surface of these solutions is the radius R_a where ρ reaches ρ_0, and the pressure vanishes.

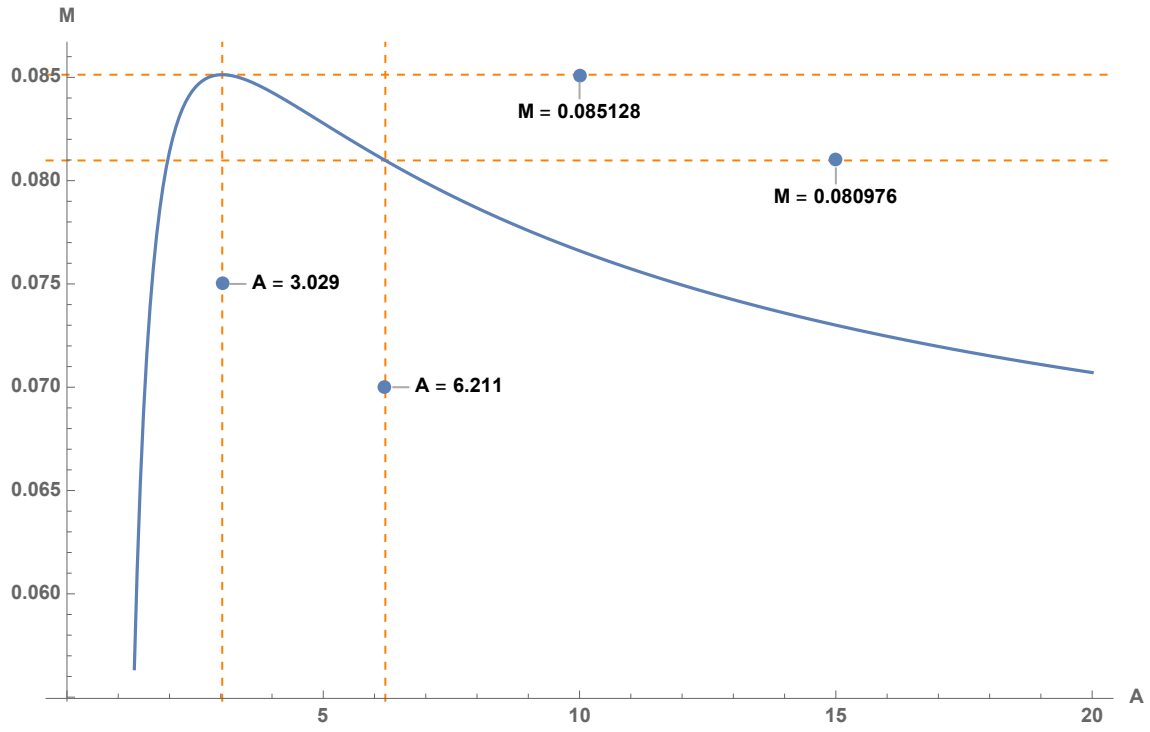


Figure 4.1: Mass vs. central density parameter A for solutions with the maximally stiff equation of state (4.21).

It is worth describing this most compact case further, since these provide first candidate toy models for highly compact CQOs. The solutions may be found by specifying a central density $\rho_c = A\rho_0$ and integrating the TOV equations (4.19) outward from $r = 0$. Plots of the total mass M and compactness C of the resulting solutions as a function of central density parameter A are shown in figs. 4.1, 4.2, and radial profiles of the density ρ and mass within a given radius are shown in figs. 4.3, 4.4. Linear stability properties change at the point where $dM/d\rho_c = 0$, and so the higher density solutions are expected

[10]This EOS has been frequently studied for the purpose of determining a theoretical maximum mass and radius for neutron stars; see *e.g.* [139, 140, 141, 142, 143, 144].

to be unstable. This gives a maximum compactness $C_m = 0.354$.

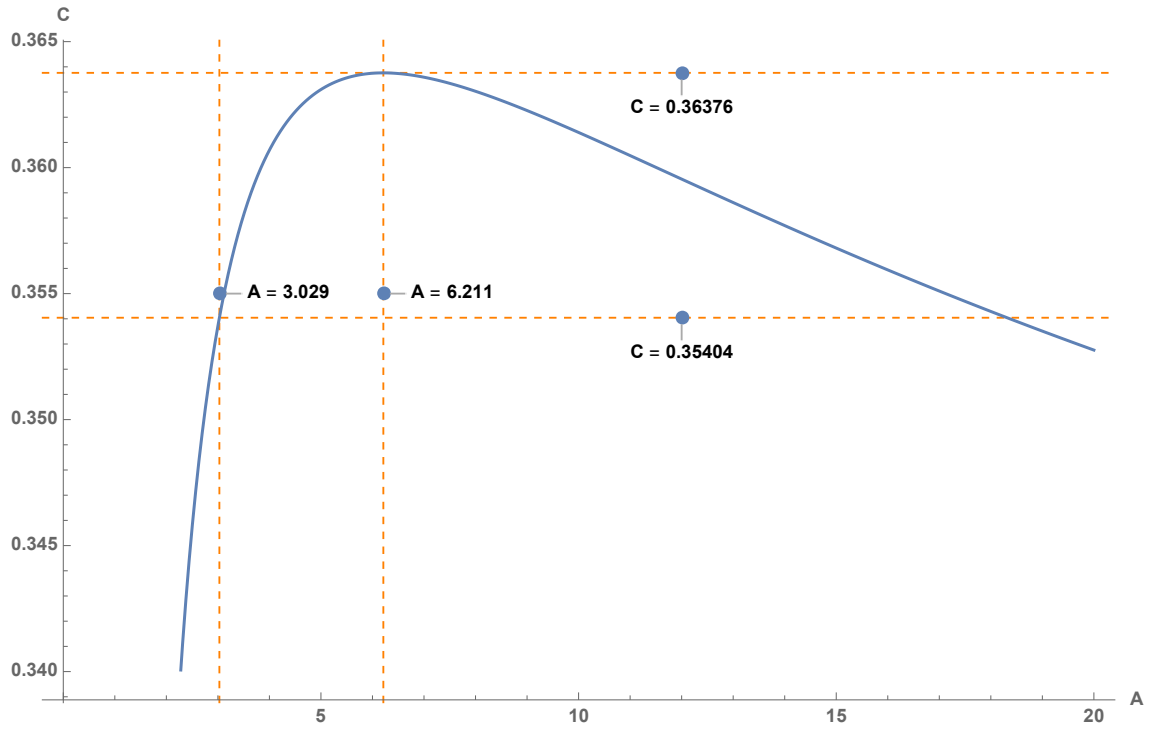


Figure 4.2: Compactness vs. central density parameter A for solutions with the maximally stiff equation of state (4.21).

The mass of the maximally compact solutions is determined in terms of the EOS parameter ρ_0 as

$$M_m = \frac{0.085\, c^4}{\sqrt{G^3 \rho_0}} \,, \tag{4.22}$$

and these have $A_m = 3.029$. So, if we want to describe such compact solutions with arbitrary masses, we need to consider a family of effective equations of state (4.21) with varying ρ_0. The scaling transformation (4.12) acts as $\rho_0 \to \widetilde{\rho_0} = \lambda^2 \rho_0$, and correspondingly from (4.22)

$$M_m \to \frac{M_m}{\lambda} \,, \tag{4.23}$$

as is seen with the Schwarzschild solution.

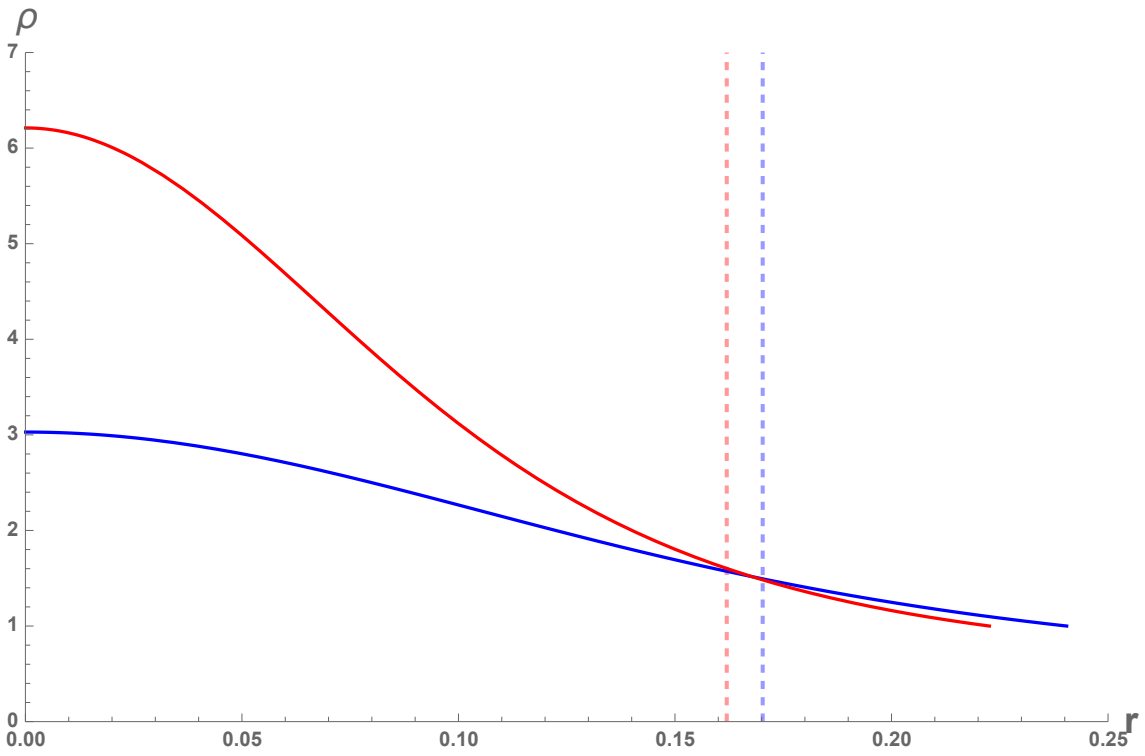


Figure 4.3: Density profile for solutions with the maximally stiff EOS (4.21). Upper (red) curve corresponds to solution with maximal C ($A = 6.211$); lower (blue) curve corresponds to solution with maximal mass ($A = 3.029$). Vertical dotted lines mark the Schwarzschild radii corresponding to the total mass of the solutions.

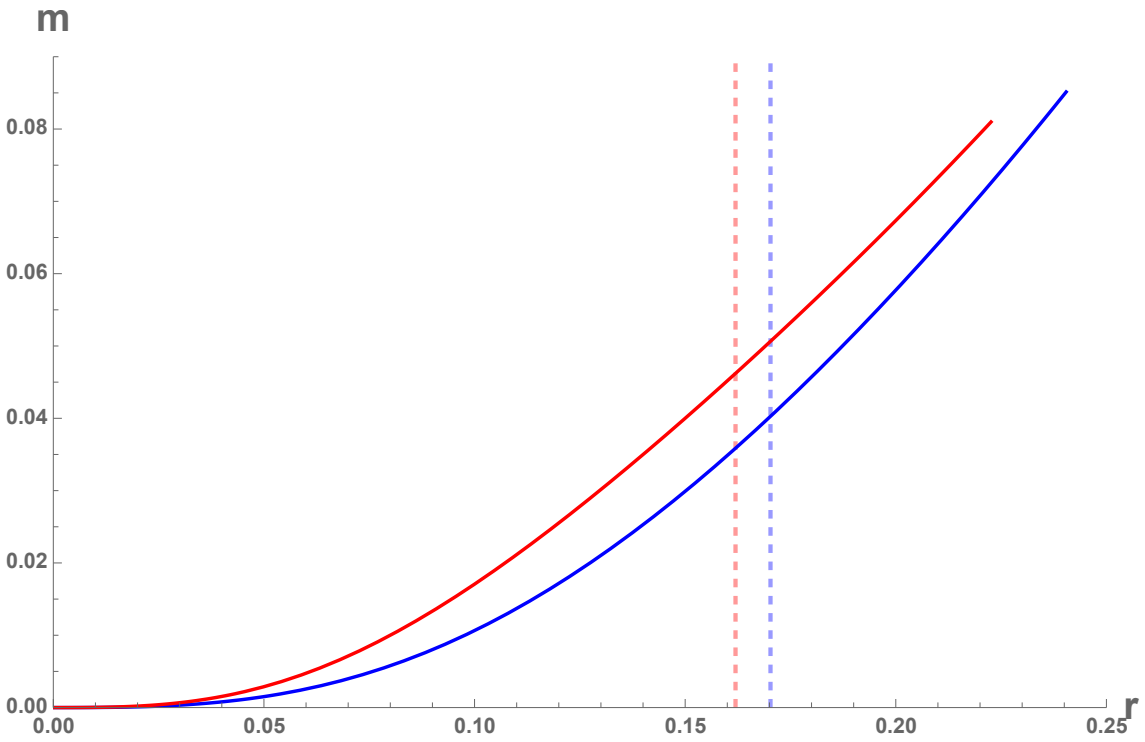


Figure 4.4: Mass profile $m(r)$ for solutions with the maximally stiff EOS (4.21). Upper (red) curve corresponds to solution with maximal C ($A = 6.211$); lower (blue) curve corresponds to solution with maximal mass ($A = 3.029$). Vertical dotted lines mark the Schwarzschild radii corresponding to the total mass of the solutions.

Since these solutions have compactness $C > 1/3$, they are inside their light rings at $r = 3M$. This suggests that departures of the GW signal due to a merger of two of these from the signal from two equal mass CBHs may be strongly obscured. An important test of this would be to calculate the gravitational wave form arising from such a merger; a useful project would be to do so with numerical simulation. However, there are also present practical limitations on such numerical simulations[11] and in particular the discontinuity in $dp/d\rho$ can be problematic for certain standard simulation routines. For this reason, the next subsection will consider solutions with improved continuity properties; it will also turn out that certain properties depend on how the density drops to zero.

Another possible issue for solutions that lie inside their light rings is that of possible non-linear instability[145, 146, 147], due to the trapping behavior of the effective gravitational potential of such a solution. This remains a subject for further exploration, and of course relies on a classical analysis which may not apply to CQOs. A pragmatic approach is to study evolution of binaries of such solutions, for example initiated not far from the orbital radius of plunge/merger; if instabilities are relevant on such timescales, they should be evident in the evolution. In addition, such objects can become linearly unstable once they acquire spin[148, 149]. If instabilities interfere with use of such solutions for testing GW departures, another approach is to adjust ρ_c just to the point where a light ring or instability ceases to exist; the resulting solutions are still expected to be highly compact, and to still provide information about gravitational obscuration of signals from mergers of CQOs.

[11] We thank L. Lehner and D. Neilsen for discussions on this.

4.4.2 Matched polytropes

Improved continuity properties can be achieved by considering an EOS corresponding to the stiffest EOS (4.21) at high energy densities, but which then transitions to a polytropic EOS at an energy density $B\rho_0$, with $B > 1$;

$$p = \begin{cases} \rho - \rho_0, & \text{if } \rho > B\rho_0 \\ K(\rho/\rho_0)^\gamma, & \text{if } \rho < B\rho_0 \ . \end{cases} \tag{4.24}$$

Here K and γ are fixed by the requirement that p and its first derivative be continuous at $B\rho_0$, so that the EOS is C^1:

$$K = \frac{B-1}{B^\gamma}\rho_0 \ , \tag{4.25}$$

$$\gamma = \frac{B}{B-1} \ . \tag{4.26}$$

The improved continuity properties of (4.24) suggest that the corresponding solutions are potentially useful, particularly for simulation with numerical GR. These have similar features to those of the maximally compact case (4.21), and in particular can achieve very high compactness. They are also in some ways similar to models of neutron stars based on hybrid EOSs, but we will consider EOS parameters attaining much higher compactness than that of neutron stars, or of other simple EOSs such as a purely polytropic EOS.

It is important to emphasize that our ρ is the energy density of the solution (that is, T^0_0 in Schwarzschild coordinates). In the modeling of neutron stars, the term 'polytrope' is often used for simple toy EOSs where the pressure is a monomial of a 'rest mass density' ρ_m instead. In that context, the neutron star is composed of matter with a conserved quantum number, namely baryon number. Then parametrizing the rest mass

density as $\rho_m = m_b n$, with m_b a fixed average baryon mass and n a conserved baryonic number density, allows for this additional conservation law to be accounted for when dynamics are turned on. The energy density is then related to this number density and pressure using an argument based on the first law of thermodynamics. For example, see [150] on the use of piecewise-polytropic EOSs to model general NS EOSs, and [151] has considered matching the extremal EOS (4.21) onto such an EOS. Of course our EOSs, as toy models of quantum-gravitational corrections to CBHs, need not have any such conserved quantities (and surely should *not* have exactly-conserved baryon number). Matching our extremal core EOS to an envelope EOS where the pressure is a monomial of the energy density should allow for a unified numerical treatment of the two different regions of the solution.

Specifically, one can once again solve Einstein's equations together with the TOV equation. The EOS is now determined by ρ_0 and B. For a given EOS, spherically-symmetric, static solutions are determined by the central density $\rho_c = A\rho_0$. These solutions have cores with the linear EOS in (4.24), and envelopes with the polytropic EOS in (4.24). Example profiles of these solutions are shown in fig. 4.5. The compactness of these solutions, as a function of A and B, is shown in fig. 4.6.[12] Clearly solutions exist, for a range of B, with compactness $C > 1/3$. The maximal compactness for such linearly-stable solutions is obtained in the (singular) limit of the EOS, $B \to 1$. As before, we expect the mass of such solutions to scale as $M \propto 1/\sqrt{\rho_0}$.

The C^1 EOS (4.24) thus furnishes solutions that may possibly be more suitable for simulation of inspiral and merger via numerical GR methods. We next turn to discussion

[12]While the matched polytropic EOS is well-defined up to the line $A = B$, as $B \to A$ the solutions become predominantly composed of the polytropic envelopes, which leads to lower compactness and also to longer numerical integration time. In Figure 4.6 the upper cutoff corresponds to solutions where the outer radius of the solution was at three times the radius of the inner boundary, so the omitted solutions are $> 3/4$ envelope in terms of radial extent. As is evident, the plotted region contains the parameter space of greatest interest, namely where the solutions are both ultracompact and linearly stable.

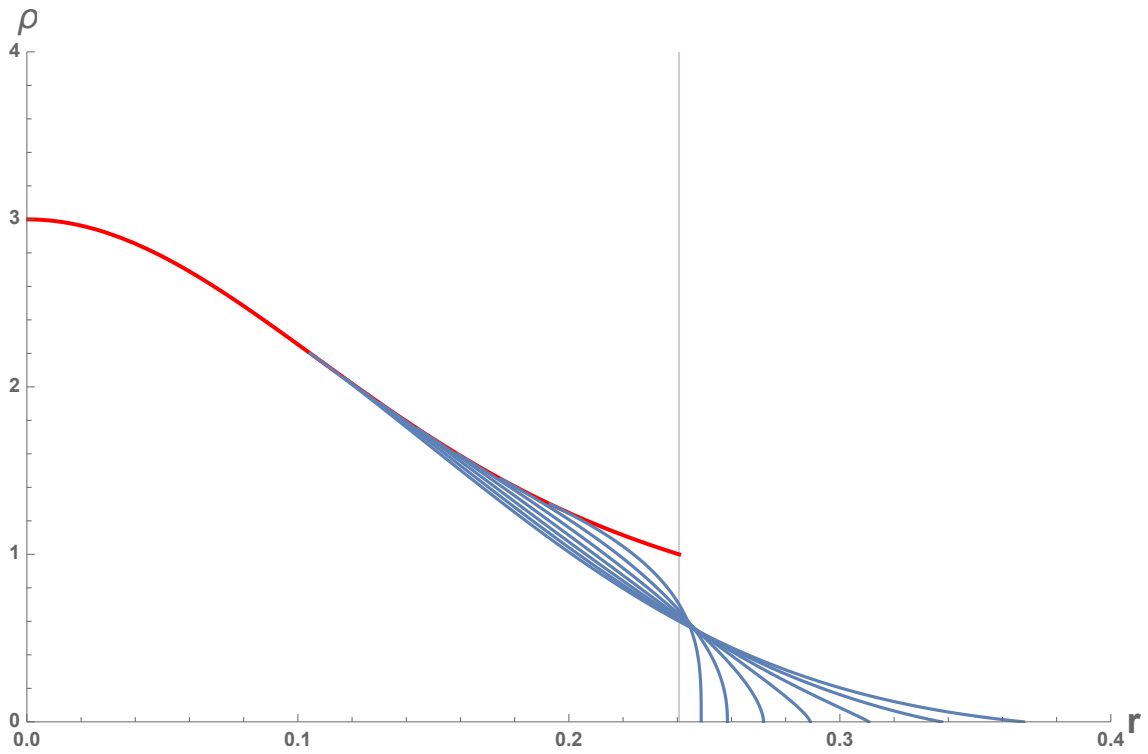


Figure 4.5: Density vs. radius curves for matched solutions with EOS (4.24), with range of B from 1.3 to 2.2 (lower, blue curves), and for corresponding extremal solution with EOS (4.21) (upper, red curve).

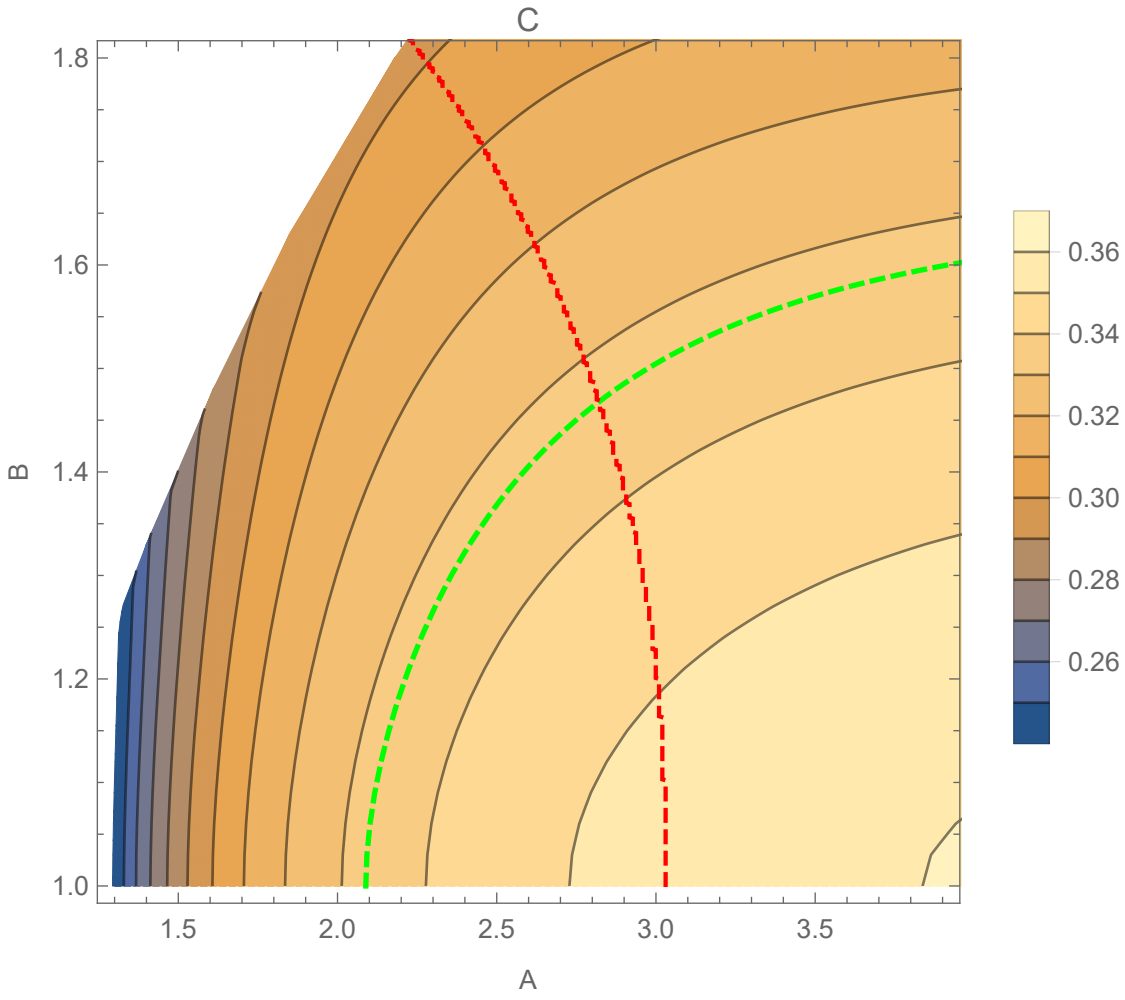


Figure 4.6: Compactness of matched solutions with EOS (4.24), as a function of the parameters A and B. The red line denotes the stability boundary, where $dM/d\rho_c$ vanishes; solutions to the left of this line are expected to be linearly stable. The green line demarcates compactness $C = 1/3$.

of some general aspects of such evolution.

4.5 Gravitational wave tests of compact quantum structure

If consistency with quantum mechanics dictates that CBHs are replaced by compact quantum objects with different properties, it is important to understand the possible sensitivity of gravitational wave observations, with LIGO/VIRGO or LISA, to this new structure. Since we don't yet have a first-principles description of such objects that follows from a complete quantum theory of gravity, a first step is to find approximate or effective characterizations of the deviations from CBH behavior, and try to determine how these deviations might manifest themselves in modifications to GW signals.[13] Indeed, precisely because we don't yet have a complete quantum theory describing black hole-like objects, any observational (or experimental) evidence for deviations from GR could provide extremely useful guidance, and should be searched for by all available means. A way to begin to understand and characterize such possible deviations is by introducing parameterizations of structure and dynamics of objects replacing CBHs, and investigating the GW sensitivity and how it depends on those parameterizations. This can help focus the search for possible departures from GR. In cases where we can provide tractable models for the new dynamics, these can be investigated with numerical GR methods.

We can distinguish three levels of detail in characterizing behavior of candidate CQOs: their description in terms of simple effective parameters, modeling of such objects in toy models or effective dynamical descriptions, and a complete description in a more

[13]In the regime where departures from GR are small, including inspiral and plunge up to the point of significant interactions, useful approaches may include the post-Einsteinian framework[152] or effective field theory[153].

fundamental theory of quantum gravity.

4.5.1 Effective parameters

The first level of detail focuses on the sizes of certain key parameters[105, 106, 107]. For example, the departure of CQO structure from that of a CBH may extend to a characteristic radius $R_a = R + \Delta R_a$ outside the horizon radius R of the CBH with the same mass.[14] The CQO structure may also be "hard" or "soft." A characteristic of this distinction is the typical spatial variation scale, or momentum transfer scale for particles as they scatter from the structure; a simple parameterization of this is as $1/L$, where L is a length scale describing the variation of the structure. Obviously $L \lesssim \Delta R_a$, and L may be much smaller, *e.g.* a microscopic size. Another characteristic is the strength $\mathcal{A}$ of the departures from GR; a benchmark for this is the amplitude for scattering of excitations from a CQO to depart from scattering from a CBH. A fourth parameter is the timescale T_q at which a CQO exhibits behavior departing from that of a CBH. In order for CQO dynamics to resolve quantum problems with BHs, this timescale is expected to lie in the range from $\sim R \log R$ – a short timescale in astrophysical terms – to $\sim R^3$, much longer than the age of the Universe for stellar-sized or larger BHs. Other potentially important parameters include tidal deformability, quantified by the Love numbers, and absorption cross sections, which can depend on wavelength.

These parameters play an important role in governing expected departure from GR predictions for GW signals. For example, departures will only be found for CQOs with age longer than T_q. For such CQOs, changes in Love numbers can lead to small departures in the GW signal from inspiral. Then, as CQOs plunge to merger, important departures from GR behavior can be expected at CQO separations $\sim 2(R+\Delta R_a)$, where

[14] For simplicity we ignore spin dependence, but in the more general spinning case the "height" ΔR_a of the gravitational atmosphere may vary *e.g.* by an order one amount as a function of angle.

the structures come into contact. This expectation holds for strong departures, $\mathcal{A} \sim 1$, but not necessarily if $\mathcal{A} \ll 1$, and the departures are expected to depend on other efective parameters such as L. A model for such departures[107] is merger of neutron stars, which give an example of large deviations in GW signals from those of CBHs, due to hard, $\mathcal{O}(1)$ structure outside the would-be horizon.

For example, a typical massive remnant scenario has hard (L microscopic), $\mathcal{A} \sim 1$ structure, but without a more detailed model, ΔR_a could range from microscopic values to $\gtrsim R$. Only in the latter case would one expect significant modifications to GW signals.[15] Love numbers and absorption cross sections also depend on the details of the model.

The soft gravitational atmosphere case has $\Delta R_a \sim L \sim R$, or more generally $\Delta R_a \sim R^q$, $L \sim R^p$, for some $p, q > 0$, to achieve "soft" scales for large CQOs. There are two variants, the strong one[123] with $\mathcal{A} \sim 1$, and the weak one[124] with $\mathcal{A} \sim 1/\sqrt{N}$, where N characterizes the large number of internal states. The strong case is expected to modify the GW signal, but also the weak case can lead to modified absorption cross sections of GWs with wavelength $\sim R$, and thus also yield departures in gravitational wave signals.

The EOS-based models considered in the preceding section also illustrate possible such parameters. The departures from the Schwarzschild metric extend over scales $\Delta R_a \sim R$, as can be seen from figs. 4.3, 4.4. Likewise, the characteristic variation scale of the geometry of these solutions is $L \sim R$; the gravitational departures are "soft" in this sense. Note, however, that if the EOS (4.21) or (4.24) gives an effective description of fluctuations of the geometry or other fields at microscopic distances, then in this more fundamental dynamics $L \ll R$. This could then reveal itself in the interaction properties

[15] This assumes that massive remnants merge to form BHs, and that $T_q \gtrsim R \log R$; exceptions will be discussed below.

of two such objects. This can be illustrated by the analogous collision of two neutron stars. The macroscopic geometries of the neutron stars vary on scales $L \gtrsim R$. However, when the surfaces of neutron stars approach in a collision, the interactions of the neutron condensates of the two stars are important, and are characterized by hard scales $L \ll R$. Absorption into or scattering from such objects, if it involves interactions other than with the macroscopic gravitational field, may also be characterized by scales $L \ll R$. With such hard structure, the models of section 4.4 behave like massive remnants, although if one considers only their average gravitational field they behave more like soft gravitational atmospheres.

4.5.2 Love numbers

Love numbers, characterizing tidal deformability, are particularly relevant parameters for investigating deviations during inspiral. With an EOS such as (4.21) or (4.24), one may calculate these. For the case of the matched EOS (4.24), a plot of the numerically-calculated Love number k_2 is shown in fig. 4.7. We calculate the $\ell = 2$ polar tidal Love number (TLN) using the method outlined in [154],[16]; it is defined as $k_2 = 3\lambda M^{-5}/2$, where λ is the proportionality constant between the quadrupole moment Q and tidal field $\mathcal{E}$, $Q_{ij} = -\lambda \mathcal{E}_{ij}$. The definition of k_2 is normalized to the mass of the objects (rather than the radius), as proposed in [156], since generic models of CQOs need not have well-defined radii.

We utilize `Mathematica` [157] to numerically solve the TOV equations for the matched polytropes and then to calculate the first-order $\ell = 2$ response to an external quadrupolar tidal field. This allows us to calculate the TLN k_2 which encodes information about the internal structure of the object. As explained in [154], this constant is sensitive to the boundary conditions imposed at the outer radius of the star R. As seen in Figure 4.7,

[16] For a general analysis of $\ell \geq 2$, see [155].

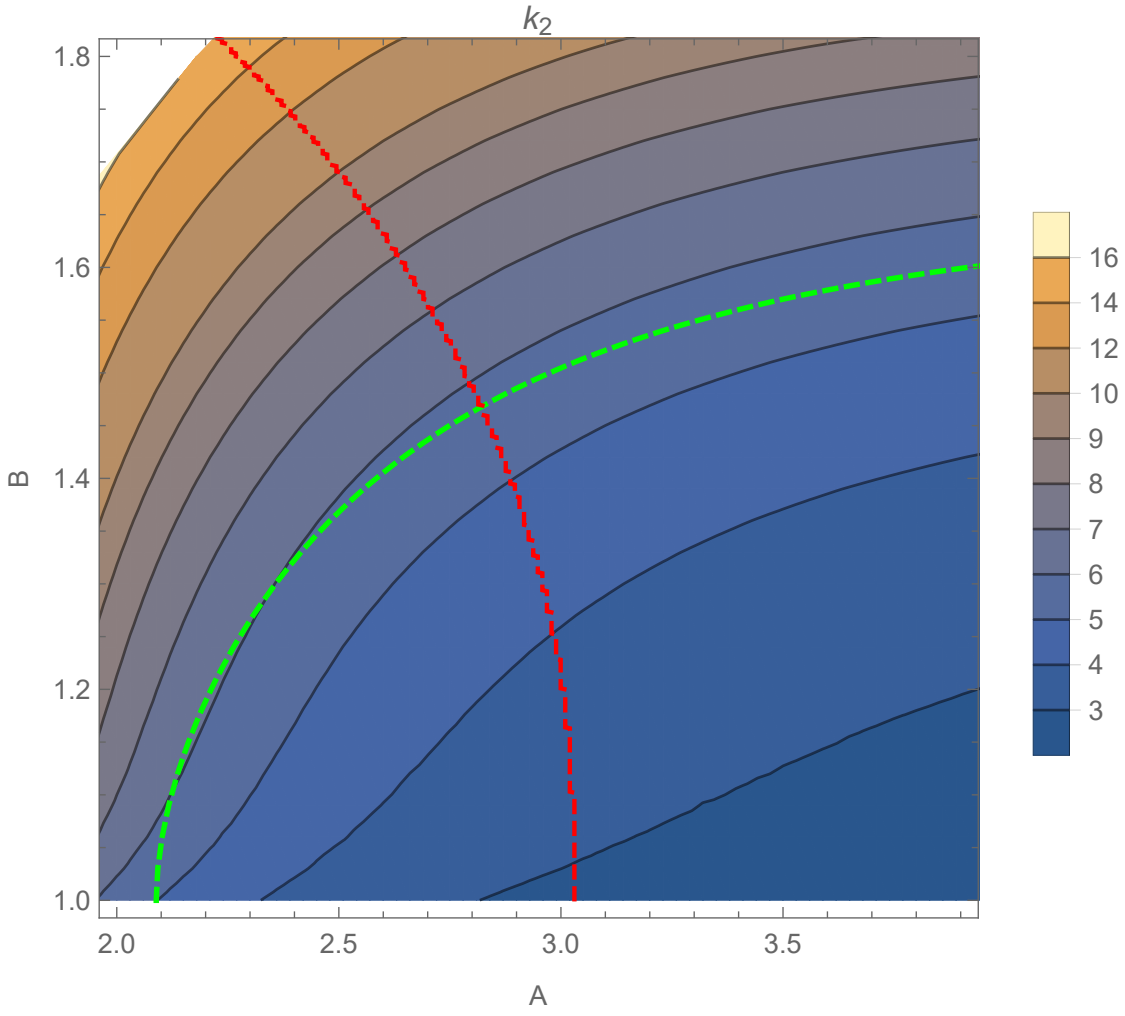


Figure 4.7: Love number k_2 of matched solutions with EOS (4.24), as a function of the parameters A and B.

values of k_2 range from $\sim 2-6$ in the region of parameter space in which the solutions are ultracompact and linearly stable. We will comment below in 4.5.3 on the physical effects of k_2 during merger, and its measurability. (Discussion of uncertainty in these calculations of k_2 appears in the appendix.)

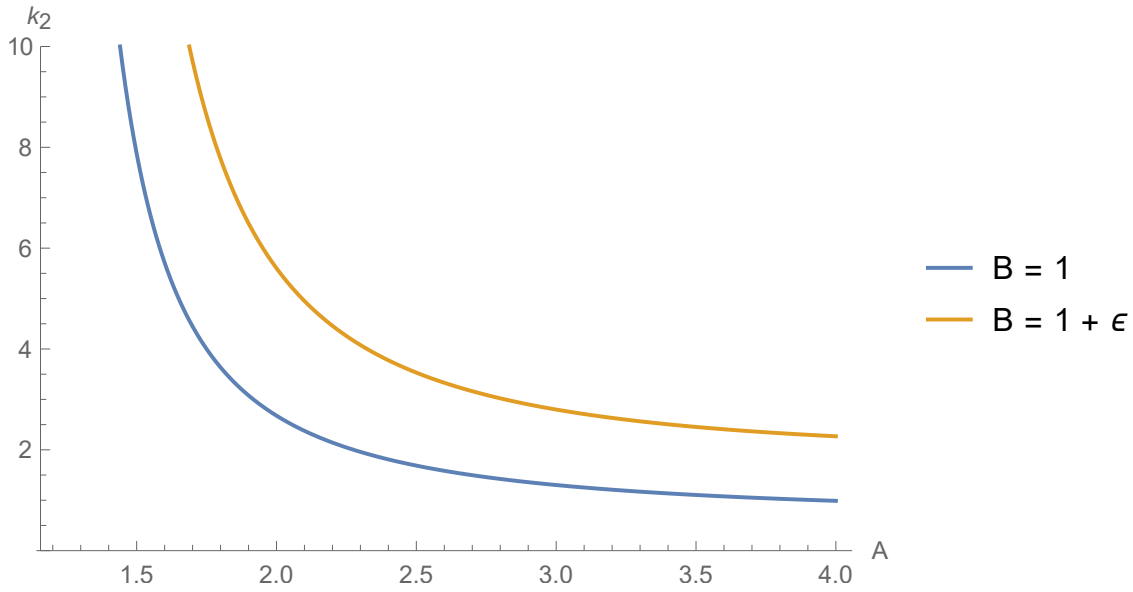


Figure 4.8: Tidal Love numbers of the extremal solutions with EOS (4.21) ("$B = 1$"), compared to those with the matched EOS (4.24), in the limit approaching $B = 1$.

It is important to note that while our matched polytropes have a continuous family of EOSs parametrized by B, the solutions of the TOV equations with these EOSs are not continuous in the limit $B \to 1$. This is visible already in Figure 4.5, where one can see that the outer radius of the extremal EOS $B = 1$ has $\rho(R) = \rho_0$, whereas the energy density falls to zero at the outer radius for any $B \neq 1$. As the TLN is sensitive to the boundary conditions at $r = R$, this difference in boundary behavior significantly affects the TLN calculation. In Figure 4.8 we show the TLNs of the extremal solutions and of the matched polytropic solutions in the limit $B \to 1$ and find that the presence of the envelope roughly doubles the TLN, even in the limit of vanishing size. This serves as one illustration of

the necessity of including parameters beyond ΔR_a in an effective description of CQOs, as despite having the same compactnesses, the macroscopic, observable effects of these objects in inspiral differ significantly.

4.5.3 Evolution: effective models and expectations

The effective parameters described above may be useful in characterizing the signal departures from that of CBHs. For a more precise determination of these departures, one needs to consider the second level of detail, using models for dynamics of CQOs. Details of dynamics can be important; for example, even in the massive remnant scenario with $\Delta R_a \sim R$, GW signal departures may be suppressed through gravitational obscuration (absorption into the final BH). One approach to such dynamics is via evolving solutions with effective EOSs.

Thus, for example, we would like to understand departures from CBH behavior in the gravitational wave signal arising from the collision of two solutions with effective EOS (4.21) or (4.24). Ideally, this could be addressed via numerical simulation of the inspiral and merger of two such solutions. In turn, understanding the signal departure then can give further insight into the roles of the effective parameters ΔR_a, L, and k_2, in governing gravitational wave signals from other models for CQOs.

In fact, given the parameters we have discussed, we can describe some anticipated features of this evolution and the signal departures.

Inspiral

To begin with, consider the inspiral phase. Here, the principal modification to the GW signal is expected to arise from the tidal deformability of the compact objects, as parameterized by the Love number k_2, and there is a clear and precise connection between

this parameter and the predicted signal deviation.

This TLN affects the signal at fifth post-Newtonian order and adds linearly to the phase of the waveform in frequency-space as

$$\tilde{h}(f) = \mathcal{A}(f) e^{i[\psi_{PP}(f)+\psi_{TD}(f)]}, \tag{4.27}$$

where f is the frequency, $\mathcal{A}$ is the amplitude, ψ_{PP} is the would-be phase for a merger of point particles, and ψ_{TD} the effect from the tidal deformability of the merging objects. This is related to the TLN k_2 as [158]

$$\psi_{TD}(f) = -\frac{3}{8}\frac{v^5}{\mu\mathcal{M}^4}\left[\left(11\frac{M_2}{M_1}+\frac{\mathcal{M}}{M_1}\right)M_1^5 k_2^{(1)} + 1 \leftrightarrow 2\right], \tag{4.28}$$

where $v = (\pi\mathcal{M}f)^{1/3}$ is the inspiral velocity, $\mathcal{M}$ and μ are the total and reduced masses of the binary, and M_i and $k_2^{(i)}$ are the individual masses and TLNs. This effect has been used to constrain the tidal deformability of neutron stars [159], which places nontrivial constraints on the neutron star EOS already from the first observation of a binary merger (see *e.g.* [160]).

The TLNs of static CBHs vanish exactly. This interesting result was first noted in [161], and further studied in [162, 163, 164, 165, 166, 167]. Contrastingly, other compact objects generically have non-zero tidal deformability, which makes this effect a good discriminating feature (as suggested in [168]). Ref. [156] used Fisher matrix methods to systematically compute the sensitivity of GW detectors to this parameter for compact objects, and finds broadly that Advanced LIGO at design sensitivity may be able to constrain TLNs down to $k_2 \sim 100$ across a broad range of binary masses; the analysis of [169] used similar methods and is in broad agreement.[17] We thus use this number as a

[17]The effect of tidal deformations in modifying the "contact frequency" has also been used to constrain some simple models of boson stars (which are not ultracompact) as being the sources of LIGO's 'black

benchmark for near-term sensitivity to tidal effects. Neutron star models have tidal Love numbers of this magnitude. However, it is clear from Figure 4.7 that the tidal effects of the present very compact CQO models are far too small to be measurable with Advanced LIGO. In [156], a study of compact objects with $\Delta R_a \approx l_P$ found $k_2 \approx \mathcal{O}(10^{-3})$, together with a universal logarithmic dependence of the TLNs on the location of the surface in the $\Delta R_a \to 0$ limit, in agreement with $k_2 = 0$ for CBHs.[18] In order to distinguish a CQO merger from a CBH merger by its tidal deformability alone, space-based detectors appear necessary. The possibility of observing strong gravity effects with these machines should serve as additional motivation for their construction, as well as for further detailed study of their capabilities[172, 156, 173]. Ref. [156] shows that current designs of future space-based GW detectors may be able to do up to two orders of magnitude better in optimistic detection scenarios, though it has recently been pointed out in [172] that the effect of tidal heating dominates for LISA binaries. (Ref. [173] suggests even greater LISA sensitivity to highly-spinning objects.) It may also be possible to extract signatures of departures from CBHs by "stacking" signals from multiple events, as in [174].[19]

The structure of objects of moderate compactness can also significantly shift the end of inspiral – objects can for example begin to interact before they reach what would be the ISCO for CBHs[175, 127]. However, while further investigation is warranted, such effects are not expected to be important for objects with compactness in the range $C \gtrsim 1/3$. Such objects are expected to have important modifications due to later interactions after they have entered the plunge phase, as they begin to merge. This observation and the preceding challenges emphasize the importance of moving past inspiral and gaining detailed understanding of the behavior of CQOs during plunge, where their deviations

hole' mergers [170], though this does not take advantage of all of the constraining power of the effects of tidal deformability.

[18]For work to distinguish tidal parameters for neutron stars see [160, 171].

[19]It also may be worth using such methods with binary neutron star templates even at high masses, to explore for possible departures. We thank L. Lehner for pointing out the possible role of such stacking.

from CBHs will be more pronounced.

Plunge and Merger

Larger deviations are expected when the model CQOs approach the point where they merge. For equal mass CQOs with mass M, inspiral transitions to plunge at a separation $d \sim 24M$, corresponding to the mutual innermost stable circular orbit. So objects with compactness $\gtrsim 1/12$ will have a plunge phase, terminated by this merger at separation $d \sim 2R_a$. The GW signal departs from that of a CBH collision both because the objects encounter the gravitational field modifications, and because they increasingly disrupt each other's structure. Neutron star collisions, for example as modeled in [117], furnish an example of some of these possible modifications[106]. In neutron star simulations, one finds a significant increase in the GW amplitude when the stars begin to merge (see *e.g.* fig. 2 of [117]), but a decrease in the emitted power spectrum; a scaled up version of the examples of [117], using the scaling transformation (4.8), (4.9), for example, already appears inconsistent with LIGO data.

While similar features are expected for simple CQO models, such as those given above, CQOs may be much more compact than neutron stars, which have compactnesses $C \lesssim 1/5$. In the case where the compactness approaches, or exceeds, $C = 1/3$, one expects some signal obscuration, as noted above, since the departures due to merger are generated "deep in the gravitational potential." This is not necessarily a sharp boundary. Indeed, such a configuration has a significant angular momentum; this means for example that the prograde and retrograde light rings of the ultimate object have different radii. If one assumes that most of the perturbations are prograde, the fact that the prograde light orbits tend to cluster towards $r \sim M$ for high spin then suggests the possibility of reduced obscuration. One also expects the GW signal to depend on other details of the model for the colliding objects, including how their structure interacts.

Given the uncertainties, a particularly interesting project would be to simulate the CQO models described above via numerical methods. It appears that already some important questions – such as the role of obscuration – can begin to be addressed even in the simple models with effective EOS given in section 4.4. An example of a concrete question is whether recent GW detections – *e.g.* the first LIGO detection of a merger of two $\sim 30M_\odot$ objects – are capable of distinguishing a CBH merger from a merger of objects governed by the EOS (4.24), if the EOS parameters are such that the solutions are highly compact, $C \gtrsim 1/3$. We hope to see such models studied via numerical GR in the near future. As an intermediate step, it may also be possible to formulate hybrid waveforms which approximately capture important aspects of the GW signatures for model CQOs, by matching tidally-corrected inspiral waveforms to parameterizations of waveforms for plunge and merger, and then to the quasinormal regime[176].

4.5.4 Quantum dynamics and expectations

We would of course like to be describing CQO evolution within the context of a complete quantum theory of quantum gravity, providing a consistent description of quantum analogs of black holes, but the field has not sufficiently advanced. The models described above may supply some insight into how sensitive observations are to this more complete quantum dynamics. However, a key question is how accurately the models capture important features of the full quantum evolution.

As was noted in section 4.2, there are multiple contenders for scenarios for the quantum completion of black hole evolution.

In the massive remnant category, one possibility that has been repeatedly considered is that of a massive remnant with $\Delta R_a \ll R$. Firewalls[103] fit in this category. If there is a viable fuzzball scenario, it is not known if it produces $\Delta R_a \sim R$ or $\Delta R_a \ll R$,

but the latter has been suggested[177] and would fit in this category. Such objects have also been considered, and given the name "ClePhOs," in [109]. However, there is so far no dynamical theory or effective model that produces any of these objects, and allows study of their evolution, and an important question is whether such configurations can exist in a consistent description. Possibly, such highly-compact solutions could be modeled with an anisotropic stress tensor[134], avoiding the Buchdahl bound (4.20), with a stress tensor violating other conditions (*e.g.* gravastars), or by other means. If such a highly compact configuration does give the correct physics, it is important to develop a consistent dynamical description for it, even if it is in an effective model.

If such configurations *were* physical, the next question is whether observations would be sensitive to their features. The case $\Delta R_a \ll R$ appears difficult, although there is possible sensitivity through TLNs[173]. Electromagnetic images are determined by trajectories of photons in the vicinity of the light ring, and so are not necessarily sensitive to such a configuration. Likewise, given the preceding discussion surrounding obscuration, it appears even less likely that the collision of two such highly-compact objects would substantially alter gravitational wave signals.

Of course, one proviso in this is if such objects coalesce to form another such object that does not behave like a black hole. There is no compelling reason for this to happen; if such objects exist, they are plausibly expected to coalesce to form black holes that *later* transition to a ClePhO, after a time at least $\sim R \log R$. But, if a ClePhO *were* to form promptly, at times $\ll R \log R$, then it could be possible for the surface of the object to reflect gravitational waves, and produce echoes[114, 115, 116] of its formation. However, such a scenario obviously requires a sequence of non-trivial assumptions.

A promising alternative to such a hard scenario is that of a soft gravitational atmosphere[123, 124]. This can be described in terms of metric perturbations h (or, more generally, other field perturbations) that depend on the quantum state of the black hole. It is not clear

how a soft atmosphere scenario could have dynamics summarized in terms of an effective EOS. The strong version of [123] has perturbations with size $\langle h \rangle \sim 1$, and thus could possibly yield an observational signal, but the more complete nonlinear dynamics is needed for its prediction.[20]

The weak scenario of [124] involves perturbations such that $\langle h \rangle$ can be exponentially small in the black hole entropy, representing a smaller departure from a GR-based description. While this may seem more plausible, it naïvely looks problematic for observation. However, due to the large number of black hole internal states, quantum scattering and absorption cross sections from such an object can receive $\mathcal{O}(1)$ corrections, which are particularly important for modes with wavelength $\sim R$; this follows from an extension of the estimates for transition rates given in [124] to the case with scattered radiation. If these provide the leading quantum corrections, that can produce an observational effect on gravitational wave modes, which in a merger typically have wavelengths characterized by the same scale. It may be possible to parameterize such absorption effects and analyze their effects on the gravitational signal. This may be even more straightforward in the case of extremal mass ratio binaries where absorption into the larger mass object can be parameterized and its effect on the coalescence and radiation inferred[178, 179];[21] these investigations are left for future work.

[20] Possible electromagnetic signals are discussed in [113].

[21] We thank S. Hughes for a discussion on this question.

Appendix A

Uncertainty in k_2 calculations

The main source of uncertainty in our calculation of k_2 comes from the determination of the outer radius R, which is defined as the location at which the pressure vanishes. Due to the stiffness of our envelope EOS, the energy density falls quite steeply near the outer radius - especially as $B \to 1$, as seen in Figure 4.5. As a result, our numerical implementation of the TOV equations turns into a 'stiff system of differential equations', which causes `Mathematica`'s numerical solution to fail at R_{end}, some small distance before the true outer radius $R - R_{\text{end}} \lll R$, when the pressure has not yet reached precisely zero.

For a rough sense of the uncertainty this gives our calculation, we extrapolate the quickly-falling pressure past the point at which the solution fails and find where it hits zero. We assign an outer radius uncertainty ΔR to be the difference between this radius and where the solution stopped at R_{end}. We then assign an uncertainty to the TLN of $\Delta k_2 \equiv k_2'(R_{\text{end}})\Delta R$, where k_2' is the derivative of the TLN with respect to the outer radius at which it is calculated. While ΔR is very small, the TLN is sensitive exactly to the behavior of the solution at the boundary, which changes rapidly, so it is not obvious a priori that the resulting uncertainty should be negligible. Nevertheless, in Figure A.1

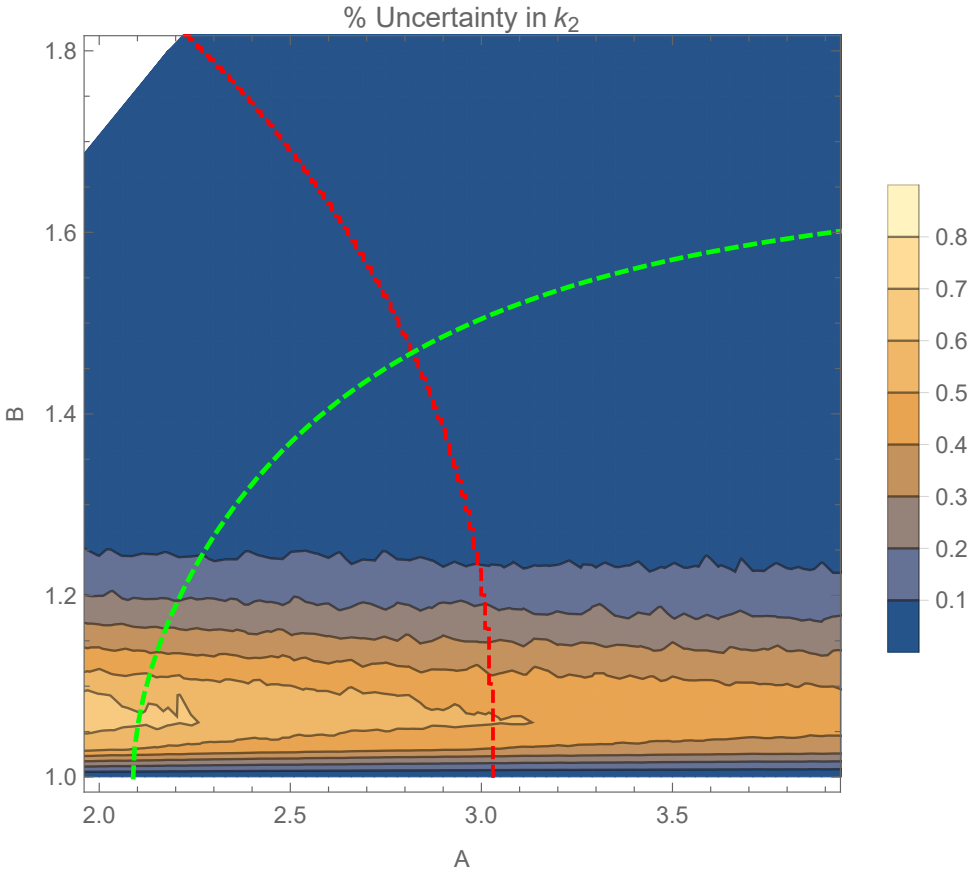


Figure A.1: Uncertainity in k_2

we plot the percent uncertainty $\frac{k_2'(R_{\text{end}})\Delta R}{k_2(R_{\text{end}})} \times 100$, which suggests that the calculation is under reasonable control everywhere.

Bibliography

[1] R. M. Wald, *General relativity*. University of Chicago press, 2010.

[2] S. Deser, P. Van Nieuwenhuizen and D. Boulware, *Uniqueness and nonrenormalizability of quantum gravitation*, *General Relativity and Gravitation* (1975) 1.

[3] G. Hooft, *Dimensional reduction in quantum gravity*, *arXiv preprint gr-qc/9310026* (1993) .

[4] L. Susskind, *The world as a hologram*, *Journal of Mathematical Physics* **36** (1995) 6377.

[5] J. M. Maldacena, *The Large N limit of superconformal field theories and supergravity*, *Adv. Theor. Math. Phys.* **2** (1998) 231 [hep-th/9711200].

[6] D. Marolf, *Unitarity and holography in gravitational physics*, *Physical Review D* **79** (2009) 044010.

[7] N. Ashby, *Relativity in the global positioning system*, *Living Reviews in relativity* **6** (2003) 1.

[8] R. A. Hulse and J. H. Taylor, *Discovery of a pulsar in a binary system*, *The Astrophysical Journal* **195** (1975) L51.

[9] B. P. Abbott, R. Abbott, T. Abbott, M. Abernathy, F. Acernese, K. Ackley et al., *Observation of gravitational waves from a binary black hole merger*, *Physical review letters* **116** (2016) 061102.

[10] A. Sengupta, *The sensitivity of the advanced ligo detectors at the beginning of gravitational wave astronomy*, .

[11] K. Danzmann and A. Rüdiger, *Lisa technology—concept, status, prospects*, *Classical and Quantum Gravity* **20** (2003) S1.

[12] N. Bartolo, C. Caprini, V. Domcke, D. G. Figueroa, J. Garcia-Bellido, M. C. Guzzetti et al., *Science with the space-based interferometer lisa. iv: Probing*

inflation with gravitational waves, *Journal of Cosmology and Astroparticle Physics* **2016** (2016) 026.

[13] E. H. T. Collaboration et al., *First m87 event horizon telescope results. i. the shadow of the supermassive black hole*, *arXiv preprint arXiv:1906.11238* (2019) .

[14] S. E. Gralla, D. E. Holz and R. M. Wald, *Black hole shadows, photon rings, and lensing rings*, *Physical Review D* **100** (2019) 024018.

[15] K. Akiyama, J. C. Algaba, A. Alberdi, W. Alef, R. Anantua, K. Asada et al., *First m87 event horizon telescope results. vii. polarization of the ring*, *The Astrophysical Journal Letters* **910** (2021) L12.

[16] S. B. Giddings, S. Koren and G. Treviño, *Exploring strong-field deviations from general relativity via gravitational waves*, *Phys. Rev. D* **100** (2019) 044005 [1904.04258].

[17] E. T. Newman and A. Janis, *Note on the kerr spinning-particle metric*, *Journal of Mathematical Physics* **6** (1965) 915.

[18] E. T. Newman, E. Couch, K. Chinnapared, A. Exton, A. Prakash and R. Torrence, *Metric of a rotating, charged mass*, *Journal of mathematical physics* **6** (1965) 918.

[19] C. W. Misner, K. S. Thorne and J. A. Wheeler, *Gravitation*. Macmillan, 1973.

[20] R. Ruffini and J. A. Wheeler, *Introducing the black hole.*, *Physics Today* (1971) .

[21] W. Israel, *Event horizons in static vacuum space-times*, *Physical review* **164** (1967) 1776.

[22] W. Israel, *Event horizons in static electrovac space-times*, *Communications in Mathematical Physics* **8** (1968) 245.

[23] B. Carter, *Axisymmetric black hole has only two degrees of freedom*, *Physical Review Letters* **26** (1971) 331.

[24] J. D. Bekenstein, *Black-hole thermodynamics*, *Physics Today* **33** (1980) 24.

[25] S. W. Hawking, *Gravitational radiation from colliding black holes*, *Physical Review Letters* **26** (1971) 1344.

[26] J. D. Bekenstein, *Black holes and entropy*, *Phys. Rev. D* **7** (1973) 2333.

[27] J. M. Bardeen, B. Carter and S. W. Hawking, *The four laws of black hole mechanics*, *Communications in mathematical physics* **31** (1973) 161.

[28] T. Jacobson, *Introductory lectures on black hole thermodynamics*, *Institute for Theoretical Physics University of Utrecht* (1996) .

[29] S. M. Carroll, *Spacetime and geometry*. Cambridge University Press, 2019.

[30] S. W. Hawking, *Particle creation by black holes*, *Communications in mathematical physics* **43** (1975) 199.

[31] S. W. Hawking, *Breakdown of predictability in gravitational collapse*, *Physical Review D* **14** (1976) 2460.

[32] W. G. Unruh, *Notes on black-hole evaporation*, *Physical Review D* **14** (1976) 870.

[33] R. D. Sorkin, *On the entropy of the vacuum outside a horizon*, in *Tenth International Conference on General Relativity and Gravitation (held Padova, 4-9 July, 1983), Contributed Papers*, vol. 2, pp. 734–736, 1983.

[34] L. Bombelli, R. K. Koul, J. Lee and R. D. Sorkin, *Quantum source of entropy for black holes*, *Physical Review D* **34** (1986) 373.

[35] T. Jacobson, *Thermodynamics of spacetime: the einstein equation of state*, *Physical Review Letters* **75** (1995) 1260.

[36] G. T. Horowitz and J. Polchinski, *Gauge/gravity duality*, *Approaches to quantum gravity* (2009) 169.

[37] S. Weinberg and E. Witten, *Limits on massless particles*, *Physics Letters B* **96** (1980) 59.

[38] G. 't Hooft, *A planar diagram theory for strong interactions*, in *The Large N Expansion In Quantum Field Theory And Statistical Physics: From Spin Systems to 2-Dimensional Gravity*, pp. 80–92, World Scientific, (1993).

[39] G. T. Horowitz, ed., *Black holes in higher dimensions*. Cambridge Univ. Pr., Cambridge, UK, 2012.

[40] J. Bardeen and G. T. Horowitz, *Extreme kerr throat geometry: A vacuum analog ofads2*s2*, *Physical Review D* **60** (1999) .

[41] E. Witten, *Anti-de Sitter space and holography*, *Adv. Theor. Math. Phys.* **2** (1998) 253 [hep-th/9802150].

[42] G. Trevino, *Reconstruction of an AdS Radiation/Boson Star Bulk Geometry Using Light-cone Cuts*, *JHEP* **11** (2017) 111 [1708.03331].

[43] S. Hernández-Cuenca, G. T. Horowitz, G. Treviño and D. Wang, *Boundary Causality Violating Metrics in Holography*, 2103.05014.

[44] S. Ryu and T. Takayanagi, *Holographic derivation of entanglement entropy from AdS/CFT*, *Phys. Rev. Lett.* **96** (2006) 181602 [hep-th/0603001].

[45] V. E. Hubeny, M. Rangamani and T. Takayanagi, *A Covariant holographic entanglement entropy proposal*, *JHEP* **07** (2007) 062 [0705.0016].

[46] X. Dong, A. Lewkowycz and M. Rangamani, *Deriving covariant holographic entanglement*, *JHEP* **11** (2016) 028 [1607.07506].

[47] V. Balasubramanian, B. D. Chowdhury, B. Czech, J. de Boer and M. P. Heller, *Bulk curves from boundary data in holography*, *Phys. Rev. D* **89** (2014) 086004 [1310.4204].

[48] M. Headrick, R. C. Myers and J. Wien, *Holographic Holes and Differential Entropy*, *JHEP* **10** (2014) 149 [1408.4770].

[49] B. Czech and L. Lamprou, *Holographic definition of points and distances*, *Phys. Rev. D* **90** (2014) 106005 [1409.4473].

[50] B. Czech, L. Lamprou, S. McCandlish and J. Sully, *Integral Geometry and Holography*, *JHEP* **10** (2015) 175 [1505.05515].

[51] V. Balasubramanian, B. Czech, B. D. Chowdhury and J. de Boer, *The entropy of a hole in spacetime*, *JHEP* **10** (2013) 220 [1305.0856].

[52] B. Czech, X. Dong and J. Sully, *Holographic Reconstruction of General Bulk Surfaces*, *JHEP* **11** (2014) 015 [1406.4889].

[53] R. C. Myers, J. Rao and S. Sugishita, *Holographic Holes in Higher Dimensions*, *JHEP* **06** (2014) 044 [1403.3416].

[54] A. Hamilton, D. N. Kabat, G. Lifschytz and D. A. Lowe, *Holographic representation of local bulk operators*, *Phys. Rev. D* **74** (2006) 066009 [hep-th/0606141].

[55] D. Kabat, G. Lifschytz and D. A. Lowe, *Constructing local bulk observables in interacting AdS/CFT*, *Phys. Rev. D* **83** (2011) 106009 [1102.2910].

[56] N. Engelhardt and G. T. Horowitz, *Towards a Reconstruction of General Bulk Metrics*, *Class. Quant. Grav.* **34** (2017) 015004 [1605.01070].

[57] M. Gary, S. B. Giddings and J. Penedones, *Local bulk S-matrix elements and CFT singularities*, *Phys. Rev. D* **80** (2009) 085005 [0903.4437].

[58] I. Heemskerk, J. Penedones, J. Polchinski and J. Sully, *Holography from Conformal Field Theory*, *JHEP* **10** (2009) 079 [0907.0151].

[59] J. Maldacena, D. Simmons-Duffin and A. Zhiboedov, *Looking for a bulk point*, *JHEP* **01** (2017) 013 [1509.03612].

[60] D. Astefanesei and E. Radu, *Boson stars with negative cosmological constant*, *Nucl. Phys. B* **665** (2003) 594 [gr-qc/0309131].

[61] D. Marolf, W. Kelly and S. Fischetti, *Conserved Charges in Asymptotically (Locally) AdS Spacetimes*, 1211.6347.

[62] A. C. Wall, *Maximin Surfaces, and the Strong Subadditivity of the Covariant Holographic Entanglement Entropy*, *Class. Quant. Grav.* **31** (2014) 225007 [1211.3494].

[63] A. Buchel, S. L. Liebling and L. Lehner, *Boson stars in AdS spacetime*, *Phys. Rev. D* **87** (2013) 123006 [1304.4166].

[64] M. Gleiser, *Stability of Boson Stars*, *Phys. Rev. D* **38** (1988) 2376.

[65] M. Gleiser and R. Watkins, *Gravitational Stability of Scalar Matter*, *Nucl. Phys. B* **319** (1989) 733.

[66] T. D. Lee and Y. Pang, *Stability of Mini - Boson Stars*, *Nucl. Phys. B* **315** (1989) 477.

[67] V. E. Hubeny, H. Liu and M. Rangamani, *Bulk-cone singularities \& signatures of horizon formation in AdS/CFT*, *JHEP* **01** (2007) 009 [hep-th/0610041].

[68] R. Aros, M. Contreras, R. Olea, R. Troncoso and J. Zanelli, *Conserved charges for gravity with locally AdS asymptotics*, *Phys. Rev. Lett.* **84** (2000) 1647 [gr-qc/9909015].

[69] L. F. Abbott and S. Deser, *Stability of Gravity with a Cosmological Constant*, *Nucl. Phys. B* **195** (1982) 76.

[70] M. Henneaux and C. Teitelboim, *Asymptotically anti-De Sitter Spaces*, *Commun. Math. Phys.* **98** (1985) 391.

[71] P. T. Chrusciel and G. Nagy, *The Mass of space - like hypersurfaces in asymptotically anti-de Sitter space-times*, *Adv. Theor. Math. Phys.* **5** (2002) 697 [gr-qc/0110014].

[72] A. Ashtekar and A. Magnon, *Asymptotically anti-de Sitter space-times*, *Class. Quant. Grav.* **1** (1984) L39.

[73] R. Aros, M. Contreras, R. Olea, R. Troncoso and J. Zanelli, *Conserved charges for even dimensional asymptotically AdS gravity theories*, *Phys. Rev. D* **62** (2000) 044002 [hep-th/9912045].

[74] E. W. Mielke, *Affine generalization of the Komar complex of general relativity*, *Phys. Rev. D* **63** (2001) 044018.

[75] B. R. Iyer, C. V. Vishveshwara and S. V. Dhurandhar, *Ultracompact ($r < 3m$) objects in general relativity*, *Classical and Quantum Gravity* **2** (1985) 219.

[76] S. Hernández-Cuenca and G. T. Horowitz, *Bulk reconstruction of metrics with a compact space asymptotically*, *Journal of High Energy Physics* **2020** (2020) .

[77] S. Gao and R. M. Wald, *Theorems on gravitational time delay and related issues*, *Class. Quant. Grav.* **17** (2000) 4999 [gr-qc/0007021].

[78] C. Akers, J. Koeller, S. Leichenauer and A. Levine, *Geometric Constraints from Subregion Duality Beyond the Classical Regime*, 1610.08968.

[79] N. Engelhardt and S. Fischetti, *The Gravity Dual of Boundary Causality*, *Class. Quant. Grav.* **33** (2016) 175004 [1604.03944].

[80] T. Jacobson, *When is g(tt) g(rr) = -1?*, *Class. Quant. Grav.* **24** (2007) 5717 [0707.3222].

[81] V. Balasubramanian and P. Kraus, *A Stress tensor for Anti-de Sitter gravity*, *Commun. Math. Phys.* **208** (1999) 413 [hep-th/9902121].

[82] R. Emparan, C. V. Johnson and R. C. Myers, *Surface terms as counterterms in the AdS / CFT correspondence*, *Phys. Rev. D* **60** (1999) 104001 [hep-th/9903238].

[83] P. Saad, S. H. Shenker and D. Stanford, *JT gravity as a matrix integral*, 1903.11115.

[84] D. Marolf and H. Maxfield, *Transcending the ensemble: baby universes, spacetime wormholes, and the order and disorder of black hole information*, *JHEP* **08** (2020) 044 [2002.08950].

[85] R. Bousso and E. Wildenhain, *Gravity/ensemble duality*, *Phys. Rev. D* **102** (2020) 066005 [2006.16289].

[86] S. S. Gubser, I. R. Klebanov and A. M. Polyakov, *Gauge theory correlators from noncritical string theory*, *Phys. Lett. B* **428** (1998) 105 [hep-th/9802109].

[87] D. Harlow and D. Stanford, *Operator Dictionaries and Wave Functions in AdS/CFT and dS/CFT*, 1104.2621.

[88] T. Banks, M. R. Douglas, G. T. Horowitz and E. J. Martinec, *AdS dynamics from conformal field theory*, hep-th/9808016.

[89] L. Susskind and E. Witten, *The Holographic bound in anti-de Sitter space*, hep-th/9805114.

[90] C. Fefferman and C. R. Graham, *Conformal invariants*, in *Élie Cartan et les mathématiques d'aujourd'hui*, no. S131 in Astérisque, pp. 95–116, Société mathématique de France, (1985).

[91] K. Skenderis and B. C. van Rees, *Real-time gauge/gravity duality*, *Phys. Rev. Lett.* **101** (2008) 081601 [0805.0150].

[92] K. Skenderis and B. C. van Rees, *Real-time gauge/gravity duality: Prescription, Renormalization and Examples*, *JHEP* **05** (2009) 085 [0812.2909].

[93] J. J. Halliwell and J. B. Hartle, *Integration Contours for the No Boundary Wave Function of the Universe*, *Phys. Rev. D* **41** (1990) 1815.

[94] M. Headrick, V. E. Hubeny, A. Lawrence and M. Rangamani, *Causality & holographic entanglement entropy*, *JHEP* **12** (2014) 162 [1408.6300].

[95] D. Berenstein and D. Grabovsky, *The Tortoise and the Hare: A Causality Puzzle in AdS/CFT*, 2011.08934.

[96] LIGO Scientific, Virgo collaboration, *GWTC-1: A Gravitational-Wave Transient Catalog of Compact Binary Mergers Observed by LIGO and Virgo during the First and Second Observing Runs*, *Phys. Rev. X* **9** (2019) 031040 [1811.12907].

[97] S. Doeleman et al., *Imaging an Event Horizon: submm-VLBI of a Super Massive Black Hole*, 0906.3899.

[98] S. B. Giddings, *Black holes and massive remnants*, *Phys. Rev. D* **46** (1992) 1347 [hep-th/9203059].

[99] S. B. Giddings, *Locality in quantum gravity and string theory*, *Phys. Rev. D* **74** (2006) 106006 [hep-th/0604072].

[100] S. B. Giddings, *Black hole information, unitarity, and nonlocality*, *Phys. Rev. D* **74** (2006) 106005 [hep-th/0605196].

[101] S. D. Mathur, *Fuzzballs and the information paradox: A Summary and conjectures*, 0810.4525.

[102] S. B. Giddings, *Nonlocality versus complementarity: A Conservative approach to the information problem*, *Class. Quant. Grav.* **28** (2011) 025002 [0911.3395].

[103] A. Almheiri, D. Marolf, J. Polchinski and J. Sully, *Black Holes: Complementarity or Firewalls?*, *JHEP* **02** (2013) 062 [1207.3123].

[104] J. Maldacena and L. Susskind, *Cool horizons for entangled black holes*, *Fortsch. Phys.* **61** (2013) 781 [1306.0533].

[105] S. B. Giddings, *Possible observational windows for quantum effects from black holes*, *Phys. Rev. D* **90** (2014) 124033 [1406.7001].

[106] S. B. Giddings, *Gravitational wave tests of quantum modifications to black hole structure – with post-GW150914 update*, *Class. Quant. Grav.* **33** (2016) 235010 [1602.03622].

[107] S. B. Giddings, *Astronomical tests for quantum black hole structure*, *Nature Astron.* **1** (2017) 0067 [1703.03387].

[108] K. Yagi and L. C. Stein, *Black Hole Based Tests of General Relativity*, *Class. Quant. Grav.* **33** (2016) 054001 [1602.02413].

[109] V. Cardoso and P. Pani, *The observational evidence for horizons: from echoes to precision gravitational-wave physics*, 1707.03021.

[110] L. Barack et al., *Black holes, gravitational waves and fundamental physics: a roadmap*, *Class. Quant. Grav.* **36** (2019) 143001 [1806.05195].

[111] R. Carballo-Rubio, F. Di Filippo, S. Liberati and M. Visser, *Phenomenological aspects of black holes beyond general relativity*, *Phys. Rev. D* **98** (2018) 124009 [1809.08238].

[112] S. B. Giddings, *Hawking radiation, the Stefan–Boltzmann law, and unitarization*, *Phys. Lett. B* **754** (2016) 39 [1511.08221].

[113] S. B. Giddings and D. Psaltis, *Event Horizon Telescope Observations as Probes for Quantum Structure of Astrophysical Black Holes*, *Phys. Rev. D* **97** (2018) 084035 [1606.07814].

[114] V. Cardoso, E. Franzin and P. Pani, *Is the gravitational-wave ringdown a probe of the event horizon?*, *Phys. Rev. Lett.* **116** (2016) 171101 [1602.07309].

[115] V. Cardoso, S. Hopper, C. F. B. Macedo, C. Palenzuela and P. Pani, *Gravitational-wave signatures of exotic compact objects and of quantum corrections at the horizon scale*, *Phys. Rev. D* **94** (2016) 084031 [1608.08637].

[116] J. Abedi, H. Dykaar and N. Afshordi, *Echoes from the Abyss: Tentative evidence for Planck-scale structure at black hole horizons*, *Phys. Rev. D* **96** (2017) 082004 [1612.00266].

[117] C. Palenzuela, S. L. Liebling, D. Neilsen, L. Lehner, O. L. Caballero, E. O'Connor et al., *Effects of the microphysical Equation of State in the mergers of magnetized Neutron Stars With Neutrino Cooling*, *Phys. Rev. D* **92** (2015) 044045 [1505.01607].

[118] C. M. Will, *Putting General Relativity to the Test: Twentieth-Century Highlights and Twenty-First-Century Prospects*, *Einstein Stud.* **14** (2018) 81.

[119] P. O. Mazur and E. Mottola, *Gravitational condensate stars: An alternative to black holes*, gr-qc/0109035.

[120] C. Rovelli and F. Vidotto, *Planck stars*, *Int. J. Mod. Phys. D* **23** (2014) 1442026 [1401.6562].

[121] S. B. Giddings, *Models for unitary black hole disintegration*, *Phys. Rev. D* **85** (2012) 044038 [1108.2015].

[122] S. B. Giddings, *Black holes, quantum information, and unitary evolution*, *Phys. Rev. D* **85** (2012) 124063 [1201.1037].

[123] S. B. Giddings, *Modulated Hawking radiation and a nonviolent channel for information release*, *Phys. Lett. B* **738** (2014) 92 [1401.5804].

[124] S. B. Giddings, *Nonviolent unitarization: basic postulates to soft quantum structure of black holes*, *JHEP* **12** (2017) 047 [1701.08765].

[125] M. Van Raamsdonk, *Building up spacetime with quantum entanglement*, *Gen. Rel. Grav.* **42** (2010) 2323 [1005.3035].

[126] G. Khanna and R. H. Price, *Black Hole Ringing, Quasinormal Modes, and Light Rings*, *Phys. Rev. D* **95** (2017) 081501 [1609.00083].

[127] G. F. Giudice, M. McCullough and A. Urbano, *Hunting for Dark Particles with Gravitational Waves*, *JCAP* **10** (2016) 001 [1605.01209].

[128] C. Palenzuela, P. Pani, M. Bezares, V. Cardoso, L. Lehner and S. Liebling, *Gravitational Wave Signatures of Highly Compact Boson Star Binaries*, *Phys. Rev. D* **96** (2017) 104058 [1710.09432].

[129] M. Bezares and C. Palenzuela, *Gravitational Waves from Dark Boson Star binary mergers*, *Class. Quant. Grav.* **35** (2018) 234002 [1808.10732].

[130] N. Sanchis-Gual, C. Herdeiro, J. A. Font, E. Radu and F. Di Giovanni, *Head-on collisions and orbital mergers of Proca stars*, *Phys. Rev. D* **99** (2019) 024017 [1806.07779].

[131] S. L. Liebling and C. Palenzuela, *Dynamical Boson Stars*, *Living Rev. Rel.* **15** (2012) 6 [1202.5809].

[132] H. Andreasson, *Sharp bounds on 2m/r of general spherically symmetric static objects*, *J. Diff. Eq.* **245** (2008) 2243 [gr-qc/0702137].

[133] S. Karmakar, S. Mukherjee, R. Sharma and S. D. Maharaj, *The Role of pressure anisotropy on the maximum mass of cold compact stars*, *Pramana* **68** (2007) 881 [0708.3305].

[134] G. Raposo, P. Pani, M. Bezares, C. Palenzuela and V. Cardoso, *Anisotropic stars as ultracompact objects in General Relativity*, *Phys. Rev. D* **99** (2019) 104072 [1811.07917].

[135] D. E. Kaplan and S. Rajendran, *Firewalls in General Relativity*, *Phys. Rev. D* **99** (2019) 044033 [1812.00536].

[136] H. A. Buchdahl, *General Relativistic Fluid Spheres*, *Phys. Rev.* **116** (1959) 1027.

[137] A. Fujisawa, H. Saida, C.-M. Yoo and Y. Nambu, *Maximum mass of a barotropic spherical star*, *Class. Quant. Grav.* **32** (2015) 215028 [1503.01517].

[138] J. M. Lattimer, *The nuclear equation of state and neutron star masses*, *Ann. Rev. Nucl. Part. Sci.* **62** (2012) 485 [1305.3510].

[139] P. Haensel and J. Zdunik, *A submillisecond pulsar and the equation of state of dense matter*, *Nature* **340** (1989) 617.

[140] K. Brecher and G. Caporaso, *Obese 'neutron'stars*, *Nature* **259** (1976) 377.

[141] C. E. Rhoades, Jr. and R. Ruffini, *Maximum mass of a neutron star*, *Phys. Rev. Lett.* **32** (1974) 324.

[142] V. Kalogera and G. Baym, *The maximum mass of a neutron star*, *Astrophys. J. Lett.* **470** (1996) L61 [astro-ph/9608059].

[143] N. K. Glendenning, *Limiting rotational period of neutron stars*, *Phys. Rev. D* **46** (1992) 4161.

[144] S. Koranda, N. Stergioulas and J. L. Friedman, *Upper limit set by causality on the rotation and mass of uniformly rotating relativistic stars*, *Astrophys. J.* **488** (1997) 799 [astro-ph/9608179].

[145] J. Keir, *Slowly decaying waves on spherically symmetric spacetimes and ultracompact neutron stars*, *Class. Quant. Grav.* **33** (2016) 135009 [1404.7036].

[146] V. Cardoso, L. C. B. Crispino, C. F. B. Macedo, H. Okawa and P. Pani, *Light rings as observational evidence for event horizons: long-lived modes, ergoregions and nonlinear instabilities of ultracompact objects*, *Phys. Rev. D* **90** (2014) 044069 [1406.5510].

[147] P. V. P. Cunha, E. Berti and C. A. R. Herdeiro, *Light-Ring Stability for Ultracompact Objects*, *Phys. Rev. Lett.* **119** (2017) 251102 [1708.04211].

[148] J. L. Friedman, *Generic instability of rotating relativistic stars*, *Commun. Math. Phys.* **62** (1978) 247.

[149] V. Cardoso, P. Pani, M. Cadoni and M. Cavaglia, *Ergoregion instability of ultracompact astrophysical objects*, *Phys. Rev. D* **77** (2008) 124044 [0709.0532].

[150] J. S. Read, B. D. Lackey, B. J. Owen and J. L. Friedman, *Constraints on a phenomenologically parameterized neutron-star equation of state*, *Phys. Rev. D* **79** (2009) 124032 [0812.2163].

[151] P. Negi and M. Durgapal, *Stable ultracompact objects and an upper bound on neutron star masses*, *Astronomy and Astrophysics* **353** (2000) 641.

[152] N. Loutrel, N. Yunes and F. Pretorius, *Parametrized post-Einsteinian framework for gravitational wave bursts*, *Phys. Rev. D* **90** (2014) 104010 [1404.0092].

[153] R. A. Porto, *The effective field theorist's approach to gravitational dynamics*, *Phys. Rept.* **633** (2016) 1 [1601.04914].

[154] T. Hinderer, *Tidal Love numbers of neutron stars*, *Astrophys. J.* **677** (2008) 1216 [0711.2420].

[155] K. S. Thorne and A. Campolattaro, *Non-radial pulsation of general-relativistic stellar models. i. analytic analysis for l¿= 2*, *The astrophysical journal* **149** (1967) 591.

[156] V. Cardoso, E. Franzin, A. Maselli, P. Pani and G. Raposo, *Testing strong-field gravity with tidal Love numbers*, *Phys. Rev. D* **95** (2017) 084014 [1701.01116].

[157] W. R. Inc., "Mathematica, Version 12.2."

[158] E. E. Flanagan and T. Hinderer, *Constraining neutron star tidal Love numbers with gravitational wave detectors*, *Phys. Rev. D* **77** (2008) 021502 [0709.1915].

[159] LIGO Scientific, Virgo collaboration, *GW170817: Observation of Gravitational Waves from a Binary Neutron Star Inspiral*, *Phys. Rev. Lett.* **119** (2017) 161101 [1710.05832].

[160] E. Annala, T. Gorda, A. Kurkela and A. Vuorinen, *Gravitational-wave constraints on the neutron-star-matter Equation of State*, *Phys. Rev. Lett.* **120** (2018) 172703 [1711.02644].

[161] H. Fang and G. Lovelace, *Tidal coupling of a Schwarzschild black hole and circularly orbiting moon*, *Phys. Rev. D* **72** (2005) 124016 [gr-qc/0505156].

[162] T. Binnington and E. Poisson, *Relativistic theory of tidal Love numbers*, *Phys. Rev. D* **80** (2009) 084018 [0906.1366].

[163] T. Damour and A. Nagar, *Relativistic tidal properties of neutron stars*, *Phys. Rev. D* **80** (2009) 084035 [0906.0096].

[164] N. Gürlebeck, *No-hair theorem for Black Holes in Astrophysical Environments*, *Phys. Rev. Lett.* **114** (2015) 151102 [1503.03240].

[165] E. Poisson, *Tidal deformation of a slowly rotating black hole*, *Phys. Rev. D* **91** (2015) 044004 [1411.4711].

[166] P. Pani, L. Gualtieri, A. Maselli and V. Ferrari, *Tidal deformations of a spinning compact object*, *Phys. Rev. D* **92** (2015) 024010 [1503.07365].

[167] P. Landry and E. Poisson, *Tidal deformation of a slowly rotating material body. External metric*, *Phys. Rev. D* **91** (2015) 104018 [1503.07366].

[168] R. A. Porto, *The Tune of Love and the Nature(ness) of Spacetime*, *Fortsch. Phys.* **64** (2016) 723 [1606.08895].

[169] N. Sennett, T. Hinderer, J. Steinhoff, A. Buonanno and S. Ossokine, *Distinguishing Boson Stars from Black Holes and Neutron Stars from Tidal Interactions in Inspiraling Binary Systems*, *Phys. Rev. D* **96** (2017) 024002 [1704.08651].

[170] N. K. Johnson-Mcdaniel, A. Mukherjee, R. Kashyap, P. Ajith, W. Del Pozzo and S. Vitale, *Constraining black hole mimickers with gravitational wave observations*, *Phys. Rev. D* **102** (2020) 123010 [1804.08026].

[171] P. Landry and R. Essick, *Nonparametric inference of the neutron star equation of state from gravitational wave observations*, *Phys. Rev. D* **99** (2019) 084049 [1811.12529].

[172] A. Maselli, P. Pani, V. Cardoso, T. Abdelsalhin, L. Gualtieri and V. Ferrari, *Probing Planckian corrections at the horizon scale with LISA binaries*, *Phys. Rev. Lett.* **120** (2018) 081101 [1703.10612].

[173] A. Maselli, P. Pani, V. Cardoso, T. Abdelsalhin, L. Gualtieri and V. Ferrari, *From micro to macro and back: probing near-horizon quantum structures with gravitational waves*, *Class. Quant. Grav.* **36** (2019) 167001 [1811.03689].

[174] H. Yang, V. Paschalidis, K. Yagi, L. Lehner, F. Pretorius and N. Yunes, *Gravitational wave spectroscopy of binary neutron star merger remnants with mode stacking*, *Phys. Rev. D* **97** (2018) 024049 [1707.00207].

[175] D. Lai and A. G. Wiseman, *Innermost stable circular orbit of inspiraling neutron star binaries: Tidal effects, postNewtonian effects and the neutron star equation of state*, *Phys. Rev. D* **54** (1996) 3958 [gr-qc/9609014].

[176] L. Lehner. private communication.

[177] B. Guo, S. Hampton and S. D. Mathur, *Can we observe fuzzballs or firewalls?*, *JHEP* **07** (2018) 162 [1711.01617].

[178] S. O'Sullivan and S. A. Hughes, *Strong-field tidal distortions of rotating black holes: Formalism and results for circular, equatorial orbits*, *Phys. Rev. D* **90** (2014) 124039 [1407.6983].

[179] S. O'Sullivan and S. A. Hughes, *Strong-field tidal distortions of rotating black holes: II. Horizon dynamics from eccentric and inclined orbits*, *Phys. Rev. D* **94** (2016) 044057 [1505.03809].